MODULATION OF IONOTROPIC GLUTAMATE RECEPTORS IN RETINAL NEURONS BY THE AMINO ACID D-SERINE

by

Bryan Arthur Daniels

Submitted in partial fulfillment of the requirements
for the degree of Doctor of Philosophy

at

Dalhousie University
Halifax, Nova Scotia
March 2011

DALHOUSIE UNIVERSITY

DEPARTMENT OF ANATOMY/ NEUROSCIENCE

The undersigned hereby certify that they have read and recommend to the Faculty of Graduate Studies for the acceptance of the thesis entitled "MODULATION OF IONOTROPIC GLUTAMATE RECEPTORS IN RETINAL NEURONS BY THE AMINO ACID D-SERINE" submitted by Bryan Arthur Daniels in partial fulfillment of the requirements for the degree of Doctor of Philosophy.

Dated: March 2, 2011

External Examiner: _____

Research Supervisor: _____

Examining Committee _____

_____

_____

Departmental Representative: _____

DALHOUSIE UNIVERSITY

DATE: March 2, 2011

AUTHOR: Bryan Arthur Daniels

TITLE: MODULATION OF IONOTROPIC GLUTAMATE RECEPTORS IN RETINAL NEURONS BY THE AMINO ACID D-SERINE

DEPARTMENT OR SCHOOL: Department of Anatomy/ Neuroscience

DEGREE: PhD CONVOCATION: May YEAR: 2011

_____

Signature of Author

Dedication

To my parents.

Your love and support has been unconditional and unwavering.

The trials that you have encountered and overcome are

a constant reminder of the power we all have,

regardless of the situation.

Thank you

Table of Contents

List of Tables

List of Figures

Abstract

D-Serine is regarded as an obligatory co-agonist required for the activation of NMDA-type glutamate receptors (NMDARs). In the retina D-serine and a second NMDAR coagonist, glycine, are present at similar concentration and the cells that produce and release them are in close apposition. This arrangement allows for an abundant supply of coagonists and under certain conditions the NMDAR coagonist binding site could be saturated. There is also evidence suggesting that D-serine can act in an inhibitory manner at AMPA/kainate-type glutamate receptors (GluRs). Glutamate receptor activation can lead to direct and indirect elevation of intracellular calcium (Ca^{2+}) concentration ($[Ca^{2+}]_i$). Therefore, in this thesis, I predominantly used Ca^{2+} imaging techniques to study the effect of D-serine on GluR activation in the mammalian retina. I first describe a novel method I developed to load retinal cells with Ca^{2+} indicator dye using electroporation and show that retinas remain viable and responsive following electroporation. This technique was used to explore the excitatory role of D-serine at NMDARs and its potential inhibition of AMPA/kainate receptors using cultured retinal ganglion cells (RGCs) and isolated retina preparations. Using cultured RGCs I demonstrated that D-serine and glycine enhance NMDAR-mediated Ca^{2+} responses in a concentration-dependent manner and are equally effective as coagonists. In isolated retinas I showed that D-serine application enhanced NMDA-induced responses consistent with sub-saturating endogenous coagonist concentration. Degradation of endogenous D-serine reduced NMDAR-mediated Ca^{2+} responses supporting the contribution of this coagonist to NMDAR activation in the retina. Using imaging and two different electrophysiological approaches, I found that D-serine reduced AMPA/kainate receptor-mediated responses in cultured RGCs and isolated retinas at concentrations that are saturating at NMDARs. Antagonist experiments suggest that the majority of inhibition is due to D-serine acting on AMPA receptor activity. Degradation of endogenous D-serine enhanced AMPA/kainate-induced responses of some cells in isolated retina suggesting that, under these conditions, D-serine concentration may be sufficient to inhibit AMPA receptor activity. Overall, the work in this thesis illustrates the utility of electroporation as a method to load Ca^{2+}-sensitive fluorescent dyes into retinal cells and highlights the potential role for D-serine as a modulator of ionotropic GluRs in the CNS.

List of Abbreviations Used

a.u.	arbitrary units
ADAR	adenosine deaminase that acts on RNA
Asc-1	alanine-serine-cysteine transporter 1
GABA	γ-aminobutyric acid
AMPA	α-amino-3-hydroxy-5-methyl-4-isoxazoleproprionic acid
AMPAR	AMPA receptor
Ca^{2+}	calcium
CP-AMPAR	calcium-permeable AMPA receptor
CNS	central nervous system
7-Cl KYNA	7-chloro kynurenic acid
CNG	cyclic-nucleotide-gated
DAAO	D-amino acid oxidase
DAG	diacyl glycerol
DCKA	dichloro kynurenic acid
DsDa	D-serine deaminase
EC_{50}	effective concentration for half maximal response
EAAT	excitatory amino acid transporter
EPSC	excitatory postsynaptic current
GPCR	G-protein-coupled receptor
GCL	ganglion cell layer
GluR	glutamate receptor
GlyT-1	glycine transporter -1
HBSS	Hanks balanced salt solution
HEK	human embryonic kidney
HA-966	1-hydoxy-3-aminopyrrolid-2-one
INL	inner nuclear layer
IPL	innerplexiform layer
$[Ca^{2+}]_i$	intracellular calcium concentration
IP3	ionositol 1,4,5-triphosphate
iGluR	ionotropic glutamate receptor
KAR	kainate receptor
KYNA	kynurenic acid
LTP	long term potentiation
MEA	multi electrode arra
mGluR	metabotropic glutamate receptor
NMDA	N-methyl-D-aspartate
NMDAR	NMDA receptor
ONL	outer nucear layer

OPL	outer plexiform layer
PDE	phosphodiesterase
PSD	postsynaptic density
K^+	potassium
RGC	retinal ganglion cell
Na^+	sodium
ASCT	system alanine-serin-cysteine transporter
TTX	tetrodotoxin
TRP	transient receptor potential
TMD	transmembrane domain
vGluT	vesicular glutamate transporter
VGCC	voltage gated calcium channel
WCR	whole cell recording

Acknowledgements

Many people have contributed to my success as graduate student and have help to shape my development as a scientist and a person. I would love to thank you all, but my thesis would be twice as long.

Dr. William Baldridge. Your guidance, patience and willingness to put others before yourself is known throughout Dalhousie and the scientific community. It has been my privilege to work with you and know you personally during an MSc and PhD. Any success that I may achieve for the remainder of my scientific career will be a direct reflection of your excellent tutelage and unwavering enthusiasm. Your wonderful family has accepted my own into their lives and that will always be appreciated.

Drs. Steven Barnes, **David Clarke** and **Kazue Semba**. Thank you for your support and advice in serving as my advisory committee. You have always made yourselves available, not only during committee meetings, to address any questions and concerns I have had or just to talk about science, life or even music.

Dr. Robert Miller. It was a difficult time arranging a PhD defense, with many emails exchanged and dates constantly changed. Your patience and maintained enthusiasm is greatly appreciated. Thank you for making time to travel to the east coast to serve as my external examiner.

My Baldridge Lab Teammates. In particular, **Dr. Andrew Hartwick**, for showing me how to balance family and science, **Jianing Yu**, for your obvious love of science, **Stuart Trenholm**, for your constant need to learn and have fun, **Dr. Luis PdSM**, for being yourself and **Janette Nason** for your excellent technical assistance.

Past and present members of the Retina Lab. All of you have made the sometimes lonely world of research a pleasurable experience on a daily basis. Through collaborations with **John Vessey**, **Leah Wood** and **Dr. Francois Tremblay** and discussions with **Drs. Gautam Awatramani**, **Melanie Kelly** and **Balwantray Chauhan** I have been exposed to several areas of research I would not have encountered otherwise.

The Retina Lab Supertechnicians. **Michelle Archibald**, **Kelly Stevens** and **Christine Jollimore**. I am sure that I have solicited all of you for assistance for more than my fair share. I shall pay you in gratitude.

To the only other people that will likely read this thesis, the future students. Best wishes for your scientific endeavours.

Brothers, **Gerard**, **Carl** and **Damian.** For the endless encouragement and many laughs. Now let's go play some golf.

My beautiful wife, **Nicole**, and our crazy kids, **Breana**, **Marcus** and **Myles**. You are simply the best. I love you all.

Chapter 1: Introduction

The Retina

Vision is one of five faculties that allow us to perceive the outside world. Light is captured, converted to an electrochemical signal and organized into distinct pathways by the retina and sent to the brain for further processing. Although sometimes ignored when discussing the brain and spinal cord, the retina is indeed a part of the central nervous system (CNS). The retina is arguably one of the best morphologically and physiologically described CNS tissues due to its discrete layering and accessibility. It has been a model choice for the study of neuroscience for over a century and was used frequently by the legendary neuroscientist Santiago Ramón y Cajal.

The retina consists of three distinct neuronal layers, each with specific cell types that extend communicative processes that compile the two interspersed synaptic (plexiform) layers (Fig. 1.1). In the dark photoreceptors (rods and cones) in the outer nuclear layer (ONL) continuously release the excitatory neurotransmitter glutamate onto dendrites of horizontal cells and bipolar cells of the inner nuclear layer (INL). Photons of light are focused onto the retina, pass through all of its layers and are captured by the outer segments of photoreceptors leading to the closure of cyclic nucleotide gated (CNG) channels and subsequent reduction in glutamate release at synapses in the outer plexiform layer (OPL). In bipolar cells this generates two distinct pathways based on sign-conserving synaptic transmission via ionotropic glutamate receptors (iGluRs), the OFF pathway, and sign-inverting synaptic transmission via metabotropic GluRs (mGluRs), the

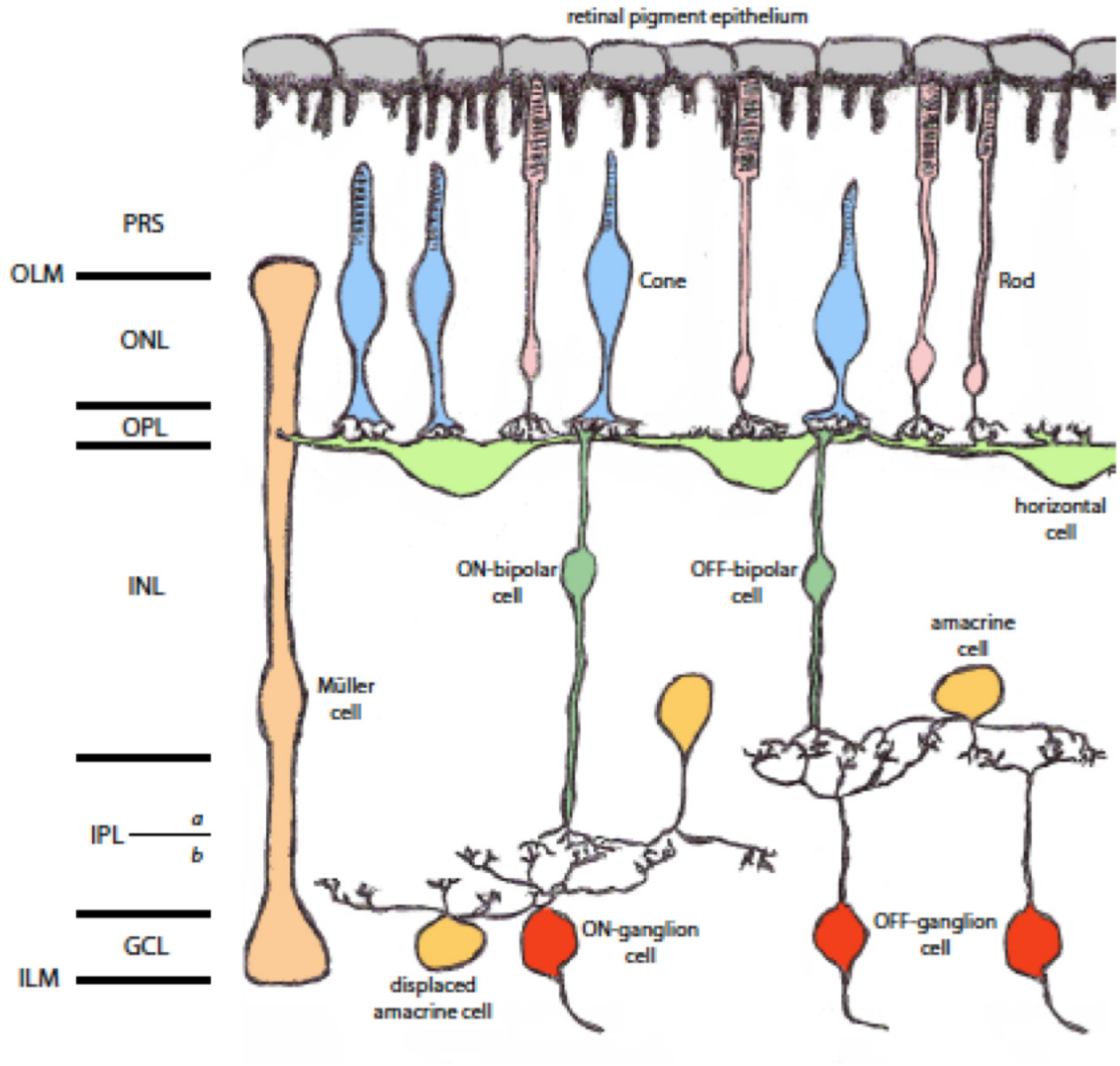

Figure 1.1 Schematic of the retina. Pigment epithelial cells line the posterior chamber of the eye adjacent to outer segments of the photoreceptors (PRS). The retina is divided in to 3 nuclear layers that contain the somata of the different neuronal constituents; the outer nuclear layer (ONL), the inner nuclear layer (INL) and the ganglion cell layer (GCL). Synaptic contacts between neurons of the ONL and the INL are made in the outer plexiform layer (OPL), while the inner plexiform layer (IPL) is where connections are made between neurons in the INL and GCL. Müller glial cells span almost the entirety of the retina and their most distal processes form the outer limiting membrane (OLM) and their proximal endfeet form the inner limiting membrane (ILM).

ON pathway. Bipolar cells in turn provide excitatory (iGluR-mediated) input to retinal ganglion cells (RGCs), at synapses within the inner plexiform layer (IPL) and RGC somata located within the ganglion cell layer (GCL), whose axons exit the back of the eye, becoming the optic nerve, and pass information on to visual and non-visual centers in the brain. The photoreceptor, bipolar cell, RGC pathway describes the "vertical pathway" of retinal processing. "Lateral pathways," involving horizontal cells (somata located in the INL) and amacrine cells (somata located in the INL and GCL), modulate the vertical pathway and are concerned with spatial and temporal aspects of the visual signal. Several excellent in depth reviews of retinal and visual processing are available (Masland, 2001b; Wassle, 2004; Sanes & Zipursky, 2010).

The work presented in this thesis comprises recordings from RGCs and amacrine cells of the GCL. Although the namesake of this layer is the output cell of the retina, so-called displaced amacrine cells account for > 50 % of its neuronal content in rodents (Jeon *et al*., 1998). Amacrine cells can be distinguished from RGCs because the average soma size is smaller and they do not have axons. Depending on the species under observation, and the techniques used to identify cell types, there are at least 10 distinct morphologically distinct RGC types with numbers ranging as high as 22 (for example Cajal, 1892; Masland, 2001b, a; Sun *et al*., 2002b, a; Volgyi *et al*., 2009). Similarly, approximately 20-40 morphologically defined amacrine cells have been identified (Young & Vaney, 1990; Strettoi & Masland, 1996; Masland, 2001a) across a number of species. Of these, at least 4-17 types are displaced amacrine cells (Perry & Walker, 1980; Wassle *et al.*, 1987; Perez De Sevilla Muller *et al.*, 2007). In general these retinal

neurons are categorized based upon soma size, dendritic arborization and positioning of the dendritic tree in the IPL.

The sheer variety of morphologically identifiable RGCs and amacrine cells implies that there must be some function associated with this form. Indeed, in every cell type that has also been probed physiologically there are distinctions that solidify the classifications. Ganglion cells are broadly classified into two physiological types, ON-center and OFF-center RGCs, which are segregated at the first retinal synapse by differential GluR expression on bipolar cells. ON-center cells respond with an increased action potential firing rate at light onset to a spot of light positioned over the center of their receptive-field and a reduced firing rate when the surround is stimulated. OFF-center RGCs respond in the opposite fashion to the same stimuli. Morphologically, this distinction is clearly seen because the IPL consists of five lamina and the dendrites of ON-center cells stratify in the three layers closer to the GCL, sublamina *b*, while OFF-center cell dendrites stratify in the two layers closer to the INL, sublamina *a* (see Fig. 1.1). Other RGCs are bistratified with dendrites in both sublaminae resulting in ON-OFF cells. Interestingly, at least two ON-center RGCs receive ON inputs in sublamina *a* via *en passant* synapses from ON cone bipolar cells (Hoshi *et al*., 2009).

Morphologically identified amacrine cell types can also be distinguished physiologically based upon the retinal circuits in which they are involved. Like RGCs, different amacrine cells have processes that terminate in specific laminae of the IPL and these have been assigned to unique retinal circuits. For example, the A17 is a wide-field (> 500 μm dendritic diameter) amacrine cell that receives excitatory inputs from rod bipolar cells (in sublamina *b*) and provide inhibitory input to the same and other rod

bipolar cells (Menger & Wassle, 2000; Chavez *et al.*, 2010). One of the best characterized amacrine cell, the AII amacrine cell, is a narrow-field (dendritic spread of 30-70 μm), bistratified cell with dendrites in sublamina *a* and *b* (Kolb & Famiglietti, 1974; Vaney *et al.*, 1991). The AII receives input from rod bipolar cells in sublamina *b* and provides input to cone bipolar cells in sublamina *a*. AII cells are electrically coupled to one another as well as to ON-cone bipolar cells allowing rod signals to be transmitted by the ON cone pathway. AII cells contain glycine and release this inhibitory neurotransmitter to allow rod signals to pass to the OFF cone pathway.

Amacrine cells are typically inhibitory interneurons, modulating synaptic transmission from bipolar to ganglion cells. Identification of the neurotransmitter(s) and neuromodulator(s) that they release provides another method to physiologically define them. By far the most abundant neurotransmitters released by amacrine cells are glycine and γ-aminobutyric acid (GABA). Approximately 40-50% of amacrine cells, typically narrow-field cells, contain glycine and at least half of those express glycine transporter-1 (GlyT-1; Menger *et al.*, 1998; Shen & Jiang, 2007; Wassle *et al.*, 2009). Similarly, an additional ~40% of amacrine cells are GABA-ergic (Vaney, 1990; Marquardt *et al.*, 2001) and are predominantly wide-field cells. Although other neuroactive substances, such as dopamine and acetylcholine, are found colocalized with or independent of glycine and GABA, theses inhibitory neurotransmitters account for up to 90% of amacrine cells.

Glutamate Receptors

The amino acid L-glutamic acid (glutamate) is the primary excitatory neurotransmitter in the central nervous system (CNS). Although it was identified and

proposed as such in the 1960's (Krnjevic & Phillis, 1963) this has only really been fully accepted for approximately the past 25 years. It is by far the most abundant neurotransmitter found in the CNS (Fonnum, 1984; Moriyama & Yamamoto, 2004) in part because it is also a source of the primary inhibitory neurotransmitter GABA, synthesized by glutamate α-decarboxylation. Given its ubiquity it is not surprising that dysfunctions in glutamatergic neurotransmission lead to severe deficits and clinical manifestations. There are two main classes of glutamate receptors (GluRs), metabotropic and ionotropic (Table 1.1), both of which are found in the retina.

Metabotropic GluRs (mGluRs) are family C, 7 transmembrane domain, G-protein-coupled receptors (GPCRs) that have a large N-terminal extracellular domain where the glutamate binding site is located (Conn & Pin, 1997). There are eight different types of mGluRs (1-8) that are further categorized into three groups based on sequence homology and their signaling cascade (Conn & Pin, 1997). Group I mGluRs (1, 5) are coupled to G_q/G_{11} and activation leads to stimulation of phospholipase C, and in some cases adenylyl cyclase, and subsequent calcium (Ca^{2+}) mobilization due to the generation of inositol 1,4,5-trisphosphate (IP_3) and diacylglycerol (DAG). Group II (2, 3) and group III (4, 6, 7, 8) mGluRs couple $G_{i/o}$ and inhibit adenlyl cyclase as well as modulate specific ion channels such as potassium (K^+) and voltage gated calcium channels (VGCC). For a comprehensive review of mGluRs see Niswender and Conn (2010).

More widely known are the ionotropic glutamate receptors (iGluRs) that mediate fast excitatory neurotransmission (Table 1.1). The three types of iGluRs, α-amino-3-hydroxy-5-methyl-4-isoxazoleproprionic acid (AMPA), kainate and N-methyl-D-aspartate (NMDA) receptors are so named based upon their different preferential full

agonist. Glutamate, or glutamate receptor agonist, binding leads to the influx of sodium (Na^+), K^+ and Ca^{2+} (depending on the receptor) ions through the channel pore causing a depolarization of the cell. If sufficient the resultant change in membrane potential can cause the opening of voltage-gated Na^+ and Ca^{2+} channels leading to the generation of action potentials and further Ca^{2+} influx, respectively. The work in this thesis has incorporated several techniques to look at theses three properties of GluR activation. Calcium imaging was used to directly measure changes in intracellular Ca^{2+} concentration ($[Ca^{2+}]_i$), patch clamp electrophysiology was used to measure changes in whole-cell currents and multi-electrode array recordings were used to measure spiking activity. There are a multitude of excellent reviews on glutamate receptors (for example Hollmann & Heinemann, 1994; Nakanishi *et al.*, 1998; Thoreson & Witkovsky, 1999; Mayer, 2005).

Over the past decade there has been a slow change to adopt a new GluR nomenclature that better reflects iGluR subunits. To date my own writings have employed the old nomenclature, but in this thesis I used the new nomenclature as outlined by The International Union of Pharmacology Committee on Receptor Nomenclature and Drug Classification (NC-IUPHAR; see Collingridge *et al*., 2009).

Non-NMDA iGluRs, AMPA receptors (AMPARs) and kainate receptors (KARs) are often considered together because together they drive fast excitatory transmission. The four AMPAR subunits, GluA1-4 (formerly GluR1-4), are encoded by distinct genes (*GRIA1-4*). The preferred agonist, AMPA, is extremely specific for AMPARs versus other GluRs. Each subunit can form functional homotetramers in expression systems (Keinanen *et al*., 1990), however, *in vivo*, AMPAR-gated channels are mostly

Table 1.1

Ionotropic Glutamate Receptors

Receptor	Subunit	Former name	Gene
AMPA	GluA1$_{flip/flop}$	GluR1	*GRIA1*
	GluA2$_{flip/flop}$	GluR2	*GRIA2*
	GluA3$_{flip/flop}$	GluR3	*GRIA3*
	GluA4$_{flip/flop}$	GluR4	*GRIA4*
Kainate	GluK1	GluR5	*GRIK1*
	GluK2	GluR6	*GRIK2*
	GluK3	GluR7	*GRIk3*
	GluK4	KA1	*GRIK4*
	GluK5	KA2	*GRIK5*
NMDA	GluN1$_{1a-4a/1b-4b}$	NR1	*GRIN1*
	GluN2A	NR2A	*GRIN2A*
	GluN2B	NR2B	*GRIN2B*
	GluN2C	NR2C	*GRIN2C*
	GluN2D	NR2D	*GRIN2D*
	GluN3A	NR3A	*GRIN3A*
	GluN3B	NR3B	*GRIN3B*
Orphan	GluD1	GluRδ1	*GRID1*
	GluD2	GluRδ2	*GRID2*

**Subscript text indicates relevant splice variants*

heterotetramers consisting of GluA1/2 or GluA2/3 (Wenthold *et al*., 1996), although not necessarily present in equal amounts. For example, the use of conditional knockouts in a small population of CA1 neurons in hippocampus has enabled the quantification of GluA1- versus GluA3- containing synaptic AMPARs (81 and 16%, respectively; Lu *et al*., 2009). There are five KAR subunits, GluK1-5 (formerly GluR5-7, KA1-2) encoded by distinct genes (*GRIK1-5*). The preferred agonist, kainate, activates both kainate and AMPA receptors, even though it has weak affinity for the latter. Specific antagonists for KARs have been lacking and therefore our knowledge of KAR physiology has been largely restricted to studies using expression systems (see Jane *et al*., 2009). Similar to AMPARs, GluK1-3 subunits can all form functional homotetrameric receptors, although homomeric GluK3 receptors have a 2-3 fold greater EC_{50} (effective concentration for half-maximal response) for most GluR agonists (Schiffer *et al*., 1997). On the other hand GluK4 and 5 do not form functional receptors under homomeric expression. Functional evidence from hippocampus and striatum suggest that KARs are physiologically expressed as heterotetramers containing GluK1/5, GluK2/5 or GluK1/2 (Chergui *et al*., 2000; Mulle *et al*., 2000; Christensen *et al*., 2004).

There at least four distinctions between AMPA and kainate receptors, in addition to sequence homology, highlighting their differences despite the fact that they are so often considered together. First, there are clear differences in the kinetics of AMPAR- and KAR-mediated components of excitatory postsynaptic currents (EPSCs). Relative to AMPARs, the KAR-mediated portion of the EPSC is slow (Castillo *et al.*, 1997; Vignes *et al.*, 1997; Vignes & Collingridge, 1997), displaying a delayed activation and prolonged decay (Bureau *et al*., 2000). Second, each AMPAR subunit has two splice variants

termed *flip* and *flop* due to alternative splicing of the extracellular binding domain. While some GluK subunits are subject to alternative splicing it affects only trafficking and regulation as opposed to channel activity (Pinheiro & Mulle, 2006). In general, the *flop* isoforms of GluA2-4 desensitize much faster than their *flip* counterparts, but there is no difference in desensitization rate when comparing the GluA1 isoforms (Mosbacher *et al*., 1994). Related are findings that GluA2 and 3 *flop* versus *flip* variants have a faster channel closure while there is no difference between GluA1 channel closure times (Pei *et al*., 2007; Pei *et al*., 2009). Throughout the CNS these isoforms are expressed differentially with respect to cell type and developmental stage. In the adult mouse retina GluA mRNA has been identified in all major classes of neurons, except photoreceptors, with the *flop* isoform predominating greatly. However, in ganglion cells there is near equal expression of GluA3 *flip* and *flop* mRNA (Jakobs *et al*., 2007). In rat brain [^{3}H]-AMPA binding studies show that GluA1-3 *flip* is mostly expressed prenatally and *flop* postnatally (Standley *et al*., 1995). In the developing mouse retina *flop* versus *flip* mRNA is expressed at a ratio of 2:1 for all GluAs at postnatal day 8 (P8; Namekata *et al*., 2006). This ratio increases to ~13:1 for GluA1 by P40 and remains unchanged for the other subunits while the total mRNA for each subunit decreases (Harada *et al*., 1998; Namekata *et al*., 2006). Considering that GluA1 *flip* and *flop* are similar with respect to desensitization rate and channel closure, it is unclear what influence this change might have on retinal synaptic physiology.

A third notable difference between AMPARs and KARs is that the latter requires external monovalent ions bound to the receptor to function. In the absence of external ions GluK2-containing outside-out patches were completely unresponsive to glutamate

puff application while GluA1-containing patches responded normally (Wong *et al*., 2006). A single amino acid residue at position 770, methionine (Met 770) for GluK2 and lysine for GluA1, was identified as a potential candidate for this difference (Paternain *et al*., 2003). Mutant GluK2 subunits, with a substituted lysine, restored channel functioned in the absence of external ions (Wong *et al*., 2006). Further work identified that anions and cations bind at distinct sites in a binding pocket containing Met 770 and are coupled together stabilizing the dimer interface of GluK2 subunits (Plested & Mayer, 2007; Wong *et al.*, 2007; Plested *et al.*, 2008). However, the role ion co-activation plays in the modulation of KAR activity is unclear given that the external ionic concentration is normally within a range that should have little influence on receptor activation.

Finally, depending on post-transcriptional modifications and subunit expression, both AMPARs and KARs can be calcium-permeable or relatively -impermeable. Amino acid 607, in transmembrane domain (TMD) II, of GluA2 normally contains a glutamine residue (Q) but is commonly an arginine (R) residue in the case of neuronal expression (see Palmer *et al*., 2005) due to nuclear RNA-editing. The so-called Q/R editing site is accessible to RNA-specific adenosine deaminase (ADAR) 2 that acts on mRNA and converts adenosine to inosine (Sommer *et al*., 1991). Homomeric or heteromeric channels formed with unedited GluA2 and GluA1, 3 and 4 are permeable to divalent cations and have inwardly rectifying I/V curves. However inclusion of a single edited GluA2 subunit yields a channel with lower conductance, that is not permeable to divalent cations and is linear or slightly outwardly rectifying (Hume *et al*., 1991). Similarly, GluK1 and 2 are subject to Q/R editing by ADAR1 that contributes to their divalent cation permeability and current rectification. They are also subject to editing on TMD I

that, in concert with Q/R editing, also influences divalent cation permeability (Kohler *et al*., 1993). In general, animal models have shown > 99% of GluA2 is of the edited form (Sommer *et al*., 1991; Christensen *et al*., 2000) so that the presence of GluA2 alone is sufficient to indicate that an AMPAR is calcium-impermeable. Alternatively, there is greater variability of editing concerning GluK1 and 2 with estimates ranging form 30-60% and 70-90% edited, respectively (Belcher & Howe, 1997; Bernard *et al.*, 1999; Christensen *et al.*, 2000). In human grey matter similar numbers are reported for edited GluA2, GluK1 and GluK2 but in white matter (oligodendrocyte expression) there is substantially less Q/R editing (Kawahara *et al*., 2003). Since a given neuron may express calcium-permeable and impermeable AMPA and KA receptors it can be difficult to delineate what their respective roles are. Much more is known about calcium-permeable AMPARs (CP-AMPARs) because there are multiple antagonists specific for CP-AMPARs.

The NMDAR-gated channel is a tetrameric or pentameric structure that is formed by heteromeric subunits and there are 7 genes (*GRIN1, 2A-D, 3A-B*) that encode each subunit. The GluN1 subunit, formerly NR1, is an absolute requirement for a functional NMDAR channel (Meguro *et al*., 1992) and 8 splice variants have been identified ($GluN1_a$-4_a and $GluN1_b$-4_b). These splice variants are involved in different aspects of the NMDAR life cycle including assembly and membrane insertion (Stephenson *et al*., 2008). Homomeric expression of GluN1 form functional NMDARs that respond weakly to glutamate and other appropriate agonists (Moriyoshi *et al*., 1991). However, when co-expressed with other NMDAR subunits currents are greatly potentiated (Kutsuwada *et al*., 1992; Meguro *et al*., 1992). Four isoforms of the GluN2 subunit, formerly NR2,

(GluN2A-D) have been cloned (Ikeda *et al*., 1992; Monyer *et al*., 1992) and the kinetic properties of NMDAR channels vary depending on which of these is expressed. For example, the efficacy of glutamate increases incrementally from GluN2A, EC_{50} = 1.7 μM, through to GluN2D, EC_{50} = 0.4 μM (see Hollmann & Heinemann, 1994). Similarly, brief (1 ms) glutamate application show that the deactivation time course for GluN1/N2A was ~50 ms, for GluN2B or C-containing was ~ 280 ms and for GluN2D-containing was nearly 2 sec (Vicini *et al*., 1998). Splice variants have also been identified for GluN2 and 3 but it is unclear what physiological function they serve (Rafiki *et al*., 2000; Cull-Candy *et al*., 2001).

There are two GluN3 subunits (formerly NR3), GluN3A and B, and they have a lower expression throughout the CNS than all other subtypes. Like GluN2 they do not assemble into functional homotetramers. Instead they form channels with GluN1/N2 and these channels have a lower unitary conductance than GluN1/N2 alone (Ciabarra *et al*., 1995; Das *et al*., 1998). While GluN3A is expressed throughout the CNS (Ciabarra *et al*., 1995; Wong *et al*., 2002) GluN3B is relatively restricted to motoneurons (Chatterton *et al*., 2002), although it is also expressed in other brain areas (Wee *et al*., 2008). Interestingly, either GluN3 subunit can form functional channels with GluN1 that are excited by glycine and unaffected by glutamate or NMDA when expressed in *Xenopus* oocytes (Chatterton *et al*., 2002; Awobuluyi *et al*., 2007). The GluN3A subunit was shown to have a high affinity for glycine (K_d = 40 nM) and a low affinity for glutamate (K_d = 9.8 mM) and accordingly glutamate binding to GluN1 was absent even at 300 mM (Yao & Mayer, 2006; similar results reported by Nilsson *et al.*, 2007). In cultured hippocampal neurons glycine could not elicit GluN3-mediated responses and the authors

posited that excitatory glycine NMDARs do not occur in neurons (Matsuda *et al*., 2003). Recently excitatory glycinergic Ca^{2+} responses were elicited from CNS myelin and were absent in GluN3A knockout animals (Pina-Crespo *et al*., 2010). These findings suggest that the GluN1/N3 NMDAR may indeed have a physiological role that may be restricted to non-neuronal elements.

There are several modulatory sites directly located on NMDARs that govern its capacity to function as an ion channel (see McBain & Mayer, 1994). Within the channel pore a divalent cation binding site is occupied by a magnesium ion (Mg^{2+}) at transmembrane potentials more negative than -40 mV. This "Mg^{2+} block" is relieved in a voltage-dependent manner as the cell is depolarized, with maximal relief occurring at potentials between -40 and -30 mV (Nowak *et al*., 1984). Due to the influence of the Mg^{2+} block, studies of NMDARs are often performed under conditions that minimize extracellular Mg^{2+}. Another binding site on the NMDAR is the so-called "glycine" binding site that must be occupied when glutamate binds in order for the channel to be activated (Kleckner & Dingledine, 1988). NMDA currents have been identified in the absence of a co-agonist (Moriyoshi *et al*., 1991; Yamazaki *et al*., 1992b) but trace amounts of glycine found in experimental solutions may account for this discrepancy.

One of the most remarkable and defining features of NMDAR channels are their high permeability to Ca^{2+}. It is this property that seems to be key to the involvement of NMDARs in processes such as long term potentiation (LTP; Harris *et al*., 1984), synaptogenesis (Constantine-Paton & Cline, 1998) and glutamate excitotoxicity (Sucher *et al*., 1997). While other GluRs can also allow Ca^{2+} influx, it is significantly greater through NMDAR channels, with the exception of the GluN1/N3 excitatory glycine

channel. For example the ratio of divalent to monovalent cation permeation for NMDARs relative to CP-AMPARs is more than four-fold greater (Hollmann & Heinemann, 1994). Furthermore NMDAR channels are more selective for the species of divalent cation that can pass through the pore (Ca^{2+}, barium, cadmium but not Mg^{2+}, cobalt or nickel) whereas CP-AMPA and –KA receptors pass both Ca^{2+} and Mg^{2+}. Mutagenesis studies revealed that it is the Q/R editing site (like AMPA and KA receptors) that governed divalent cation permeability. NMDAR subunits, with the exception of GluN3, have an asparagine (N) at this site leading to high Ca^{2+} permeability and selectivity over Mg^{2+} (Hume *et al*., 1991; Burnashev *et al*., 1992). The adjacent N residue (N+1), particularly on GluN2 subunits, is responsible for the voltage-dependence associated with Mg^{2+} (Wollmuth *et al*., 1998). Alternatively GluN3 subunits have a glycine at the Q/R site and an arginine at N+1 thus accounting for their lowered Ca^{2+} permeability and resistance to the Mg^{2+} block (Matsuda *et al*., 2002). I find it truly extraordinary that a single amino acid can account for many of the differences that distinguish iGluRs.

The least well-characterized GluRs are the 'Orphan' delta receptors, GluD1 and 2 (formerly GluRδ1 and 2), so-called as it is unknown what activates them, that are encoded by the genes *GRID1* and *GRID2*. The GluDs were identified based on their sequence homology with the GluAs (17-28%). GluD1 has low expression throughout the brain during development and is more restricted to the hippocampus and cochlear inner hair cells in adulthood (Lomeli *et al*., 1993; Gao *et al*., 2007) while GluD2 has high expression in Purkinje cells of the cerebellum (Yamazaki *et al*., 1992a; Lomeli *et al*., 1993). Interestingly, human embryonic kidney (HEK) 293 cells expressing GluDs do not

respond to glutamate, AMPA or kainate nor do they bind tritiated GluR agonists (Lomeli *et al*., 1993; Mayat *et al*., 1995). When coexpressed with other GluRs there is no alteration in receptor properties compared to when GluD is absent. However, GluD2 knockouts show abnormalities such as reduced muscle coordination, impaired long-term depression and Purkinje cell synapse formation indicating that they must be integrally involved in the motor system (Hirano *et al*., 1995; Kashiwabuchi *et al*., 1995). Similarly, the recent GluD1 knockout show reduced hearing at high frequency but surprisingly no apparent difference in hippocampal physiology, such as LTP and synaptic transmission (Gao *et al*., 2007).

Glutamate Neurotransmission in the Retina

To identify the role of glutamate in the distinct circuits in the retina pharmacological manipulation of physiological recordings and the identification of GluR mRNA/protein expression have been employed. Many studies have identified the cellular localization of GluRs in the retina and all subtypes have been reported across a wide variety of species. It is clear that GluR expression is heterogeneous, as would be expected given the multitude of cell types in the retina, but it has been difficult to match specific receptor and neuronal subtypes. Localization studies have provided a good overview of GluR expression between major classes of retinal cells and the different retinal layers and physiological recordings have enabled more precise classifications of distinct circuit elements.

Photoreceptors are light responsive neurons and thus would not necessarily be expected to receive glutamatergic excitatory input. However, they do express some

functional GluRs that may modulate their activity. For example, mGluR8 expression at photoreceptor terminals could modulate the release of glutamate onto bipolar cells and horizontal cells (Koulen *et al*., 1999). GluA2/3 expression has been identified in photoreceptors of fish, frog, turtle and guinea pig (Peng *et al*., 1995; Vandenbranden *et al*., 2000; Vitanova, 2007a, b) and not in rat or mouse (Hack *et al*., 2001; Jakobs *et al*., 2007), but the role that they might play is unclear. Kainate receptor mRNA (GluK1, 2 and 5) is expressed in mouse rods (Jakobs *et al*., 2007) and GluK 2/3 subunits are expressed on rods terminals in primate retina (Harvey & Calkins, 2002). Glutamate activation of these receptors could serve to keep terminals depolarized to maintain release (as suggested by Harvey and Calkins) or serve in a modulatory capacity given the metabotropic-like effects that can be attributed to KARs (see Rodriguez-Moreno & Sihra, 2007). The GluN1 subunit has been identified on photoreceptor terminals (Fletcher *et al*., 2000) but presumably is not functional because other NMDAR subunits have not been found nor did NMDA affect photoreceptor $[Ca^{2+}]_i$ (Koulen *et al*., 1999).

Postsynaptic to photoreceptors glutamate acts at three cell types, horizontal cells, OFF-center bipolar cells and ON- center bipolar cells, each with distinct patterns of GluR expression. Horizontal cells respond to glutamate in a sign conserving fashion, predominantly expressing GluA2/3, GluK2/3 and to a lesser extent GluA1/4 (Peng *et al*., 1995; Brandstatter *et al*., 1997). Functionally, the specific AMPAR antagonist GYKI 52466 almost completely blocks glutamate-induced and light-evoked horizontal cell currents (the latter by hyperpolarizing the cell) suggesting that AMPARs are the preferred receptor (Yang *et al*., 1998). A typical cone synapse involves three invaginating post-synaptic processes with a central bipolar cell dendrite and a horizontal cell dendrite on

either side (termed a triad). Ultrastructural evidence indicates that GluK2/3 expression predominantly occurs in only one of the two horizontal cell processes (Brandstatter *et al*., 1997). Furthermore, nearly all horizontal cells contain CP-AMPARs and these contribute greatly to the glutamate-evoked current (Sun *et al*., 2010).

OFF-center bipolar cells are also sign conserving in their response to glutamate. Jakobs and colleagues (2007) showed iGluR mRNA expression of predominantly GluA1, GluK1, GluK5 and GluN1 in mouse, with no distinction by bipolar cell type. The GluN1 expression probably does not correspond to functional NMDAR since other subunits were not identified, which is consistent with the predominant view that there are no NMDAR channels on bipolar cells. An elegant study by Steve DeVries (2000) illustrated that three different OFF-center bipolar cells were almost exclusively driven by synaptically-activated AMPARs or KARs depending on the subtype. This allows OFF-center bipolar cells to process temporal information differentially because, as discussed previously, AMPAR exhibit a faster activation/inactivation time course than do KARs. Synaptic terminals of OFF-center bipolar cells likely express group III mGluRs that act as autoreceptors to regulate glutamate release. As glutamate release from OFF-center bipolar cells was increased, increased mGluR III activation acted to reduce release (Awatramani & Slaughter, 2001), likely in order to keep RGC activity within a specified operating range.

There is evidence for the expression of multiple mGluRs by many retinal neurons. For example, amacrine and ganglion cells express receptors from all mGluR groups (Hartveit *et al.*, 1995; Koulen *et al.*, 1997; Tehrani *et al.*, 2000; Koulen & Brandstatter, 2002) although there is little data suggesting specificity of mGluR type by cell type. The

best characterized mGluR in the retina is mGluR6 expressed by ON-center bipolar cell dendrites and under normal conditions thought to be unique to the retina (Nakanishi *et al*., 1998). Photoreceptors continuously release glutamate in the dark and release is reduced in the light. The problem of converting the reduction of an excitatory drive to an excitation of bipolar cells is resolved by the neuronal inhibition achieved by mGluR6 activation. Experimentally we know that mGluR6 activation selectively reduces ON-center bipolar light evoked responses (Slaughter & Miller, 1981) suggesting that glutamate binding to mGluR6 functionally inhibits cells. However, the mechanism that governs this inhibition has remained elusive. Initially, it was thought that mGluR6 binding led to the closure of a cyclic-nucleotide-gated (CNG) channel via phosphodiesterase (PDE)-induced reduction of cyclic guanosine monophosphate (cGMP), but PDE and CNG channels have not found associated with bipolar cell dendrites (Wassle *et al*., 1992). Within the past 2 years the transient receptor potential M1 (TRPM1) channel has been identified as the non-selective cation channel associated with the mGluR6 cascade (Morgans *et al*., 2009; Shen *et al*., 2009; Koike *et al*., 2010). Several reports have identified iGluR (particularly AMPAR) expression in rod- and cone-driven ON-bipolar cells (Peng *et al.*, 1995; Kamphuis *et al.*, 2003b; Huang *et al.*, 2004; Hanna & Calkins, 2007), which may seem counterintuitive since it would oppose mGluR6 activity. In rat approximately 75% of ON-bipolar cells under investigation co-expressed mGluR6 and GluA2, plus other GluAs to a lesser extent, with similar quantification of genetic expression (Kamphuis *et al.*, 2003a).

The major commonality between the plethora of amacrine cells types is the glutamatergic excitatory drive that they receive from bipolar cells. Combined, they

express all GluRs types, but one division is seen based on whether input comes from rod- or cone-driven bipolar cells. Amacrine cells within the cone pathway express GluN1, 2A and 2B but those associated with the rod pathway do not express NMDARs (Fletcher *et al*., 2000). Interestingly, a clear example of the intricacy of specific GluR expression with respect to cell type lies in the reciprocal and lateral feedback circuits involving amacrine and rod bipolar cells. The A17 amacrine cell receives excitatory inputs from rod bipolar cells driven almost exclusively by AMPARs and provides feedback onto rod bipolar cells (reciprocal feedback) via GABA (Hartveit, 1999; Menger & Wassle, 2000). Work from Jeffrey Diamond's laboratory convincingly showed that Ca^{2+} influx through CP-AMPARs, not VGCCs, amplified by Ca^{2+} induced Ca^{2+} release (CICR) lead to the release of GABA on to rod bipolar cells (Chavez *et al*., 2006). To my knowledge CP-AMPAR-mediated neurotransmitter release is, so far, unique to the retina. A recent report from the same group identified a similar phenomenon in other amacrine cells involved in lateral feedback to rod bipolar cells (Chavez *et al*., 2010). However, unlike the A17 circuit CP-AMPARs were not the sole source of Ca^{2+} entry.

Ganglion cells receive glutamatergic input from bipolar cells and express the widest variety of GluRs within the retina. This has made it extremely difficulty to ascribe specificity between receptor subtype and RGC-type. Many expression studies cannot or do not determine the precise cellular location of the receptor subunit. Physiological recordings have helped to identify synaptic vs. extrasynaptic localization but are typically limited to identifying between the 3 main iGluR types. Cultured RGCs express all iGluRs as evidenced by kainate-, AMPA- and NMDA-evoked currents and calcium responses (Aizenman *et al*., 1988; Taschenberger *et al*., 1995; Mukai *et al*., 2002;

Hartwick *et al*., 2004). Electrophysiological studies demonstrate that the story is complicated at the synaptic level. At many synapses in the CNS AMPARs mediate a fast component of the postsynaptic response (i.e. an EPSC) while NMDARs mediate a slow component (Hestrin *et al*., 1990; Perkel *et al*., 1990; Silver *et al*., 1992). In ganglion cells AMPAR almost exclusively mediate the non-NMDA iGluR component of the evoked EPSCs (Lukasiewicz *et al.*, 1997; Chen & Diamond, 2002) and most, but not all, of the synapses onto individual RGCs contain GluA2/3 (Jakobs *et al*., 2008). Several studies have shown an NMDAR-mediated component of evoked RGC EPSCs (Diamond & Copenhagen, 1993; Taylor *et al.*, 1995; Chen & Diamond, 2002), however, spontaneous EPSCs (sEPSCs) do not (Taylor *et al.*, 1995; Chen & Diamond, 2002). Whole-cell patch recordings combined with postembedding immunogold electron microscopy demonstrated that the GluN2A with GluN1-1/2 subunits were predominantly located at the postsynaptic density (PSD) of OFF-ganglion cell dendrites while GluN2B with GluN1-3/4 were found outside the PSD of ON-ganglion cell dendrites (Zhang & Diamond, 2009). While differential GluN1 splice variant expression can occur in a use dependent manner (Mu *et al*., 2003) this was the first report of segregation of GluN1 and GluN2 isoforms at parallel synapses. These findings highlight some of the similarities and uniqueness of retinal circuitry and the rest of the CNS.

Glutamate synthesis and recycling in neurons can occur via glutamic acid dehydrogenase from α-ketoglutarate, aspartate aminotransferase from apsartate and glutaminase from glutamine, all of which are expressed in photoreceptors and Müller cells. Inhibition of glutaminase, *in vivo*, leads to significantly reduced bipolar cell activity (Barnett *et al*., 2000; Bui *et al*., 2009) indicating that glutamine accounts for most

glutamate production. Since activity is not completely abolished Bui and colleagues (2009) suggest that α-ketoglutarate and aspartate/alanine must also be involved. There are three vesicular glutamate transporters (vGluTs), vGluT1-3, that package glutamate into vesicles for synaptic release. The retina displays some differential expression of vGluTs as photoreceptor and bipolar cell terminals predominantly contain vGluT1, while ~10% of cones express vGluT2 (Wassle *et al*., 2006). The only cells to express vGluT3 are a small group of glycinergic amacrine cells, accounting for approximately 1% of all amacrine cells (Haverkamp & Wassle, 2004; Johnson *et al.*, 2004). Lastly, ganglion cell somas only express mRNA for vGluT2 (Mimura *et al*., 2002) and correspondingly RGC terminals express the vGluT2 protein (Fujiyama *et al*., 2003). Glutamate release is Ca^{2+}-dependent, typically due to depolarization-induced Ca^{2+} influx through VGCC. After release it is rapidly cleared from the extracellular space by high-affinity sodium-dependent excitatory amino acid transporters (EAATs). There are 5 transporters, EAAT1-5, and only EAAT 4 has not been identified in the retina. Only Müller cells express EAAT1 (or GLAST) and the other EAATs are found in several different retinal neurons and contribute to glutamate clearance (Rauen *et al*., 1998; Wiessner *et al*., 2002; Rowan *et al*., 2010). The majority of glutamate transport occurs through EAAT1 into Müller cells (Barnett & Pow, 2000) where glutamate is rapidly convert into glutamine via glutamine synthase (Derouiche & Rauen, 1995) and glutamine is shuttled back to neurons where it is converted back to glutamate, thus completing the glutamate/glutamine cycle.

Identification of the NMDAR 'Glycine' Binding Site

Throughout the 1980's there were reports that suggested that the neurotransmitter glycine might have a second role in the CNS. Glycine is a well-characterized inhibitory neurotransmitter in the CNS and binds to glycine receptors that can be blocked by the high-affinity competitive antagonist strychnine. The first solid indication of an alternative action of glycine came from a receptor autoradiography study where Bristow and colleagues (1986) showed two distinct [^{3}H]-glycine ligand binding patterns in the rat brain. One pattern corresponded to the strychnine-sensitive receptor and the other, more widespread, was strychnine-insensitive. Notably, the second binding site was remarkably similar to the pattern of [^{3}H]-glutamate binding to NMDARs (Monaghan & Cotman, 1985). The seminal work of Johnson and Ascher (1987) demonstrated, using whole-cell patch clamp recording from mouse cortical cell cultures (neurons and glia), that NMDA-induced currents were enhanced when superfusion rates were reduced. They correctly deduced that an excitatory factor must be released by some element in the culture that was washed away when superfusion was rapid. Subsequent experiments led them to screen amino acids as candidates, based on size criteria, for the unknown factor and determined that glycine (and to a lesser extent D-serine and D-alanine) could reproduced the effect of slow superfusion. Strychnine did not prevent the excitatory effect of glycine suggesting that it was acting at the unknown site identified by the aforementioned radioligand study. Outside-out patches from the cultured cortical neurons revealed that glycine enhanced NMDA currents by increasing the channel open frequency but not mean open time (Johnson & Ascher, 1987). The following year Kleckner and Dingledine's (1988) report that glycine was an absolute requirement for NMDAR

activation gave credence to the possibility that the potentiating effect of glycine was of physiological relevance.

Glycine was also shown to enhance NMDAR activity by an apparent reduction of desensitization of the receptor by allosteric modulation. Using a fast drug delivery system it was identified that NMDA- and AMPA-induced currents underwent significant desensitization (with slow and fast time-courses, respectively) and kainate-induced currents did not (Mayer & Vyklicky, 1989). Extending these findings the same group demonstrated that not only did glycine enhance the peak NMDAR-mediated current, as was already known, but it had a considerable effect on NMDAR desensitization and in a concentration-dependent manner (Mayer *et al*., 1989). Interestingly, it was determined that NMDA binding led to a decreased affinity for glycine, which was pre-equilibrated, and increasing concentrations sufficiently overwhelmed this change (Benveniste *et al*., 1990). Together with a companion paper from the same group (Vyklicky *et al*., 1990) the authors suggest that glycine is obligate for NMDARs (as previously reported Kleckner & Dingledine, 1988) and negative cooperativity between the glutamate and glycine binding site govern agonist occupancy. Similarly, the glycine binding site partial agonist, 1-hydoxy-3-aminopyrrolid-2-one (HA-966), reduced NMDAR glutamate affinity indicating that the allosteric interaction is reciprocal (Kemp & Priestley, 1991; Lester *et al.*, 1993).

Although unconfirmed, it was widely accepted that glycine bound directly on NMDARs at a distinct site from glutamate. Preliminary evidence for this existed in that (1) rat brain mRNA expressed in *Xenopus* oocytes required glycine to elicit NMDA-induced currents (Kleckner & Dingledine, 1988), (2) [^{3}H]-glycine binding mimicked [^{3}H]-glutamate binding to NMDARs (as described above), (3) [^{3}H]-glycine, [^{3}H]-TCP

and [^{3}H]-glutamate all bound to a protein (NMDAR subunit) of approximately the same molecular weight (Honore *et al*., 1989) and (4) the above mentioned negative cooperativity that influenced glutamate/glycine binding affinity. Following successful cloning of NMDARs (Moriyoshi *et al*., 1991; Ikeda *et al*., 1992; Meguro *et al*., 1992; Monyer *et al*., 1992; Yamazaki *et al*., 1992b), it was reported that glycine enhanced NMDA-induced currents in *Xenopus* oocytes injected with clone mRNA specifically for the GluN1 subunit (Moriyoshi *et al*., 1991), further supporting the idea that glycine acted at NMDARs and not at a separate receptor. Finally, site-directed mutagenesis of cysteine residues of GluN1 showed that two extracellular sites were involved in glycine potentiation of glutamate-evoked currents and the effect was not due to a change in glutamate affinity (Laube *et al*., 1993). This also demonstrated that glutamate must bind elsewhere and there is general agreement that it binds on the GluN2 subunit (Anson *et al*., 1998; Anson *et al*., 2000).

Studies supporting endogenous glycine activity at NMDARs in the CNS are numerous, typically focusing on electrophysiological recordings, LTP or cell death. Kynurenic acid (KYNA) is a metabolite of tryptophan and known to inhibit post-synaptic NMDA currents (Ganong *et al.*, 1983; Ganong & Cotman, 1986) by acting at the strychnine-insensitive glycine binding site (Kessler *et al*., 1989). Synthetic derivatives of KYNA, for example 7-chloro kynurenic acid (7-Cl KYNA) and 2,7-dichloro kynurenic acid (DCKA), are more selective for the NMDAR glycine binding site and are often used to decrease endogenous NMDAR co-agonist activity. In rat cortical slices 7-Cl KYNA attenuated NMDA-induced depolarization (Kemp *et al*., 1988). Similarly, LTP induction (associated with NMDAR activity) was prevented in rat hippocampal slices during 7-Cl

KYNA administration (Izumi *et al*., 1990; Watanabe *et al*., 1992). NMDA- and simulated ischemia-induced cell death in the rat cortical slice preparation was decreased in a dose-dependent manner with pretreatment of DCKA (Katsuki *et al*., 2004; Katsuki *et al*., 2007). These select studies indicate that the NMDAR glycine binding site is endogenously occupied and appropriate antagonists can reduce the influence of NMDAR activity.

A Physiological Role for a D-Amino Acid

Concurrent with the characterization of NMDAR glycine binding site and its physiological merit was the identification of another amino acid that endogenously bound to the glycine binding site. From the initial studies D-serine was found to act at NMDARs at least as effectively as glycine and was subsequently used as a specific, non-physiological agonist. The discovery of endogenous D-aspartate and D-serine in the mammalian CNS raised the possibility for a functional role for D-amino acids, which were largely thought to be unnatural in vertebrates (Dunlop *et al.*, 1986; Hashimoto *et al.*, 1992; Hashimoto *et al.*, 1995; Matsui *et al.*, 1995; Hashimoto & Oka, 1997). Interestingly, a clearance mechanism for D-amino acids, D-amino acid oxidase (DAAO), had been discovered by Sir Hans A. Krebs (1935; referred to as D-amino acid deaminase), but it was thought to exist to breakdown D-amino acids that had accumulated via the diet and from bacteria lining the gut wall. This notion changed nearly 65 years later with the discovery and cloning of serine racemase, a serine specific enzyme that converts L-serine to D-serine (Wolosker *et al*., 1999a; Wolosker *et al*., 1999b). Many laboratories have subsequently shown that D-serine is an endogenous NMDAR co-

agonist (Schell *et al*., 1995; Schell *et al*., 1997; Mothet *et al*., 2000; Stevens *et al*., 2003; Shleper *et al*., 2005). Specifically, D-serine has been implicated as an endogenous co-agonist because breakdown of D-serine by exogenous application of DAAO has similar effects as KYNA derivatives on post-synaptic NMDA currents (Mothet *et al*., 2000), LTP induction (Yang *et al*., 2003) and cell death (Katsuki *et al*., 2007). However, these results do not exclude glycine as an endogenous coagonist in these preparations as well. A tetrameric NMDAR channel has 2 binding sites for glutamate and 2 for D-serine and/or glycine. This has necessitated a change in nomenclature from 'the glycine binding site' to 'the coagonist binding site', yet the former is still common in the literature.

Since the discovery of endogenous NMDAR coactivation there has been significant debate over the saturation state of the coagonist binding site. Within the retina, and the rest of the CNS, there is now significant evidence that the ambient coagonist concentration is normally maintained at a concentration that permits NMDAR channel activation upon glutamate binding, but that is sub-saturating. For example, the exogenous application of D-serine enhanced NMDA-induced whole-cell currents of rat RGCs (Stevens *et al*., 2003). Light-evoked electrophysiological responses are also enhanced by D-serine application in lower vertebrates (Stevens *et al*., 2003; Gustafson *et al*., 2007) and mice (Reed *et al*., 2009). These studies outline that the NMDAR coagonist binding site is not fully occupied leaving the possibility that coagonist release/clearance could be modulated to enhance NMDAR activity. The use of coagonist binding site antagonists (KYNA derivatives, see above) has determined that there must be some coagonist normally available to NMDARs, and indeed DCKA reduced synaptic (potassium- or light-evoked) RGC EPSCs (Lukasiewicz & Roeder, 1995). However, the

use of antagonists cannot discriminate between D-serine and glycine. Application of the enzymes DAAO and D-serine deaminase (DsDa) selectively degrade D-serine relative to glycine causing reduced NMDA- and light-evoked electrophysiological responses from RGCs (Stevens *et al*., 2003; Gustafson *et al*., 2007). This confirms that D-serine contributes to the ambient extracellular coagonist concentration in retina, as it does in the brain (Mothet *et al*., 2000), but does not exclude a glycinergic contribution.

In the brain and spinal cord D-serine and glycine localization are inversely proportional to one another (Schell *et al*., 1997). The retina presents an interesting environment for NMDAR coagonist activity because, extracellularly, they are found in relatively equal concentrations with vitreal measurements suggesting concentrations of 2-5 μM (Thongkhao-On *et al*., 2004). Of course greater control of coagonist concentration would exist within the neural retina itself. D-Serine and/or serine racemase are present in Müller cells of the rat (Stevens *et al*., 2003; Williams *et al*., 2006; Kalbaugh *et al*., 2009), mouse, mudpuppy, salamander (Stevens *et al*., 2003) and human (Diaz *et al*., 2007). Originally thought of solely as a 'gliotransmitter', advancements in fixation and immunohistochemical techniques allowed for the discovery of D-serine and serine racemase in neurons as well. The majority of both are localized to glia but there is significant localization to neurons in the brain (Kartvelishvily *et al*., 2006; Williams *et al*., 2006) and even some suggestion that neuronal D-serine production might predominate (Miya *et al*., 2008; Ding *et al*., 2010). In mouse retina serine racemase is also expressed in neurons, RGCs in particular, but is markedly reduced throughout the retina from postnatal week 1 to week 18 (Dun *et al*., 2007a). Nonetheless, *in situ* hybridization revealed extensive serine racemase expression in all major classes of adult

rat retinal neurons, excluding photoreceptors (Takayasu *et al*., 2008). Alternatively, glycine is thought to be produced exclusively by neurons and in the retina predominantly by amacrine cells (Menger *et al*., 1998). As such it undergoes depolarization-induced vesicular release and is cleared from the extracellular space by a high affinity glycine transporter-1 (GlyT-1).

Extracellular D-serine clearance occurs via transport and can subsequently be broken down by DAAO. Glial cells express the system alanine, -cysteine, -serine transporter (ASCT) that exchanges neutral amino acids in a Na^+-dependent manner. Conversely, neurons express the Na^+-independent Asc-1 transporter, although some evidence indicates that neurons can also express ASCT2 (Gliddon *et al*., 2009). Comparatively, Asc-1 is considered a high affinity neutral amino acid transporter, and transport occurs very rapidly, and ASCT is lower affinity with a slower time course (see Rutter *et al*., 2007). The uptake of D-serine in the retina is exclusively Na^+-dependent and is mediated by ASCT2 that is expressed by Müller cells (O'Brien *et al*., 2005; Dun *et al*., 2007b). Because transport is dependent on Na^+ and amino acid concentration, ASCTs can be used both for uptake and release of D-serine. Once inside the cell D-serine can be stored in vesicles (Williams *et al*., 2006), although little is known how this occurs, or be broken down by DAAO, the expression of which in the brain is inversely correlated to D-serine expression (see Yoshikawa *et al*., 2004). The only published reports on DAAO localization in retina is in amphibians, that show the enzyme inside peroxisomes in the RPE, cones and Müller cells, predominantly near the outer limiting membrane (Beard *et al*., 1988; St Jules *et al*., 1992). While still not confirmed in mammals this distribution would parallel that of the brain since DAAO concentrations

are higher in the outer retina while D-serine concentrations are higher in the inner retina similar to NMDAR distribution.

Thesis Objectives

The work presented in this thesis is integrally related but consists of three different components. First, it is a study of glutamate receptor activity and its modulation. Secondly, it probes the physiological function of the amino acid D-serine. Thirdly, it places D-serine modulation of glutamate receptors in the context of retinal circuitry and discusses the functional implications, taking into consideration other parts of the CNS. In order to assess these issues I have used two different preparations. Acutely isolated retinas were used in order to study GCL neurons in their 'native' environment and, therefore, their synaptic inputs were maintained. However, because of these inputs, appropriate considerations had to be made to account for network influences. In addition, immunopurified cultures of ganglion cells, that are less encumbered by retinal circuitry and the associated network effects, were used when possible to probe cellular activity with less ambiguity. Together these two approaches complement each other and strengthen my conclusions. Along a similar vein, in some cases multiple methods of physiological recordings were used, asking the same questions using different tools, in attempt to eliminate any biases inherent in a particular methodology.

In Chapter Two I describe the development of a novel method of loading calcium indicator dye into retinal neurons in order to study neuronal activity and I used this technique throughout the remainder of the thesis. Chapter Three is a study of NMDA

receptor coactivation by the amino acid D-serine that highlights the potential for D-serine modulation in the retina. In Chapter Four I demonstrate that D-serine can act in an inhibitory manner at AMPA receptors. In its totality I believe this work adds significantly to the study of D-serine modulation of GluRs and provides the basis for continued avenues of exploration.

Chapter 2: A Novel Method to Load Ca^{2+} Indicator Dye into Retinal Neurons

Preface

The use of Ca^{2+} imaging in the study of neuroscience has proved to be a valuable tool to explore cell excitability, calcium dynamics and excitotoxicity. Many studies use isolated cultured cells that help to reduce ambiguity in interpretation of the data. However, imaging living intact tissue, such as isolated retinal preparations, allows for the study of specific cells within their native environment. I began my doctoral research using the "Stab" technique (Baldridge, 1996; Hartwick *et al*., 2004) to label ganglion cells for isolated rat retina Ca^{2+} imaging experiments. The loading was very consistent and Ca^{2+} responses were robust but I was concerned about the significant wait-time associated with this technique since back-labelling RGCs with the 10,000 MW fura dextran required 6-8 hours. The retina could potentially be compromised given the long time it remained *ex vivo* before experiments, despite the use of specialized media (Ames or Hibernate A) to maintain its health. In particular, when I started my initial D-serine project (Chapter Three) I was concerned that the endogenous D-serine concentration might change over this extended period of time. Similarly, changes in genetic and protein expression have been noted within 12 hours following optic nerve transection (Agudo *et al*., 2008; Agudo *et al*., 2009) and thus could influence the experiments.

Several attempts were made to load indicator into rat RGCs while minimizing the time between retinal extraction and the first recording. I first attempted to load low MW Ca^{2+} indicator salts from the optic nerve head with little success. Secondly, Michelle

Archibald (a technician from Dr Balwantray Chauhan's lab) kindly helped by applying indicator, *in vivo*, using gel foam soaked with dye on a transected optic nerve. I removed the retinas for imaging 18 hrs later and there was significant RGC loading. However, the dye appeared to be vesicularized and was unresponsive to bath application of high K^+ or kainate. Although this was promising, because removal at earlier time points may have revealed adequate cytosolic loading, I did not continue to explore this loading method further. Thirdly I incubated developing and adult retinas in AM indicator dyes, successfully loading glia but not neurons. Fourth, I pressure ejected fura-2 AM underneath the ILM of two retinas in multiple locations but did not see any indication of cellular loading (data not included in the thesis).

Finally, I attempted to load retinal neurons using fura-2 salt and electroporation, an approach previously demonstrated capable of loading spinal cord neurons (Bonnot *et al*., 2005). This approach was successful and led to the exclusive use of the electroporation technique for all subsequent isolated retina Ca^{2+} imaging experiments. While loading specificity of RGCs was sacrificed, the time between isolating a retina and performing an imaging experiment was now limited only by the preparation time. The experiments outlined in this chapter took place in four separate phases. (1) The initial phase demonstrating the loading of fura-2 salt into GCL cells, which were subsequently used for experiments in later chapters. (2) Once again Michelle Archibald lent her expertise and performed *in vivo* superior colliculus injections of rhodamine dextran to label RGCs. After one week I electroporated the retinas in order to establish the extent of RGC loading with fura-2. (3) I recorded the light-evoked responses from naive and electroporated retinas to establish the overall health of the retinal circuitry following

electroporation (with helpful discussions and suggestions from Dr Awatramani along the way). (4) In concert with phase three, I applied the procedure to the mouse retina. To my knowledge there are currently only three publications that have used electroporation to load Ca^{2+} indicator dye into retinal cells (Yu *et al.*, 2009; Daniels & Baldridge, 2010; Farrell *et al.*, 2010), all of which are from our research group (the Retina and Optic Nerve Laboratory, Dalhousie University). I am an author on two of these manuscripts (and helped Dr Steven Barnes' lab in using the technique for the third publication) and my contributions are reproduced in this thesis with appropriate copyright permissions (see Appendix). A group in Germany has also successfully used a similar electroporation technique to assess light-evoked Ca^{2+} transients from GCL neurons (Briggman & Euler, 2011).

Introduction

The ability to measure changes in intracellular calcium (Ca^{2+}) concentration ($[Ca^{2+}]_i$) has long been used as a method to study neuronal function and followed the advent of high affinity Ca^{2+} indicator dyes (Tsien, 1980; Grynkiewicz *et al*., 1985). There is almost a 10,000 fold difference between normal extracellular Ca^{2+} concentration and $[Ca^{2+}]_i$ so events that lead to increases in cytosolic Ca^{2+} can have profound effects. For example, Ca^{2+} influx is necessary for the synaptic release of neurotransmitter, it plays an integral part in synaptic plasticity and can signal the nucleus for gene transcription (see Berridge, 1998). Activation of glutamate receptors (GluRs) typically leads to a rise in $[Ca^{2+}]_i$ directly, i.e., N-methyl-D-aspartate (NMDA) receptors (NMDARs) or indirectly, by most α-amino-3-hydroxy-5-methyl-4-isoxazoleproprionic acid (AMPA) receptors (AMPARs)/kainate receptors (KARs), by depolarization-induced influx through voltage-gated Ca^{2+} channels and metabotropic GluR (mGluR)-mediated Ca^{2+} mobilization from intracellular stores (see Dingledine *et al*., 1999). Alternatively, excessive increases in $[Ca^{2+}]_i$ due to prolonged glutamate exposure are associated with neuronal death (termed glutamate excitotoxicity; Choi, 1985, 1988). Calcium imaging can therefore be used to study intracellular Ca^{2+} dynamics as well as ligand-gated receptor physiology and pathophysiology.

Our laboratory has a broad interest in glutamatergic Ca^{2+} dynamics in retina from a physiological perspective (Yu *et al.*, 2009; Daniels & Baldridge, 2010) and in relation to pathophysiological conditions, such as glaucoma and ischemia (Hartwick *et al.*, 2004; Hartwick *et al.*, 2005; Hartwick *et al.*, 2008). However, it has long proven challenging to load neurons with Ca^{2+} indicator dye in the adult mammalian retina, particularly in

comparison to early postnatal stages. In the first postnatal week, retinas, like cultured cells, can be bathed in membrane-permeant acetoxymethyl (AM) ester Ca^{2+} indicator dyes and ganglion cell layer (GCL) neurons can be loaded with dye (Bansal *et al.*, 2000). By postnatal day 10 (P10), however, such loading is no longer effective, presumably due to the restricted access produced by the developing inner limiting membrane (ILM). Calcium indicators can be pressure ejected underneath the ILM facilitating neuronal dye loading (Blankenship *et al.*, 2009) using the multicell bolus loading technique originally described for use in cortex (Stosiek *et al.*, 2003). Using this method it takes 1-3 hrs for sufficient loading of GCL neurons in mice < P20 (Marla Feller, personal communication). To my knowledge it is unknown if this technique works in the adult retina, where loading of Müller cells may be more prevalent. Some success has been obtained by applying Ca^{2+} indicator dyes to the cut optic nerve allowing for back-labelling to the retina after 1-1.5 hrs (Sasaki & Kaneko, 2007). Similarly, dextran-conjugated dyes can be injected into the isolated retina and substantial labelling is seen after >6 hrs (Baldridge, 1996; Hartwick *et al.*, 2004). These last two techniques are advantageous because retinal ganglion cells (RGCs) are loaded specifically but, on the other hand, they require prolonged periods for adequate retrograde labelling.

To reduce the time between preparation and experiment we have developed an electroporation technique to load GCL cells with Ca^{2+} indicator dye, a technique modified from a method developed for spinal cord by Bonnot and colleagues (2005). The precise mechanism by which cell impermeant dyes gain access to the cytosol during electroporation is unknown but it is believed that pores are formed transiently through alteration of the plasma membrane lipid bilayer by the resultant electric field allowing

dye entry into the cytoplasm (Weaver, 1995). Electroporation is commonly used to transfect genes into isolated cells or embryos (see Washbourne & McAllister, 2002) but it has also been used to facilitate entry of fluorescent dextrans into neurons in cerebellar slices (Yang *et al.*, 2004).

The primary goal of this project was to identify a protocol to load GCL neurons with Ca^{2+} indicator dye with minimal delay between killing the animal and obtaining consistent and reliable Ca^{2+} responses. Here we compare several different methodologies explored in an attempt to achieve that goal with emphasis on the protocol that we have optimized for the electroporation of dye into rat and mice GCL cells. After electroporation the GCL shows a high degree of presumptive neuronal loading with particular preference for RGCs. Using several bath-applied agents to elicit increased $[Ca^{2+}]_i$ we demonstrate that robust Ca^{2+} responses are obtainable within 20 min after electroporation and that such preparations are stable for several hours. Cell-attached spike recordings demonstrate that light responses are maintained following electroporation and are similar to non-electroporated retina responses.

Materials and Methods

Procedures were performed in accordance with the Dalhousie University Committee on Laboratory Animals. Chemicals were purchased from Sigma-Aldrich (Oakville, ON, Canada) unless otherwise stated.

Rat Retinal Wholemount Preparation

Adult Long Evans rats (250-400 g) were killed with an intraperotineal injection of sodium pentobarbital (240 mg/ml, CDMV, Dartmouth, NS, Canada) and the eyes were removed quickly. Adult black C57 mice were killed by exposure to halothane followed by cervical dislocation. For light-evoked recording experiments animals were kept in the dark for at least 20 min prior to procedure. Retinas were removed under dim light, placed directly in recording chamber and held in place by a harp (Warner Instruments, Hamden, CT, USA) or placed on a white filter paper (Millipore, Bedford, MA, USA), over a 500 μm wide hole) affixed in the chamber. For Ca^{2+} imaging experiments fura-2 pentapotassium or pentasodium salt (Invitrogen, Burlington, ON, Canada) solution was electroporated into the retina following a modified spinal cord protocol (Bonnot *et al*., 2005). Eyes were removed quickly and 4 μl of 22 mM fura-2 was injected into the vitreous through the optic nerve head. Tweezertrodes (BTX, Holliston, MA, USA) were positioned on the eye and square wave pulses applied using the ECM 830 electroporation system (BTX). The retina was dissected out under red light in room temperature Hank's Balanced Salt Solution (HBSS) bubbled with 100% oxygen. Each retina was cut into 2-4 pieces and mounted separately onto black filter paper (Millipore) GCL positioned up and left in oxygenated HBSS for at least 30 min, to allow for recovery from the procedure, before transfer to the superfusion chamber for calcium imaging.

Calcium Imaging

The recording chamber was superfused at ~2 ml/min with 100% oxygenated HBSS (10 mM HEPES, pH 7.4) at ~23ºC. Cultured RGCs (coverslips) or a piece of isolated retina (filter paper) was transferred to the chamber and allowed to equilibrate for

10-15 min. Ratiometric fura-2 dyes (K_d = 224 nM) were used and image pairs of 340 and 380 nm excitation (510 nm emission) were collected with an exposure of 400 ms each. Images were captured with a CCD camera (Sensicam, PCO, Germany) and recorded using Imaging Workbench 4 software (Molecular Devices, Sunnyvale, CA, USA) every 20 sec during baseline recordings and every 5 sec for 1 min prior to a response until >30 sec after the peak of the response. A response was measured by averaging the fura-2 ratio (340 nm/380 nm) for 5 image pairs prior to a response subtracted from the peak ratio of the response. Increases in the fura-2 ratio, quantified as arbitrary units (a.u.), are indicative of an increase in $[Ca^{2+}]_i$ and termed "Ca^{2+} responses."

RGC Retrograde Labelling

Animals were anaesthetized with ketamine (5.6 mg/kg) and the analgesic buprenorphine hydrochloride (0.02 mg/kg, Animal Resource Centre, McGill University, Montreal, PQ, CAN) was administered during the procedure and post-operatively. Animals were placed in a stereotaxic frame and access was gained to the superior colliculus through the skull, or to the optic nerve through the orbit. A 1 mm^2 piece of gel foam soaked in 15% rhodamine dextran (10,000 MW; Invitrogen) was placed on the superior colliculus or with 20% fura (10,000 MW; Invitrogen) or calcium green dextran (3,000 MW; Invitrogen) on the cut optic nerve (at least 5 mm from the back of the eye, leaving retinal blood supply intact). The gel foam was left in place, the incisions were stapled and the animal was allowed to recover. Superior colliculus loaded animals were left for one week before retinal isolation and 18-22 hrs post-operation in the case of optic nerve loading.

On-Cell Patch Recordings

The recording chamber was superfused at ~2 ml/min with 100% oxygenated HBSS (10 mM HEPES, pH 7.4) at ~36ºC. On-cell recordings were obtained using micropipettes (5-10 MΩ) filled with HBSS (pH 7.4). Liquid junction potential was corrected at 5 mV. Under infrared illumination a micropipette was used to tear a small hole in the ILM, allowing access to 3-4 GCL cells. A new micropipette was then used to obtain a gigaseal for spike recordings. Recordings were performed using a Multiclamp 700A amplifier, Digidata 1322A digitizer and pClamp 8 software and analyzed off-line with Clampfit 10 (Molecular Devices). Recordings were low pass filtered at 2-3 kHz, digitized and sampled at 10 kHz. For light stimulation a 527 nm LED was fitted to a fiber optic cable and 400 μm spot was centered over the electrode and focused onto the photoreceptors via the microscope objective.

Data Analysis

All statistical analysis was performed with Prism 4 (GraphPad, La Jolla, CA, USA) using the raw values and data were normalized for presentation only for visual clarity due to variability in absolute response size between cells. For on-cell recording firing rates were averaged from 3 sweeps per cell using the five seconds prior to light onset compared to that during the duration of the stimulus. A mixture of responses was obtained but only the responses over the course of light stimulation (ON response) were used for analysis. Data are expressed as mean ± SD.

Results

The Stab Technique

As described previously (Baldridge, 1996; Hartwick *et al.*, 2004), successful loading of Ca^{2+} indicator dye into RGCs in adult isolated rat retina was produced by injecting fura dextran (10,000 MW) into the retina. At the injection site all the cells of the retina can be loaded with indicator dye and considerable damage is done to the retina. Along with retinal cells, RGC axons also take up the dye and after 6 hrs proceed to retrogradely label RGC somata distant from the injection site. An example of this loading technique is illustrated in Figure 2.1 where RGC somata more than 200 μm away from the injection site were loaded with fura dextran via the axon bundles seen coursing through the image (arrowheads). Figure 2.1a shows an image of the raw fluorescence produced by emission (510 nm) from a single excitation wavelength (380 nm), of a group of cells with a range of fluorescence intensities. Because fura-based indicator dyes are ratiometric, the composite ratio image (ratio of raw fluorescence at 510 emission from excitation due to 340 nm/380 nm, Figure 2.1b) gives a relative indication of baseline $[Ca^{2+}]_i$. For example, cold colours (blue, cell 1 in Figure 2.1b) indicate low ratios and therefore low $[Ca^{2+}]_i$, relative to warmer colours (green to red, cell 2 in Figure 2.1b) that indicate higher ratios and greater baseline $[Ca^{2+}]_i$, although the same cells show similar raw fluorescence with 380 nm excitation in Figure 2.1a. To illustrate Ca^{2+} responses from dextran loaded cells 200μM NMDA was bath applied for 30 sec causing a rise in $[Ca^{2+}]_i$ that peaked within the first minute of the response and returned to baseline levels

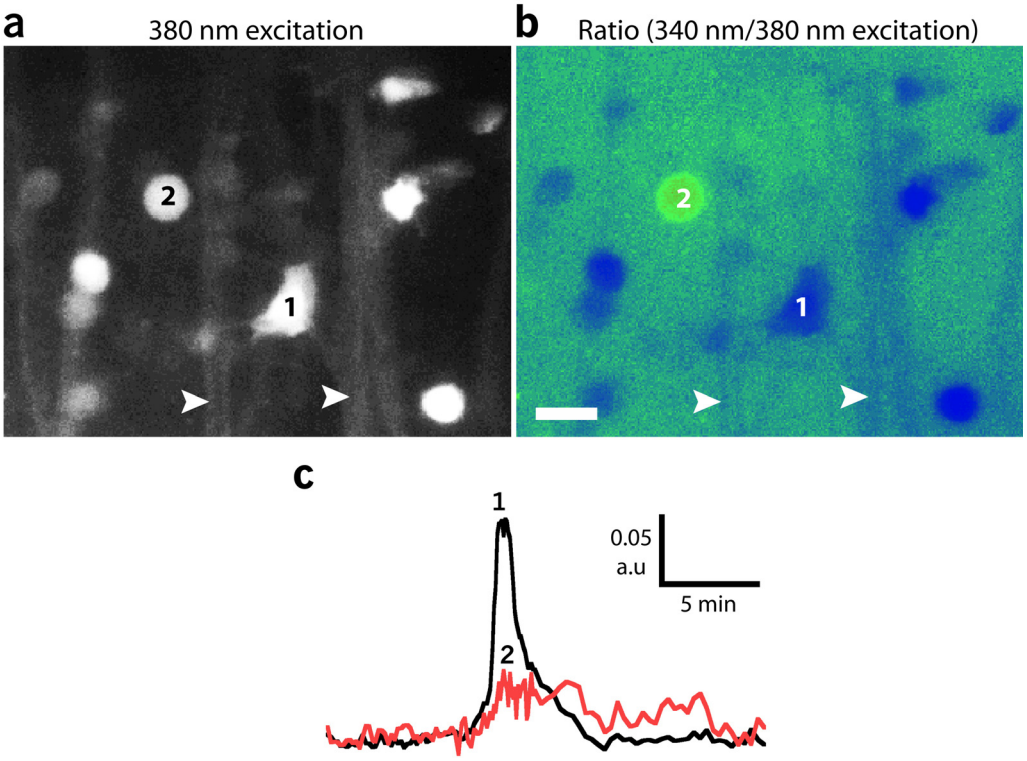

Figure 2.1 Fura dextran loading of RGCs using the stab technique. (a) A representative fluorescent photomicrograph (380 nm excitation, 510 nm emission) showing axon bundles (*arrow-heads*) that carried the dye from the injection site to RGC somata (i.e., *1* and *2*). (b) Baseline fura ratio image (340 nm/380 nm) of the same area in panel *a*. Colder colours indicate lower ratios and therefore low $[Ca^{2+}]_i$, cell *1*, and warmer colours indicate higher ratios and elevated $[Ca^{2+}]_i$, cell *2*. Scale bar = 20 µm. (c) Representative raw traces of Ca^{2+} responses from cell *1* and *2* elicited by bath application of 200 µM NMDA (30 s).

after several minutes (Figure 2.1c). Mean ± SD NMDA-induced Ca^{2+} responses were 0.24 ± 16 a.u. (n=41 RGCs from 6 retinas).

Alternative Attempts to Load GCL Neurons with Ca^{2+} Indicator Dye

There is a substantial incubation time required for adequate Ca^{2+} indicator dye loading of RGCs using the stab technique in rat (> 6 hrs; Hartwick *et al*., 2004). In order to reduce this period I attempted three different fluorescent dye-loading techniques reported to successfully load neurons in the retina (for example Bansal *et al*., 2000; Sasaki & Kaneko, 2007; Behrend *et al*., 2009; Koeberle *et al*., 2010). First, two adult rats (four eyes) were used to assess whether *in vivo* dye loading from the optic nerve was a viable option to load RGCs specifically. While the animal was under anesthesia each optic nerve was cut approximately 5 mm from the back of the eye, leaving the blood supply to the retina intact, and a piece of gel foam soaked with Ca^{2+} indicator dye positioned on the cut optic nerve. The same dye used for the stab technique, fura dextran (10,000 MW at 20%), was applied to each optic nerve of one animal and calcium green dextran (3,000 MW at 30%) was used for the second animal. After the surgery the animals recovered and the following day the animals were killed and retinas were removed just prior to imaging (18-22 hrs between surgery and imaging). Extensive fura and calcium green dextran loading of RGCs was seen in every retina. However, the appearance of the loading was punctate in virtually every cell (Figure 2.2a). This suggested that the Ca^{2+} indicator dyes were compartmentalized and therefore unlikely to report changes in cytosolic $[Ca^{2+}]_i$. Accordingly, attempts to elicit Ca^{2+} responses by 60 sec bath application of 200 μM kainate were unsuccessful in over 100 analyzed RGCs

combined from each of the four retinas (example trace from a fura dextran-loaded RGC in Figure 2.2b).

Secondly, I tried loading fura dextran, calcium green dextran, fluo-4 salt and fura-2 salt into RGCs via the optic nerve stump in the isolated eye/eyecup preparation, reported to load cells within 1-2 hrs in the rat (Sasaki & Kaneko, 2007) and salamander retina (Behrend *et al.*, 2009). Various concentrations of each dye (20-40% for dextrans and 20-60 mM for salts) were used. Eyecups were prepared by enucleation and hemisection of the eye and subsequent removal of the lens and vitreous. The optic nerve was freshly cut and a piece of tubing was glued to the sclera forming a well surrounding the resultant optic nerve stump. The Ca^{2+} indicator solution was added to the well (1-3 µl) and the preparation was kept in HBSS (Ca^{2+}-containing or Ca^{2+}-free) bubbled with 100% oxygen for 1-4 hrs. A total of 18 eyes were used for these experiments and while some axonal loading did occur (Figure 2.2c) there was never any loading of RGC somas.

The third approach used was incubation of the isolated retina in fura-2 AM ester dye, commonly used for cultured cell dye loading (see Chapters 3 and 4). Within the first 10 postnatal days RGCs in the isolated mouse retina are readily labelled with fura-2 AM, although it can take 2-6 hrs for substantial loading (Bansal *et al.*, 2000). Four P6 rat retinas were incubated in 20 µM fura-2 AM with 0.1% pluronic acid for 1 hr. Mostly presumptive Müller cell endfeet were loaded with the dye (Figure 2.3a). Müller cells are known to respond to NMDA (Puro *et al.*, 1996) and ATP (Wurm *et al.*, 2009). Accordingly, Müller cell endfeet showed robust increases in $[Ca^{2+}]_i$ in response to bath application of 200 µM NMDA (60 sec) and 10 µM adenosine triphosphate (ATP, 30 sec) producing mean ± SD responses of 0.031 ± 0.022 a.u. and 0.045 ± 0.025 a.u.,

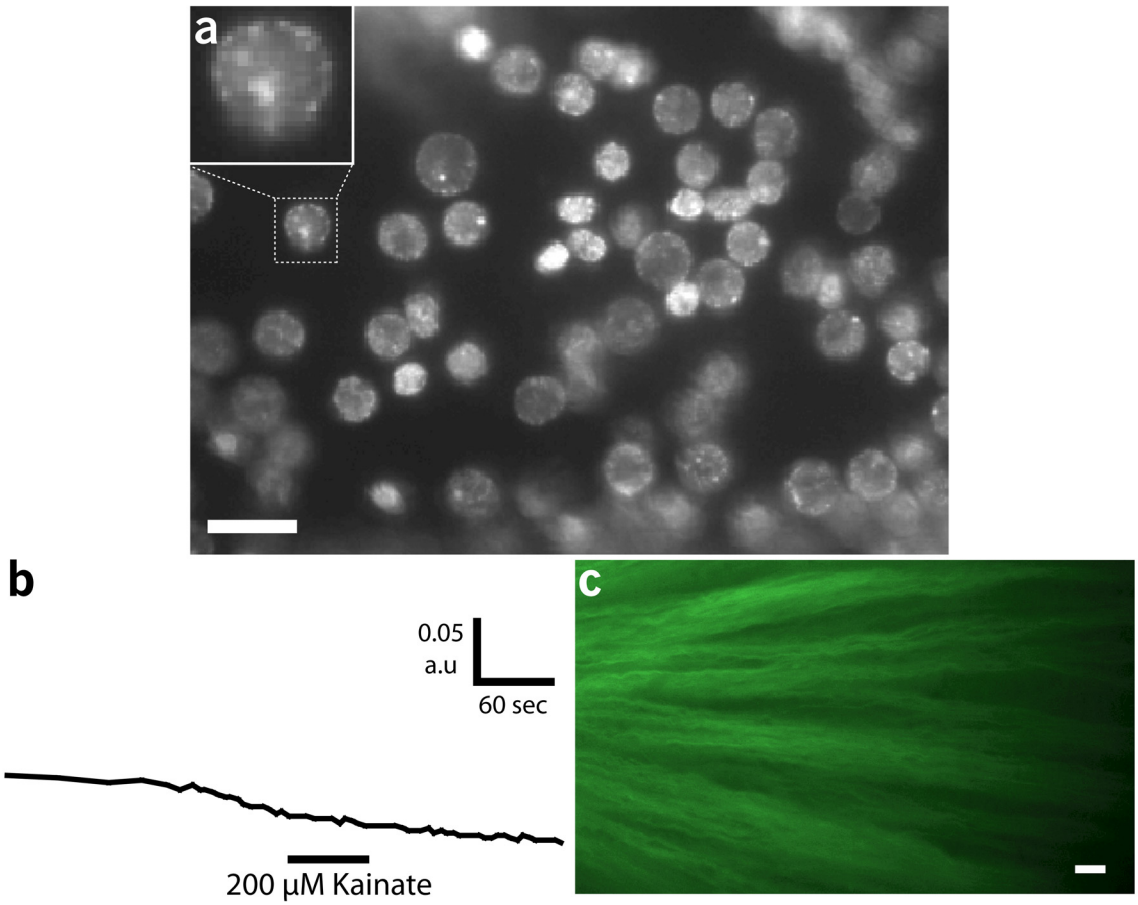

Figure 2.2 Calcium indicator loading via the optic nerve. (a) Fluorescent image (380 nm excitation, 510 nm emission) of RGCs loaded *in vivo* from the cut optic nerve with fura dextran ~20 hrs prior to isolated retina preparation. Dye loading of RGCs was punctate as seen in the inset. (b) Example trace from the cell in the inset in panel *a* showing the lack of response to a bath application of 200 µM kainate for 60 sec. (c) Fluorescent image (380 nm excitation, 510 nm emission) of axonal loading following 2 hr optic nerve incubation in 20% fura dextran. Scale bars = 20 µm

respectively (Figure 2.3c, e). Using the same protocol there was no apparent loading in two adult rat retinas. However, using the non-ratiometric dye, X-rhodamine-1 (Xrhod-1) AM, known to load glia in retinal preparations (Rillich *et al.*, 2009), at 10-50 μM with 0.1% pluronic acid for 15-30 min, yielded extensive loading of Müller cell endfeet but not neurons (Figure 2.3b) in all 14 pieces of retinas studied. Non-neuronal loading using AM dye incubation is consistent with previous results that have been obtained in the adult rat retina (for eaxample Newman, 2005). Neuronal loading was sometimes seen at the edges of the retina or where ILM integrity was compromised (not shown). Similar to P6 retinas, the Müller cell processes in the adult retina (loaded with Xrhod-1) showed robust Ca^{2+} increases in response to 200 μM NMDA and 10 μM ATP, producing mean ± SD Ca^{2+} responses of 4.4 ± 2.5% ΔF/F and 15.8 ± 4.9% ΔF/F, respectively (Figure 2.3d, f). Comparatively, the appearance of the glial cell loading between P6 and adult was quite different (Figure 2.3a, b). This could be due either to the development of the ILM in immature retinas or the different dyes used. Nonetheless, there was clearly no neuronal loading.

Fura-2 Labelling After Electroporation

The final approach to load GCL neurons with Ca^{2+} indicator dye was modified from a protocol reported by Bonnot and colleagues (2005), who successfully loaded Ca^{2+} indicator dye into neurons within the neonatal mice spinal cord. After the rat eye was enucleated 2-4 μl of cell-impermeant fura-2 salt was injected into the vitreous and the whole eye was electroporated within 15 sec of dye injection using electrodes placed on the anterior and posterior poles of the eye. Based on the electroporation settings reported for mouse spinal cord (55 mM calcium green hexapotassium salt, ~20V, seven 50 ms

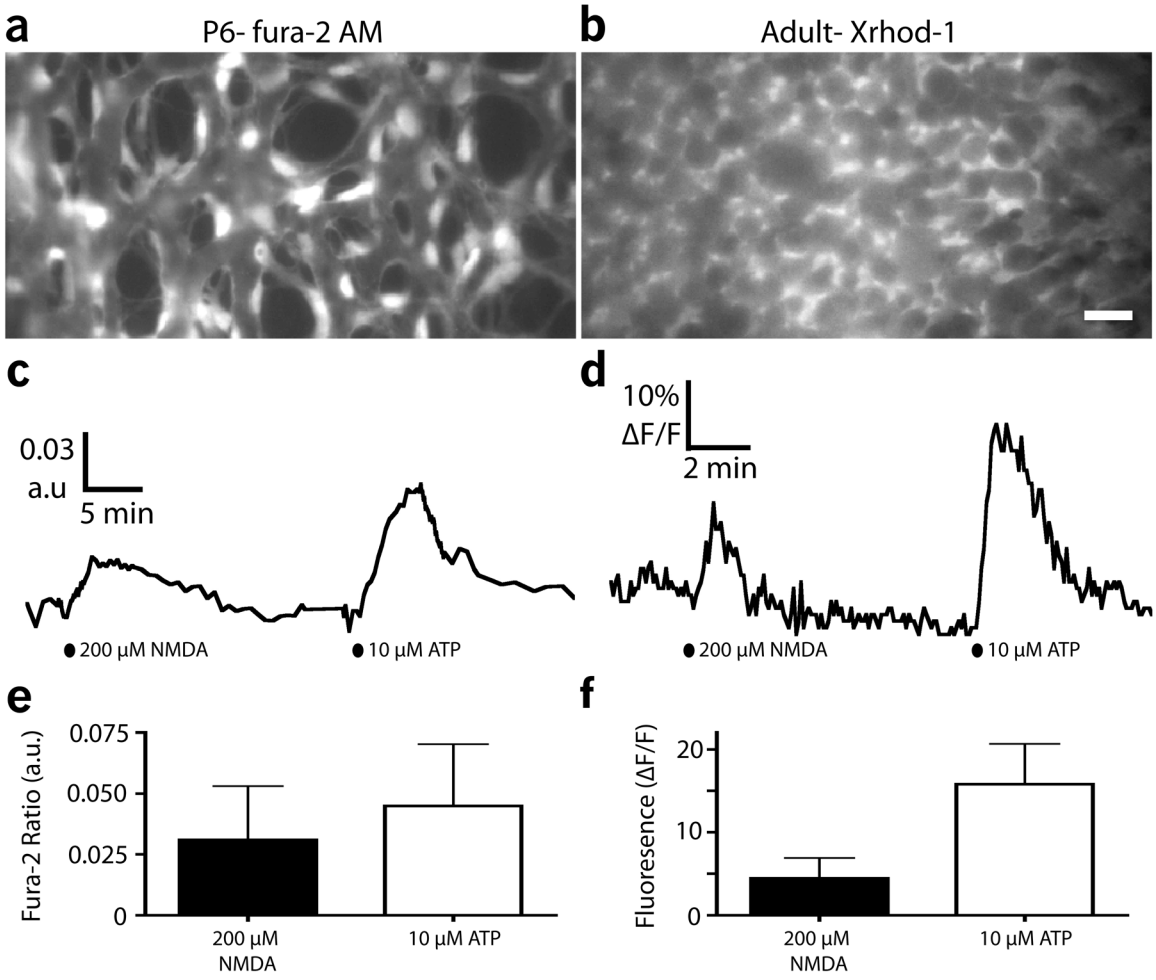

Figure 2.3 Müller cell endfeet loaded with AM Ca^{2+} indicator dyes. Fluorescent micrographs from (a) P6 rat retinas (1 hr incubation in fura-2 AM, 380 nm excitation, 510 nm emission) and (b) adult rat retina (20 min incubation in X-rhodamine-1, 560 nm excitation, 645 m emission). Example traces showing an increase (c) fura-2 ratio from a P6 retina and the (d) % ΔF/F in adult retina in response to 200 µM NMDA (60 sec) and then 10 µM ATP (30 sec). (e, f) Mean ± SD of NMDA and ATP-induced Ca^{2+} responses from (e) P6 (n=86 regions of interest from 4 pieces of retina) and (f) adult retinas (n=56 regions of interest from 3 pieces of retina). Scale bar = 20 µm

pulses at 1 Hz) I manipulated the set voltage (0-40V, effective voltage reported by electroporator was 1-3V), number of pulses (5 or 7), dye concentration (22.5-120 mM), the salt type (pentapotassium or pentasodium), the site of injection into the vitreous and position of the anode/cathode. While not every possible permutation involving the above parameters was tested, at least 50 retinas were used in order to established the parameters that maximized the number of cells loaded with maintained viability.

Initial experiments assessed different approaches to deliver dye to the retina for subsequent electroporation. Fura-2 salt solution was placed directly onto the GCL side of a piece of retina mounted on filter paper (results not included) or injected into the vitreous of an intact eye. Although GCL loading was achieved using both preparations, the retinas electroporated after being wholemounted appeared less healthy (white or opaque) than retinas that were electroporated while still within the eye. Furthermore, less than 10 cells were labelled in all 4 pieces (from one retina) combined. In contrast, retinas from electroporated eyes appeared healthier and had substantial presumptive GCL neuronal loading (described in detail below) in multiple fields of view (FOVs; 280 x 350 μm) within a single retina. Presumptive neuronal cell bodies loaded with Ca^{2+} indicator dye could be distinguished from glial cells because the former were typically round (7-25 μm diameter) compared to thin (~1 μm) Müller cell endfeet processes surrounding cell bodies. Müller cell stalks connecting the cell body to the endfeet were round but smaller (~2 μm) and astrocytes had an irregular star-like shape. The reported cell counts (below) are of presumptive neurons and each *n* is one representative FOV from a single retina unless otherwise noted. Importantly, loading was not uniform through the retina and other FOVs within an individual retina had greater, lesser or no cell loading.

I compared GCL dye-loading between two sites for the injection of fura-2 salt into the vitreous of the enucleated eye using 60 mM fura-2 salt, 40V, five 50 ms pulses at 1 Hz. (1) The injection needle was forced through the sclera just below the ora serrata, to avoid hitting the lens and to limit potential physical damage by the needle tip to the periphery of the retina. (2) Dye was injected through the optic nerve head making it easier to control the location of the injection. Examples of FOVs from retinas electroporated following sclera or optic nerve head dye injection are shown in Figure 2.4a and 2.4b, respectively. On average (± SD) 650 ± 160 cells/mm^2 were loaded with fura-2 after injection of salt through the sclera (n=10 retinas) and 841 ± 254 cells/mm^2 after injection through the optic nerve head (n=16 retinas, Figure 2.4 and Table 2.1). There were significantly (p=0.044, unpaired T-test) more cells labelled following injection of fura-2 salt through the optic nerve head compared to the sclera.

Next, the fura-2 salt concentration and the set electroporation voltage were varied. Fura-2 salt was injected into the vitreous through the optic nerve head at concentrations (in mM) of 22.5, 30, 60 or 120 and the eye was electroporated (40V, five 50 ms pulses at 1 Hz). Qualitatively, raw fluorescence was proportional to the dye concentration with the amount of GCL cell loading similar between 22.5 and 30 mM as well as between 60 and 120 mM fura-2 salt. Because of this similarity I only report the detailed comparison between 22.5 and 60 mM fura-2 salt. On average (± SD) 690 ± 227 cells/mm^2 were loaded after electroporation with 22.5 mM fura (n=10 retinas) and 904 ± 260 cells/mm^2 with 60 mM fura-2 (n=19 retinas, see Table 2.1). An unpaired T-test revealed that these values were significantly different (p=0.036). To assess the impact of the set voltage on the loading of GCL cells with Ca^{2+} indicator dye three voltages were used; 0, 20 and 40

V (fura-2 salt injected through the optic nerve head, five 50 ms pulses at 1 Hz). When dye was injected through the optic nerve head but the eye was not electroporated (0 V) some cell loading could be seen within 200 μm of the optic nerve head in some retinas or sometimes only axon loading was seen. On average (±SD) 93 ± 111 cells/mm^2 were loaded with fura 2 with no electroporation (n=7 retinas and values reported are the absolute maximum from each retina). When all other settings remained the same, but the electroporation voltage was set to 20V, an average (± SD) of 277 ± 78 cells/mm^2 were loaded with fura-2 (n=8 retinas) and this was significantly (p=0.002; unpaired T-test) different from non-electroporated retinas. When the voltage was increased to 40V an average (± SD) of 810 ± 264 cells/mm^2 were loaded with fura-2 (n=32 retinas, see Table 2.1). One-way ANOVA (with Tukey's post hoc test) revealed that the amount of loaded cells with electroporation using 40V was significantly ($p<0.001$) different than 0 and 20V. Finally, although not quantified, there was no apparent difference between the use of pentasodium vs. pentapotassium fura-2 salt or whether the cathode or anode was positioned on the cornea and a negligible qualitative increase in labelling with 7 versus 5 pulses.

I wanted to verify that electroporation was a viable method to load GCL cells in retinas regardless of developmental stage or species. Initial electroporation experiments used retinas from full-grown, adult rats (250 g at least 10 weeks old). The following experiments were performed using rats from two developmental stages, P10-14 and P17-20 (22.5 mM fura-2 salt injected through the optic nerve head, 30V, five 50 ms pulses at 1 Hz) and adult mice. Using P10-14 rats an average (± SD) of 2149 ± 418 cells/mm^2 (n=5 retinas) were loaded with Ca^{2+} indicator dye and 1190 ± 510 cell/mm^2 with P17-20

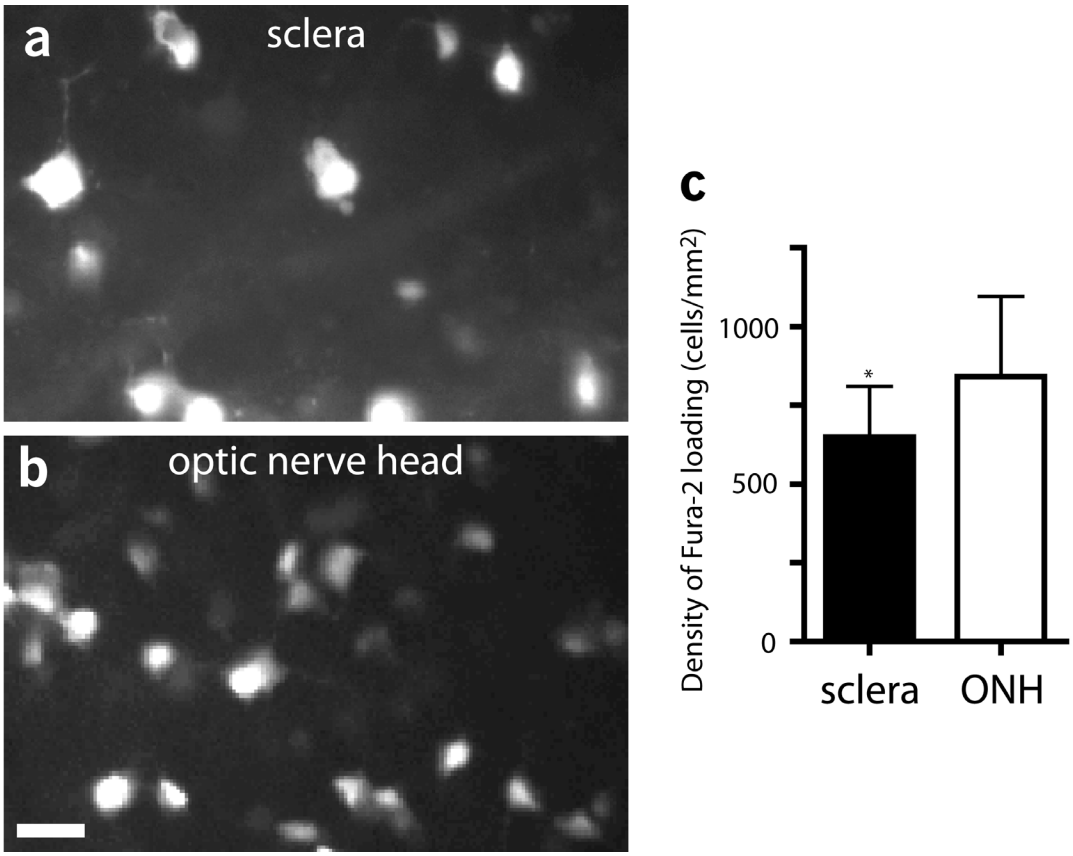

Figure 2.4 Electroporation of fura-2 salt into the adult rat retina. Fluorescent micrographs (380 nm excitation, 510 emission) illustrating loading of presumptive neurons in the GCL with fura-2 using electroporation after injection of fura-2 salt into the vitreous through the (a) anterior sclera or (b) the optic nerve head (ONH). (c) Mean ± SD number of presumptive GCL neurons loaded with fura-2 that was injected into the vitreous through the anterior sclera (n=10 retinas) or the ONH (n=16 retinas) and subsequently electroporated. *****P = 0.044, unpaired, two-tailed T-test. Scale bar = 20 μm.

rats (n=4 retinas, Figure 2.5 and Table 2.1). Loading was significantly greater in the youngest animals (P10-14; $p<0.001$) compared to P17-20 and adult rats, but there was no significant difference between the latter groups (one way ANOVA, Tukey's). For a summary of the loading in rat retina achieved using different electroporation conditions see Table 2.1.

Preliminary work in our lab using adult mouse eyes showed that electroporation also loaded GCL neurons with dye in mice, with lower voltages than used for rat (given the smaller size of the mouse eye). Three voltages (0, 15 and 30 V) were tested on two eyes each with the other parameters constant (5 x 10 ms pulses at 1 Hz after injection of 750 nl of 22.5 mM pentasodium fura-2 salt through the optic nerve head). Loading of cells could be seen even without electroporation, but was sparse and limited to relatively few cells (Figure 2.6a, ai). Applied voltages of 15 V (Figure 2.6b, bi) and 30 V (Figure 2.6c, ci) dramatically enhanced the apparent area of coverage and density of loading proportionally. Labelled cells from all conditions responded to 20 sec bath application of 10 μM kainate. The maximum number of cells in a given field of view when dye was injected through the optic nerve head with no electroporation was 41 and 22 of these responded to the kainate application (0.026 ± 0.021 a.u.). Alternatively, 266/283 cells in a representative field of view from a 30 V electroportated retina responded to the same application with an increased fura ratio of 0.066 ± 0.051.

Characterization of Fura-2 Positive GCL Cells in the Rat Retina After Electroporation

Electroporation successfully aids in loading fura-2 into retinal cells but one would not necessarily expect there to be any specificity with respect to which cells are loaded. In order to ascertain the extent of RGCs loading, RGCs were first back-labelled *in vivo*

with rhodamine dextran via the optic nerves in three adult rats (six eyes). After one week, the eyes were electroporated (22.5 mM fura-2 injected through the optic nerve, 40V, five 50 ms pulses at 1 Hz) and images of rhodamine dextran and fura-2 (380 nm excitation) were collected at five different locations (one pair from each quadrant plus one more non-overlapping FOV) from each retina (Figure 2.7). Rhodamine dextran and fura-2 labelling was not found in all regions of retina, so locations for evaluation were those that had both presumptive fura-2 GCL labelling (areas that I would normally choose for Ca^{2+} imaging experiments) and relatively uniform rhodamine labelling. Images were captured and subsequently adjusted (brightness and contrast, and digital conversion to red vs green image) and analyzed off-line. Assessment of double-labelling was determined by superimposing the rhodamne and fura-2 images and comparing cell position, shape and focal plane. When analyzed by retina (n=6 retinas) the mean ± SD number of fura-2 labelled cells was 564 ± 133 cell/mm^2 and of these, 66.7 ± 7.3% were rhodamine dextran-positive and, therefore, identified as RGCs (Figure 2.7e). Analyzing each individual retina demonstrates the variability of loading within a given retina and between different retinas. Using the 5 FOVs for each retina (n=5 FOVs for each retina) shows the range of loading and double-labelling with RGCs (Figure 2.7d, e). On average (± SD) retina 1 (yellow dot) had 786 ± 287 fura-2 labelled cells/mm^2 with 64 ± 7.4% identified as RGCs, retina 2 (blue dot) had 370 ± 258 cells/mm^2 and 60.2 ± 13.1% RGCs, retina 3 (pink dot) had 545 ± 177 cells/mm^2 and 65.1 ± 12.2% RGCs, retina 4 (red dot) had 592 ± 41 cells/mm^2 and 80.7 ±7.1% RGCs, retina 5 (black dot) had 554 ± 189 cells/mm^2 and 67.2 ± 5.1% RGCs and retina 6 had 537 ± 180 cells/mm^2 and 62.9 ± 10.1% RGCs

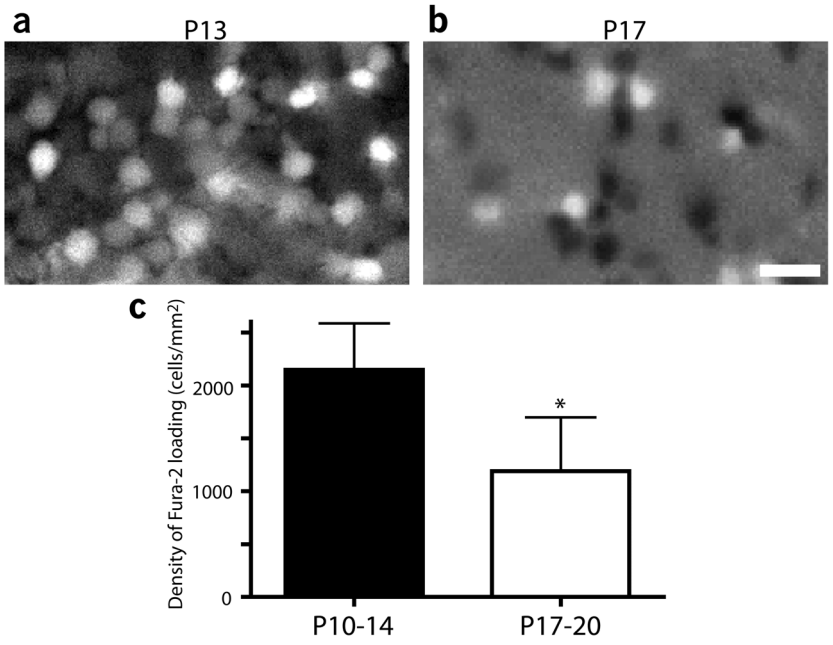

Figure 2.5 Electroporation of fura-2 salt into developing rat retinas. Representative fura-2 ratio images (340 nm/380 nm excitation) from a (a) P13 and (b) P17 rat retina following electroporation of fura-2 salt into the GCL. (c) Mean ± SD density of presumptive neuronal loading of fura-2 in the GCL after electroporation of P10-14 (n=5 retinas) or P17-20 (n=4 retinas) rat eyes. *****P = 0.019, unpaired, two-tailed T-test Scale bar = 20 μm.

Figure 2.6 Electroporation of fura-2 salt into adult mouse retina. Montages of fluorescent images (380 nm excitation, 510 nm emission) following injection of fura-2 salt into the vitreous, through the optic nerve head with (a) no electroporation, (b) 15V setting and (c) 30V setting. (ai-ci) Enlarged sections of each montage (from each yellow box, respectively) showing the pattern of loading. While there is some presumptive neuronal loading with no electroporation (arrows in *ai*) the speckled, background fluorescence is likely due to deposition of the salt in the extracellular space or inner limiting membrane. With electroporation (bi, ci) presumptive neuronal loading is more discreet, numerous and proportional to the voltage setting. Scale bars = 100 μm (montage) and 20 μm (inset).

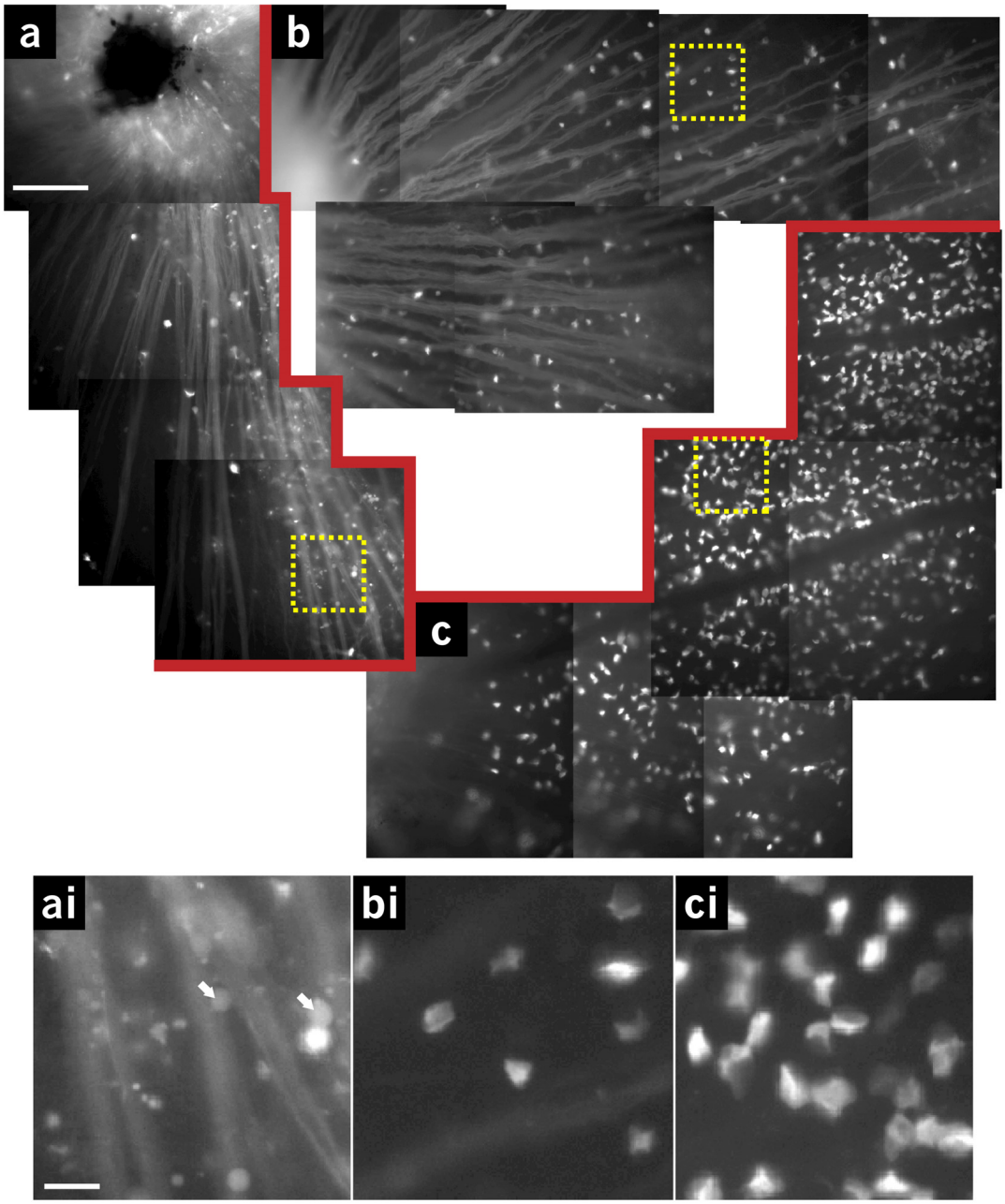
a
b
c
ai
bi
ci

Table 2.1 Summary of rat GCL fura-2 loading with electroporation

Age	Injection site	Voltage (V)	[Fura] (mM)	*n* (retina)	Density (cells/mm^2)
Adult	Sclera	40	60	10	650 ± 160
Adult	ONH	40	60	16	841 ± 254
Adult	ONH	0	22.5 - 60	7	93 ± 111
Adult	ONH	20	22.5 – 60	8	277 ± 78
Adult	ONH	40	22.5 – 60	32	810 ± 264
Adult	ONH	40	60	19	904 ± 260
Adult	ONH	40	22.5	10	690 ± 227
P10-13	ONH	30	22.5	5	2149 ± 438
P17-20	ONH	30	22.5	4	1190 ± 510

Data expressed as mean ± SD

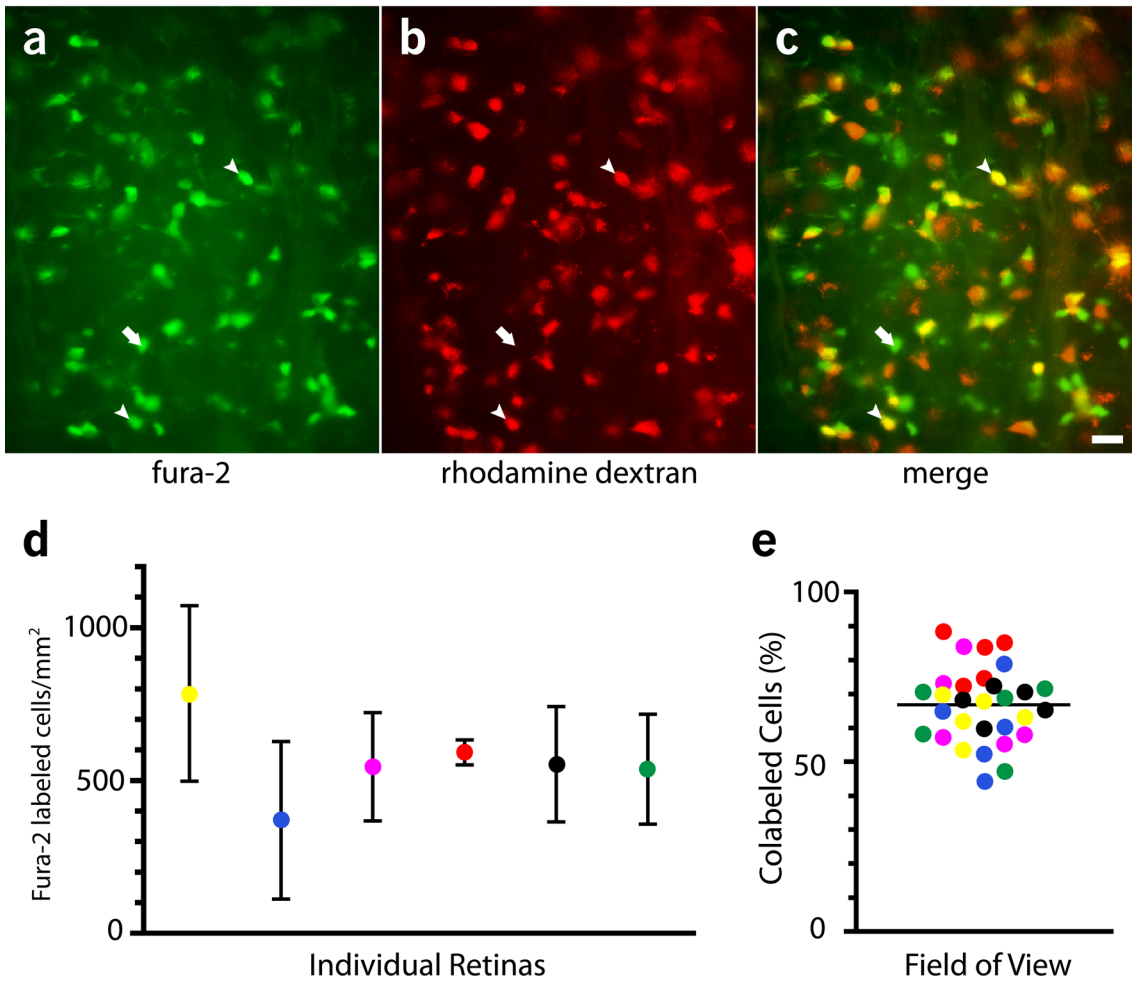

Figure 2.7 Identification of rat RGC fura-2 loading after electroporation. Images of fluorescence from the same area of (a) cells loaded with fura-2 following electroporation and (b) RGCs labelled with rhodamine dextran from the superior colliculus. (c) Fura-2 (green) and rhodamine (red) images were superimposed (merge) and yellow cells indicate fura-2 loaded RGCs (arrowheads). Presumptive amacrine cells are loaded with fura-2 but not rhodamine (arrow). Scale bar = 20 µm. (d) Mean ± SD cell density of fura-2 labelled cells for 6 different (colour-coded) retinas. (e) Distribution of double-labelled RGCs from each field of view (coloured circles) from every retina. There are 5 fields of view for each retina colour-coded to correspond to the labels in panel *d*. The black line shows the mean number of double-labelled RGCs for all retinas analyzed.

Calcium imaging of the isolated retina often showed two distinct populations of cells with respect to basal $[Ca^{2+}]_i$. As seen in Figure 2.1, the majority of cells have low ratios (coded by cool colours, i.e. blue) in the fura-2 ratio image and others have high ratios values (coded by warmer colours, i.e. green-red) indicating a relative elevation of resting $[Ca^{2+}]_i$. Nonetheless, cells with elevated basal $[Ca^{2+}]_i$ (green) are normally responsive to bath application of agonists (Fig 2.1c) indicating they are viable. However it is unclear whether this dichotomy in resting $[Ca^{2+}]_i$ is functionally 'normal' or if it is an indication of healthy vs. unhealthy cells. To explore this issue I sought to determine if the elevated basal $[Ca^{2+}]_i$ was due to increased baseline activity (action potential firing rate and/or synaptic input) by applying 1 μM TTX, to block voltage-gated Na^+ channels or a cocktail of iGluR antagonists (15 μM NBQX plus 100 μM APV or 20 μM MK-801; Figure 2.8). If elevated $[Ca^{2+}]_i$ was due to increased activity then application of TTX or the cocktail of iGluR antagonists would be predicted to reduce basal $[Ca^{2+}]_i$. Application of TTX caused a reduction in baseline Ca^{2+} in 32% of cells from 4 retinas and no change in the remainder (Figure 2.8b). Application of the iGluR antagonist cocktail caused a reduction in 3.3% of cells from 9 retinas and no change in the remaining cells. In both cases linear regression analysis showed that there was an inverse correlation between initial baseline fura-2 ratio value and the change in that value produced by TTX or iGluR blockers (Figure 2.8d, e) as cells with elevated baseline Ca^{2+} were more likely to be reduced by the antagonists. The regression slope deviation from 0 (no correlation) was significant for both conditions ($p<0.005$) however, since only a small number of cells showed a change in basal $[Ca^{2+}]_i$ r^2 values were low (0.09 and 0.07 respectively), making it difficult to interpret the meaningfulness of these findings.

Our lab has been interested in GluR activation and its contribution to Ca^{2+} signaling in RGCs and has commonly used bath application of GluR agonists paired with Ca^{2+} imaging as a primary investigative approach. Robust, repeatable Ca^{2+} responses must be obtained in order to make direct comparisons within and between cells. Typical experiments (see subsequent chapters) involve three consecutive applications of an agonist each causing a peak Ca^{2+} response and subsequent recovery to baseline. The first and third responses are the control and recovery responses, respectively, and the middle response is obtained during a treatment under investigation that is predicted to alter the Ca^{2+} response. This protocol necessitates that an agonist-induced responses can be repeated with little variability. To test whether repeatable Ca^{2+} responses could be obtained in GCL neurons, following electroporation loading of fura-2, we bath-applied 40 mM K^+ or 50 μM kainate three consecutive times and measured the change in the resulting Ca^{2+} response as a function of the initial response for each individual cell (Figure 2.9). Within cell comparisons show that K^+-induced Ca^{2+} responses were 101 ± 8% and 102 ± 8% for the second and third responses, respectively, relative to the initial response (100%, Figure 2.9b). Similarly, relative to the first kainate-induced Ca^{2+} response the subsequent response were 100 ± 10% and 98 ± 10%, respectively. There was no significant difference between the three responses for either agonist.

It could be argued that although exogenously applied agonists can induce an effect on $[Ca^{2+}]_i$ dynamics, a more physiological stimulus (light) might be more sensitive to alterations in retinal signaling, as a result of the electroporation procedure, since it would require an intact network. One advantage of studying retina is the possibility of employing a 'natural' stimulus, light, even when the retina is isolated from the eye.

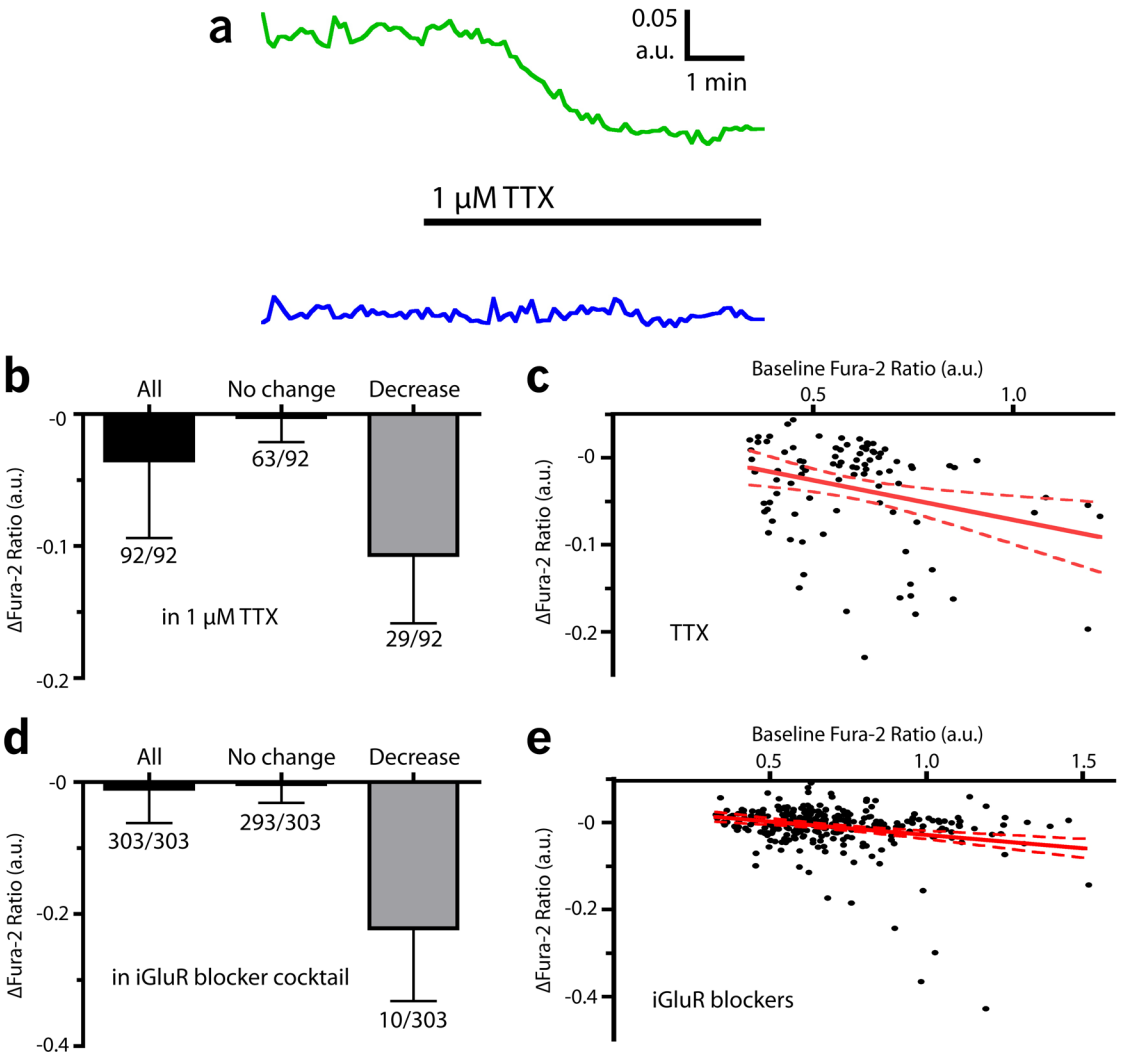

Figure 2.8 Contribution of spiking and synaptic input to baseline $[Ca^{2+}]_i$. (a) Two representative fura-2 ratio traces from cells in the same retina. During the application of 1 µM tetrodotoxin (TTX) the ratio was reduced in some cells (*green*) but unchanged in other cells (*blue*). Mean ± SD for the change in basal $[Ca^{2+}]_i$ in response to (b) TTX and (d) a cocktail of iGluR antagonists (15 µM NBQX, 20 µM MK-801) showing the total number of cells from 4 and 9 retinas, respectively. Bars show the effect of antagonists on all cells (*left*) only those that showed no change (*middle*, based on positive and negative changes in baseline) and those that showed a decrease in baseline $[Ca^{2+}]_i$ (*right*). (c, e) Scatter plots of each cells initial basal fura-2 ratio vs Δfura-2 ratio in the presence of TTX or iGluR anagonists with linear regression lines (solid red) ± 95% confidence intervals (dashed red lines).

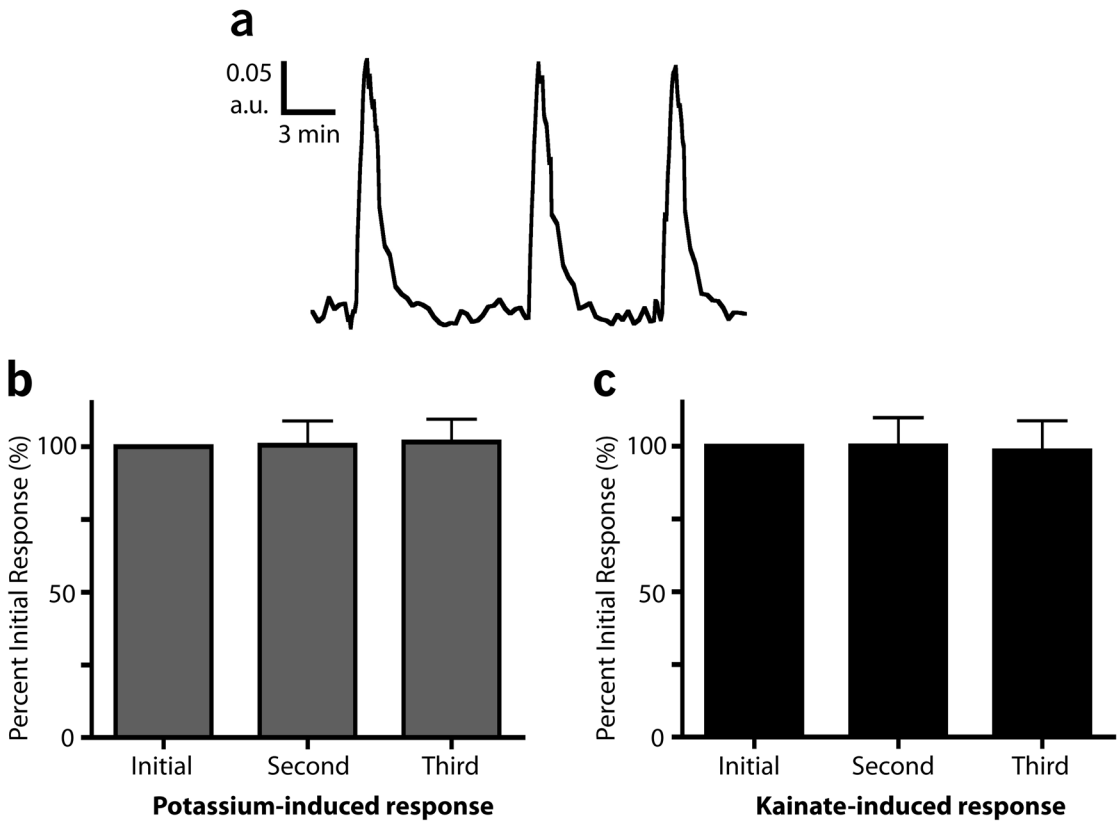

Figure 2.9 Control high-K^+ and kainate-induced Ca^{2+} responses from electroporated retinas. (a) An example trace of three consecutive Ca^{2+} responses elicited by 20 sec bath application of 40 mM K^+ solution. Mean ± SD of repeated (b) K^+ and (c) kainate-induced Ca^{2+} responses. There was no significant difference (repeated measures, one-way ANOVA) between the three responses by either treatment. The first responses with both drug applications were elicited approximately 15 min following electroporation. n = 56 cells from 4 retinas and 33 cells from 3 retinas, respectively.

Therefore, cell-attached, light evoked spike recordings were obtained to determine if electroporation adversely affected normal synaptic input to RGCs. We recorded from six spiking GCL neurons from two non-electroporated rat retinas (control) and seven neurons from two electroporated (22.5 mM fura-2 salt injected through the optic nerve head, 40V, five 50 ms pulses at 1 Hz) rat retinas (Figure 2.10). Due to technical limitations it is not known if the recordings were obtained from cells loaded with Ca^{2+} indicator dye. But the primary purpose of these experiments was to assess the impact of the electroporation on retinal function, not the specific effect of dye loading. Because background spiking of neurons made it difficult to analyze the increased spike rate at light-offset (OFF-response, arrowhead in Figure 2.10b), only the spike rate during the light stimulus was compared to the spike rate over 5 sec pre-stimulus. Therefore cells with pure OFF-responses (two and three for each condition, respectively) were not included in this data set. Prior to light onset cells from control retinas had a mean ± SD background firing rate of 4.7 ± 6.0 Hz that was significantly increased to 28.3 ± 8.1 Hz calculated over the duration of the 1 sec light stimulus (Figure 2.10c). Recordings from spiking GCL neurons in the electroporated retina were similar with basal firing rates of 2.6 ± 4.6 Hz that were significantly increased to 31.1 ± 8.7 Hz (Figure 2.10c). Similarly there was no difference in the peak firing rates (50 ms) bins between cells from non-control (73.3 ± 16.3 Hz) and electroporated (77.1 ± 31.5 Hz) retinas and the latency to spike following light onset with values of 190.3 ± 84.2 ms and 177.9 ± 66.3 ms, respectively (for summary of cell attached recordings see Table 2.2).

Table 2.2 Light-evoked responses from GCL neurons in control vs. electroporated retinas

	n	Background firing rate (Hz)	ON response (1 sec bin) (Hz)	Latency (time to spike) (ms)	Peak ON response (50 ms bins) (Hz)
Control	6	4.7 ± 6.0	28.3 ± 8.1	190.3 ± 84.2	73.3 ± 16.3
Electroporation	7	2.6 ± 4.6	31.1 ± 8.7	177.9 ± 66.3	77.1 ± 31.5
P value		*0.4807*	*0.5504*	*0.7717*	*0.795*

Data expressed as mean ± SD analyzed with unpaired, two-tailed T-test

Discussion

This work compares several methods to load Ca^{2+} indicator dyes into retinal neurons and describes a new method optimizing the electroporation of fura-2 into GCL cells of the rat and mouse retina. RGCs were loaded with fura dextran using the stab technique and Ca^{2+} responses could be elicited by application of GluR agonists. *In vivo* loading of fura dextran or calcium green dextran from the cut optic nerve also resulted in specific RGC labelling but was punctate, presumably indicating compartmentalization and thus cells were unresponsive to bath applied GluR agonists. Incubation of cut optic nerve with Ca^{2+} indicators in the eyecup preparation resulted in extensive axonal but no neuronal loading. Isolated retinas incubated in fura-2 AM caused extensive presumptive Müller cell endfeet loading in retinas from P6 rats, but not adult, whereas X-rhodamine-1 AM labelled Müller cell endfeet in adult retinas. Electroporation of fura-2 pentapotassium or pentasodium salt, injected into the vitreous of the eye, yielded extensive loading of cells in the retinas from rats as young as P10 to adulthood as well as in adult mice retina. Repeatable Ca^{2+} responses from GCL cells were elicited by depolarization with high K^+ solution and by the iGluR agonist kainate. Importantly, electroporated retinas maintained light responsiveness as determined from recordings of spiking GCL neurons.

Non-Electroporation Ca^{2+} Indicator Dye Delivery

The stab technique has served as a reliable method load Ca^{2+} indicator into the retina and offers the advantage of labelling RGCs specifically. This specificity is limited to regions distal to the injection site where axons have retrogradely delivered dye to the

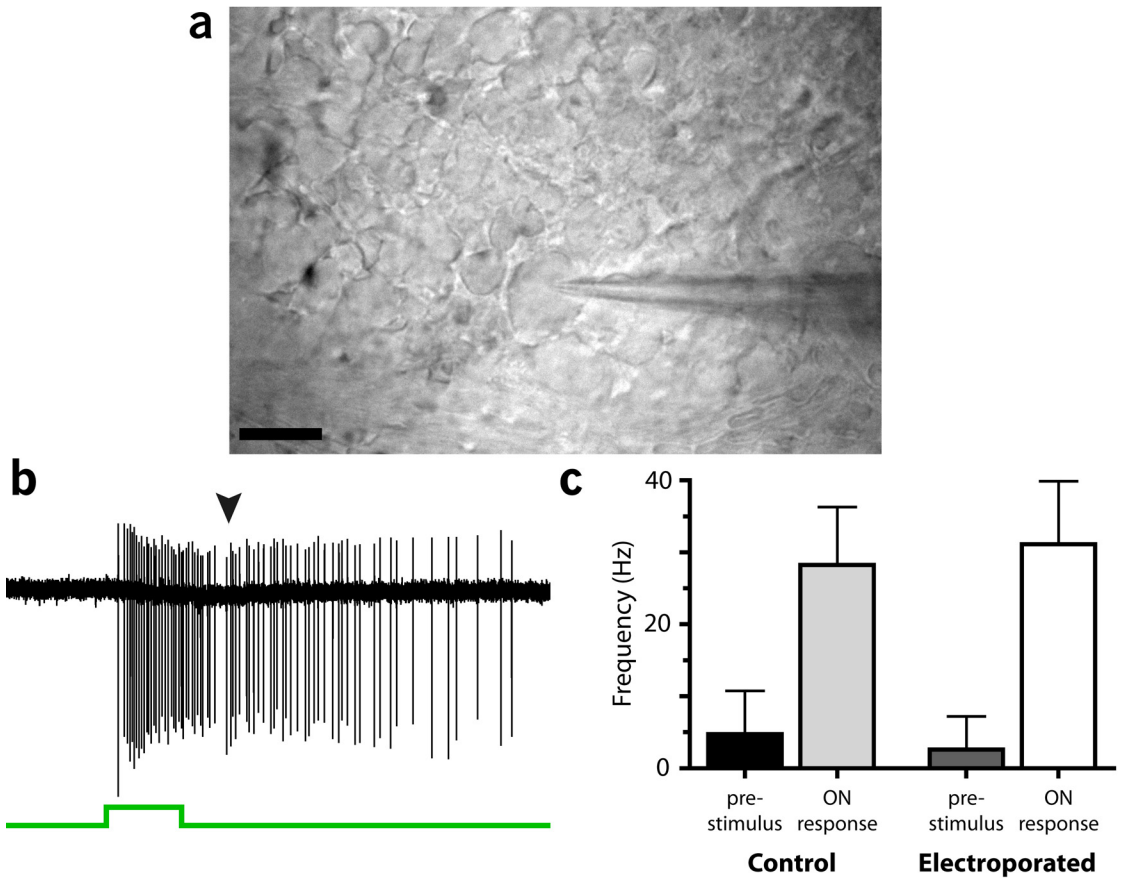

Figure 2.10 Light-evoked spike recordings from non-electroporated and electroporated rat retinas. (a) Infrared photomicrograph of a micropipette positioned for cell-attached spike recordings from a presumptive RGC. (b) An example trace of a spike-recording from a GCL neuron in an electroporated retina showing an increased spike rate (ON response) in response to a 1 sec light flash (step in green trace) of a 400 µM spot centered over the cell. A small increase can also be seen after light offset (presumptive OFF-response, indicated by the arrowhead). (c) Mean ± SD frequency of spikes in the 5 sec preceding the light flash (pre-stimulus) compared to during the 1 sec light response from cells in non-electroporated retina (control, n = 6 cells from 2 retinas) and electroporated retinas (n = 7 cells, 2 retinas). For each condition the light response significantly increased the spike frequency ($P < 0.05$; paired T-test) but there is no difference between pre-stimulus frequency or ON response frequency when comparing control to electroporated retinas (one-way ANOVA). Scale bar = 20 µm.

soma. The areas immediately surrounding the injection site show extensive cell loading from which Ca^{2+} responses can still be obtained (not shown), but in this case the cell type identity is unknown. A second advantage of the stab technique, related to loading specificity, is the relatively low background fluorescence surrounding back-labelled RGCs because the loading is restricted to one cell type and does not permeate into the surrounding tissue. However, a major concern with using this technique is the length of time required for loading RGCs (>6 hrs) and the changes that might occur over such periods.

In our hands loading via the optic nerve, both *in vivo* and using the eyecup preparation, did not load Ca^{2+} indicator into RGC cytosol. *In vivo* loading with fura and calcium green dextran was punctate, likely due to compartmentalization of the indicator dye by active transport of the dextran molecule (Fritzsch & Wilm, 1990). It is not known if dye reached the cytosol by diffusion and was subsequently vesicularized, but examining RGC loading at earlier time-points could help clarify this possibility. Secondly, the use of calcium indicator dye salts, rather than dextran conjugates, may facilitate passive diffusion instead of active transport. When dye was applied to the cut optic nerve of the eyecup preparation loading was limited to axons and somatic loading was not seen. While RGC loading has previously been reported using this technique it was rather limited in rat retina, requiring confocal microscopy to identify cell loading and with seemingly few cells loaded (Sasaki & Kaneko, 2007). Extensive loading has been achieved in the adult salamander retina (Behrend *et al.*, 2009) but this group had little success loading RGCs in the adult mammalian retina (Andrew Weitz, personal communication).

The use of AM dyes to load GCL neurons in the retina has been limited to slice preparations, isolated retinas from immature animals or animals with retinal degeneration (Bansal *et al.*, 2000; Sekaran *et al.*, 2003; Vessey *et al.*, 2005). Müller cell endfeet, and probably astrocytes, particularly after ~P14, loaded with dye with little to no loading of neurons, consistent with previous reports (Newman, 2005; Kurth-Nelson *et al.*, 2009). In early retinal development (up to P14) fura-2 AM has been successfully loaded into mouse GCL neurons (Bansal *et al.*, 2000; Unsoeld *et al.*, 2008), however even at P6 we saw only loading of Müller cell endfeet. Hypothetically, a difference in the maturation or makeup of the ILM might account for the absence of neuronal loading. Alternatively, we may not have incubated retinas in dye long enough (1-3 hrs) as Bansal and colleagues (2000) state that 2-6 hrs can be required for mouse. However, as described above, such long incubation periods may not be ideal.

Electroporation-Facilitated Ca^{2+}-Indicator Loading

Electroporation of fura-2 salts have now proven to be a viable method to load Ca^{2+} indicator dye into to GCL neurons and robust Ca^{2+} responses can be elicited within 20 min post-electroporation. One of the disadvantages of electroporation for gene transfection is the known low transfection rate, estimated at approximately 20% in cultured cells (Karra & Dahm, 2010). The low rate is almost exclusively due to transfected plasmid not reaching the nucleus and remaining in the cytosol. This disadvantage, in the case of gene transfection, may be an advantage if the goal is to load the cytosol with Ca^{2+}-sensitive dye. Although electroporation of plasmids is not directly comparable to the electroporation of dyes, our results indicate that a sufficient amount of Ca^{2+} indicator dye reaches the cytoplasm with this method. Single-cell electroporation

has also been used to load Ca^{2+} indicator into neurons in brain slices (Nevian & Helmchen, 2007). However, the approach presented in our study allows for many cells to be loaded simultaneously. In immature animals, *in vivo* and isolated retina electroporation of DNA plasmid, with comparable electroporation settings to those used here, has also been successfully used for gene transfection into retinal neurons with cells remaining viable for days after the procedure (Donovan & Dyer, 2006). Similarly, we show here that robust Ca^{2+} responses and electrically recorded light activity can be evoked from adult retinas immediately after electroporation of the adult retina in the enucleated eye.

The pattern of cellular loading in the retina using electroporation was variable, since the retina was never completely loaded, and would not be expected to load specific types of neurons in the GCL. Surprisingly, areas of the GCL with presumptive neuronal loading had a high degree of RGCs labelled. Electroporation of adult rat retinas with RGCs back-labelled from the superior colliculus with rhodamine dextran showed approximately 66% colocalization of Ca^{2+} indicator dye and rhodamine dextran in the GCL. In rat ~50% of GCL neurons are amacrine cells (Jeon *et al*., 1998) indicating a preference for RGC loading by electroporation. Furthermore, the number of RGCs labelled by Ca^{2+} indicator might be slightly underestimated since 5-10% of RGCs do not project to the superior colliculus. There are two possibilities that may account for the specificity of RGC labelling following electroporation. First, some RGCs are likely loaded retrogradely via their axons, particularly when fura-2 salt was injected through the optic nerve head and not the anterior sclera. In fact, injection of indicator through the optic nerve head alone, without electroporation, lead to some limited loading of cells, in

particular in the case of mouse retinas (Figure 2.6), and to a much lesser extent in the rat retina and sometimes not at all in the rat. While this limited loading (following optic nerve head injections) could be due to retrograde transport it would not account for the great number of cells loaded after electroporation. Secondly, on average RGC somas are larger than amacrine cells and therefore this selection bias may also be due to the enhanced cell surface area increasing the probability that indicator will enter the cell duing electroporation.

There was variation of basal $[Ca^{2+}]_i$ in cells following Ca^{2+} indicator loading, that was noticeable because of the use of the ratiometric dye fura-2. This difference in basal $[Ca^{2+}]_i$ could be related to normal differences in cell activity (ON vs OFF pathway) or abnormal differences, as a result of electroporation or retina isolation. An attempt to distinguish this difference, using TTX and iGluR blockers (Figure 2.8), was inconclusive because the effect of antagonist application was not strongly related to resting $[Ca^{2+}]_i$. Cells with elevated $[Ca^{2+}]_i$ may be unhealthy since elevated $[Ca^{2+}]_i$ has been linked to neuronal death (Choi, 1985). For example, *in vivo* optic nerve damage is known to cause elevated RGC $[Ca^{2+}]_i$ that is proportional to RGC death (Prilloff *et al.*, 2007). However, it is unclear from our results what accounts for the difference in basal $[Ca^{2+}]_i$.

To address concerns as to whether electroporation disrupts retinal circuitry, I recorded light-evoked activity from a sample of spiking GCL neurons using cell-attached patch clamp from control and electroporated retinas. These results reveal that the machinery necessary to generate light responses and pass that signal through the retina to RGCs remains intact and apparently undisturbed following electroporation. Furthermore, analysis of the ON-response showed that there was no difference between the measured

parameters from spiking GCL neurons in control and electroporated retinas. It is possible that the analysis of other properties of RGC responses might reveal changes in circuitry following electroporation. Bonnot *et al*., (2005) showed that electroporation transiently disturbed local reflex networks in the spinal cord. However, the responses returned to normal within 1 hr post electroporation. All recordings for this data set were recorded within 10-60 min post electroporation and no differences were seen. However, time series recordings from one cell over a prolonged period following electroporation could be performed in attempt to identify subtle changes.

Summary

Calcium imaging has proven to be advantageous as a method to probe cellular function and activity from many cells simultaneously. The ability to load Ca^{2+} indicator dye into neurons of the intact adult mammalian retina has been challenging. Here we have described a new method to load Ca^{2+} indicator dyes into GCL cells from developing to mature rodent retinas by electroporation. Following the procedure retinas remained light-responsive and loaded neurons showed robust repeatable Ca^{2+} responses to application of different drugs almost immediately after electroporation. Thus, electroporation adds to the current arsenal of techniques available to physiologists to probe retinal function.

Chapter 3: D-Serine Enhancement of NMDA Receptor-Mediated Ca^{2+} Responses

Preface

D-Serine is now recognized as an important signaling molecule throughout the CNS. In almost every tissue examined it has been identified as an endogenous coagonist of NMDARs and contributes to basal NMDA receptor activation. Following up on previous studies of calcium dynamics of RGCs *in vitro*, I investigated the effect of D-serine on NMDAR-mediated increases in $[Ca^{2+}]_i$. These results are presented in this chapter. However, since it was discovered that NMDARs required a coagonist there has been debate about whether the coagonist binding site is normally saturated. Are NMDARs primed with saturating concentrations of D-serine and/or glycine and just waiting for glutamate to come along or are coagonist levels dynamic, providing modulation of NMDARs? Shortly after my initial work with cultured RGCs, presented in this chapter, I became aware of interesting, but conflicting, results presented at the 2007 European Retina Meeting regarding D-serine in the retina. Jeffrey Diamond's group reported that D-serine was present at saturating levels while Robert Miller's group reported that they were sub-saturating. At that time I had done all my D-serine work in cultured cells but this controversy encouraged me to use the isolated retina preparation to determine, using Ca^{2+} imaging, if the coagonist binding site was saturated or not. Reports in the mid-1990s suggested that D-serine and glycine had different relative efficacies depending on which GluN2 subunit was expressed with GluN1. These studies used

expression systems and there were some obvious differences between the studies (discussed in this chapter). Using cultured RGCs I compared the two coagonists in a system that had a heterogeneous distribution of NMDAR subunits. Preliminary work from this chapter was presented in abstract form in 2008 at the Association for Research in Vision and Ophthalmology (ARVO) and the Canadian Neuroscience meetings. This work was subsequently published in the Journal of Neurochemistry (Daniels and Baldridge, 2010), the copyright permission for which is located in the Appendix.

Introduction

Glutamate is the primary excitatory neurotransmitter in the CNS including the retina. NMDA receptors (NMDARs) are one of several receptors that are activated by glutamate and are implicated in a host of glutamate-related processes and malfunctions such as induction of long term potentiation, synaptogenesis, schizophrenia and excitotoxicity (for review see Harris *et al.*, 1984; Sucher *et al.*, 1997; Constantine-Paton & Cline, 1998; Kristiansen *et al.*, 2007, respectively). A key feature of most NMDAR-gated channels is significant permeability to calcium ions (Ca^{2+}) and the alteration of intracellular calcium concentration ($[Ca^{2+}]_i$) allows NMDARs to influence more than just post-synaptic membrane potential. In order for NMDARs to be activated by glutamate, a second agonist (coagonist) must be bound to the receptor (Kleckner & Dingledine, 1988; but see Moriyoshi *et al.*, 1991; Nakanishi *et al.*, 1992; Curras & Pallotta, 1996) at a separate binding site that modulates NMDARs in a concentration-dependent manner (Johnson & Ascher, 1987). It is accepted that glycine is an endogenous coagonist for NMDAR activation, however within the past 15 years D-serine has emerged as an alternative (Matsui *et al*., 1995; Schell *et al*., 1997; Wolosker *et al*., 1999a; Mothet *et al*., 2000), particularly in regions of the CNS where glycine is absent or present at low levels.

There is growing evidence that D-serine serves as a NMDAR coagonist in the vertebrate retina (Stevens *et al*., 2003; Gustafson *et al*., 2007; Kalbaugh *et al*., 2009). These studies have established that exogenous ligand-mediated and post-synaptic NMDAR currents of retinal ganglion cells (RGCs) are modulated by D-serine. However, the impact of D-serine relative to glycine on RGCs has not been established definitively. Additionally, it is not clear if cells within the retina are differentially influenced by

ambient NMDAR coagonist concentration such that at any given moment some cells may be saturated with D-serine/glycine while others are not.

The influence of D-serine on electrophysiological properties of RGC NMDARs suggests that it could also be a modulator of RGC $[Ca^{2+}]_i$ but this has not yet been fully explored. To investigate the effect of D-serine on RGC NMDAR calcium dynamics we recorded changes in $[Ca^{2+}]_i$ using ratiometric calcium imaging. Immunopanned RGCs were used to determine the effective concentration range of D-serine and glycine and to compare their efficacy as NMDAR coagonists without influence from the retinal network. We found that both coagonists increase the NMDAR-mediated calcium response over ~3 log unit concentration range and that they were equally effective. There was no difference in the ability of D-serine versus glycine to enhance the glutamate-induced Ca^{2+} response or the NMDA-induced response in the absence or presence of ifenprodil, a GluN2B antagonist. NMDA-induced changes in $[Ca^{2+}]_i$ were also recorded from RGCs and other ganglion cell layer (GCL) cells in wholemount retinas to investigate the ability of exogenous and endogenous D-serine to influence NMDARs. We report that while many cells exhibit a D-serine-dependent enhancement of NMDAR-induced calcium responses, a significant proportion did not, suggesting saturation of the coagonist binding site in these cells. Finally, all RGCs examined in the wholemount retina show a decreased NMDA-induced calcium response following D-serine degradation by D-amino acid oxidase (DAAO; EC 1.4.3.3), suggesting a significant contribution of endogenous D-serine to NMDAR function.

Materials and Methods

All procedures were performed in accordance with the Dalhousie University Committee on Laboratory Animals. Chemicals were obtained from Sigma-Aldrich (Oakville, ON, Canada), unless otherwise noted.

Immunopurified RGC Cultures

Litters of Long-Evans rats (postnatal day 5-8; Charles River, Montreal, QC, Canada) were killed by overexposure to halothane vapor followed by decapitation. Retinas were dissected from 24 eyes, on average, in Hibernate-A culture medium (BrainBits, Springfield, IL, USA) with 2% B27 supplements (Invitrogen, Burlington, ON, Canada) and 10 μg ml^{-1} gentamicin. Retinas were incubated in 10 ml Ca^{2+}/Mg^{2+}-free Dulbecco's phosphate-buffered saline (DPBS; Invitrogen) with 165 units of papain (Worthington Biochemicals, Lakewood, NJ, USA), 1 mM L-cysteine, and 0.004% DNase for 30 min at 37°C, and then mechanically triturated in an enzyme inhibitor DPBS solution (with Ca^{2+} and Mg^{2+}) containing 1.5 mg ml^{-1} ovomucoid (Roche Diagnostics, Laval, QC, Canada), 1.5 mg ml^{-1} bovine serum albumin (BSA), and 0.004% DNase. The cell suspension was centrifuged at 200 g for 11 min and then washed in DPBS containing 10 mg ml^{-1} ovomocoid and BSA. Cells were resuspended in DPBS with 0.2 mg ml^{-1} BSA and 5 μg ml^{-1} insulin before incubation on panning plates. Immunopurified RGC cultures were generated from dissociated retinal cell suspensions as described previously (Barres *et al*., 1988; Hartwick *et al*., 2004) using a two-step Thy1.1-based immunopanning procedure. Immunopanned RGCs were plated onto poly D-lysine/laminin coated coverslips at a density of 5.0×10^4. Cells were maintained in 600

µl of serum-free culture medium consisting of Neurobasal-A with 2% B27 supplements, 1 mM glutamine, 50 ng ml^{-1} brain-derived neurotrophic factor (BDNF; PeproTech, Rocky Hill, NJ, USA), 10 ng ml^{-1} ciliary neurotrophic factor (CNTF; PeproTech), 5 µM forskolin and 10 µg ml^{-1} gentamicin. Cell cultures were maintained at 37°C in humidified (~80%) 5% CO_2-air atmosphere.

Cultured RGCs were prepared for calcium imaging by incubation in 5 µM fura-2 AM (Invitrogen) with 0.1% pluronic acid in Hanks Balanced Salt Solution (HBSS) at 37°C for 15-30 min. Once placed in the superfusion chamber cells were left for 10-20 min to allow for de-esterification and wash of excess fura-2 AM. Representative images of RGCs, with brightfield microscopy and the same RGCs loaded with fura-2, using the 380 nm excitation wavelength (510 nm emission) are shown in Figure 3.1a, b.

Retinal Wholemount Preparation

To load RGCs specifically with calcium indicator dye adult retinal wholemounts were prepared and RGC somas were retrogradely labelled (Baldridge, 1996; Hartwick *et al*., 2005; Hartwick *et al*., 2008). Retinas were cut into 4 pieces and mounted on black filter paper (Millipore) and a small volume (~0.5 µl) of 10-20% fura dextran solution (10,000 MW fura dextran dissolved in purified water; Invitrogen) was deposited into each wholemount (passing through all layers of the retina) using a tapered 26-guage needle mounted on a 10 µl syringe (Hamilton, Reno, NV, USA). In order to facilitate retrograde transport of fura dextran to the RGC soma via the cut axons the wholemount preparations were left in the dark in Hibernate-A medium supplemented with B27 for 8-12 hrs.

Fura-2 pentapotassium salt (Invitrogen) solution was electroporated into GCL cells using a protocol modified from spinal cord (Bonnot *et al*., 2005), characterized in

Chapter 2. Adult Long-Evans rats were killed with an intraperotineal injection of sodium pentobarbital (240 mg ml^{-1}; CDMV, Dartmouth, NS, Canada). Eyes were removed quickly and 4 µl of 30 mM fura-2 was injected into the vitreous through the optic nerve head. Tweezertrodes (BTX, Holliston, MA, USA) were positioned on the eye (cathode on the anterior pole, anode on the posterior pole) and five 40 V square wave pulses were applied for 50 ms at 1 Hz using the ECM 830 electroporation system (BTX). The retina was dissected out under red light in room temperature HBSS bubbled with 100% oxygen. Each retina was cut into 2-4 pieces and mounted separately onto black filter paper (Millipore, Bedford, MA, USA) GCL up and left in oxygenated HBSS for at least 30 min, to allow for recovery from the procedure, before transfer to the superfusion chamber for calcium imaging.

Calcium Imaging

The microscope chamber was superfused at ~1 ml min^{-1} with 100% oxygenated HBSS (without Mg^{2+} unless otherwise indicated) with 10 mM HEPES adjusted to pH 7.3-7.4 and warmed to 33-35°C. Strychnine (5-10 µM) was included in all solutions when glycine was used to block its inhibitory actions. All drugs were dissolved in HBSS on the day of the experiment and DAAO solution was made just prior to its use. Immunopurified RGCs (on coverslips) or retinal wholemount pieces (on filters) were transferred to the superfusion chamber following loading with the appropriate fura dye. Fura-2 (K_d = 140 nM) is a ratiometric dye and image pairs of 340 and 380 nm excitation were collected for 1000 ms and 700 ms, respectively. Image pairs were captured every 20-40s in the absence of any drug treatment to limit possible photo-bleaching. All drugs were bath applied by switching from the control superfusate to one containing the

appropriate treatment. During drug application image pairs were captured every 5-10s to ensure that the peak response was obtained. Increases in the fura ratio correspond to increases in $[Ca^{2+}]_i$, therefore we use these terms interchangeably.

Data Analysis

All data were analyzed using the peak change in the raw fura ratio relative to a baseline value averaged from five frames prior to a response and *n* values indicate individual cells. The number of coverslips/ pieces of retina are provided in the figure legends and each data set was obtained from at least two different cell cultures/animals. The individual Ca^{2+} response of different RGCs to glutamate agonist application varied considerably. Therefore, repeated measure statistics were used when possible and mean (± s.e.m.) results are presented as normalized data. However, the mean raw data (fura ratio values) are provided in the text. Experiments rely on the repeatability and reliability of agonist-induced Ca^{2+} responses. Multiple responses are obtained in response to the repeated application of iGluR agonists, with little deviation (<10%) in isolated retina (Figure 2.9) and cultured RGCs (Figure 3.1).

Results

D-Serine Enhances NMDAR-Mediated Calcium Increases in RGCs *In Vitro*

The ability of D-serine to enhance NMDAR currents in many cell types has been well characterized. We report here on its effects on $[Ca^{2+}]_i$, as reported by changes in the fura ratio, in immunopurified RGCs in response to multiple ionotropic glutamate receptor agonists (Figure 3.2). Bath application of 10 μM glutamate (30 sec) elicited an increase

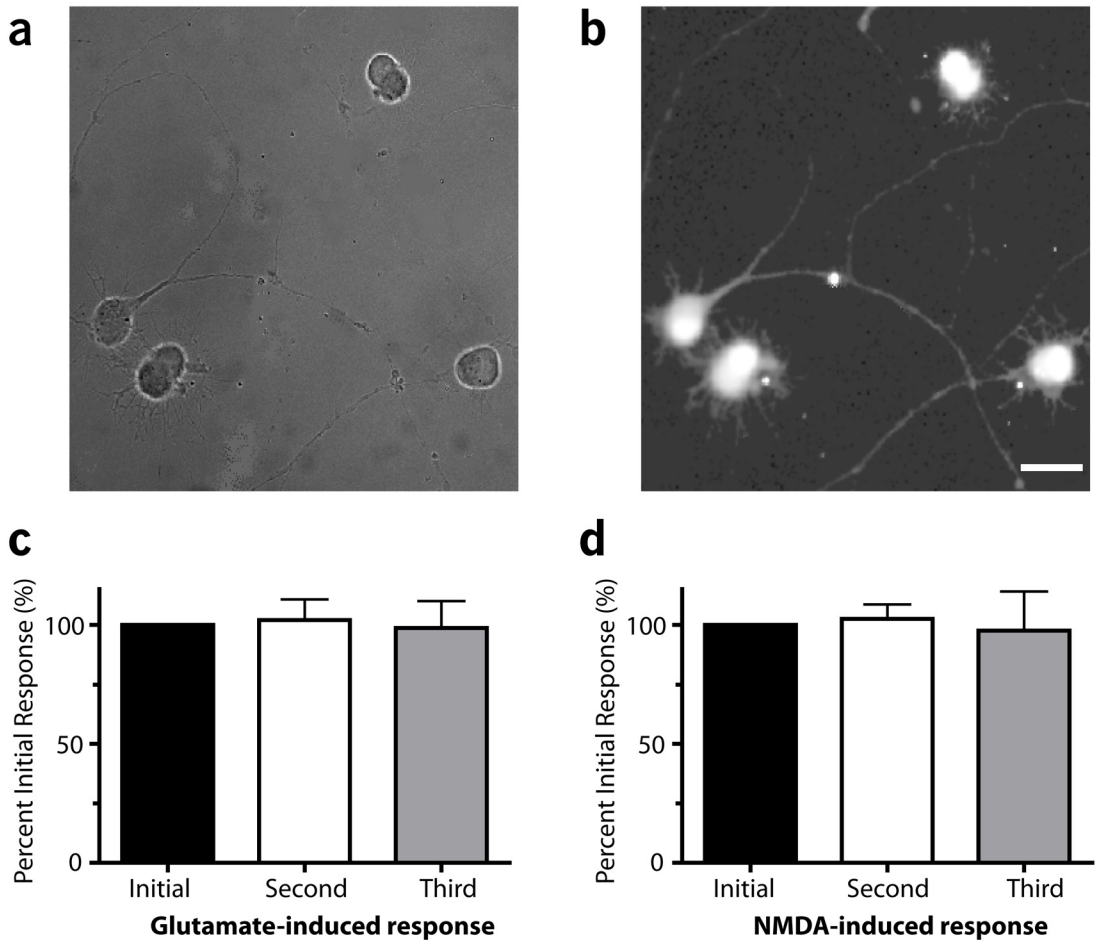

Figure 3.1 Control glutamate- and NMDA-induced Ca^{2+} responses from cultured RGCs. (a) Brightfield image of four immunopanned RGCs 2 days *in vitro*. (b) Fluorescence photomicrograph of the same RGCs loaded with fura-2 calcium indicator dye (380 nm excitation, 510 nm emission). Mean ± SD of (c) 10 μM glutamate- and (d) 100 μM NMDA-induced Ca^{2+} responses normalized to the first (initial) of three consecutive responses of each agonist (n=17 and 18 cells, respectively, each from three separate cell cultures). There is no significant difference between the three responses induced by glutamate or NMDA. Repeated measure one-way ANOVA. Scale bar = 20 μM.

of the fura ratio (Figure 3.2a) of 0.22 ± 0.06 a.u on average (Figure 3.2b). After recovery from the initial response 10 μM D-serine was coapplied with glutamate and caused a significantly ($P = 0.002$) greater $[Ca^{2+}]_i$ increase to 0.67 ± 0.12 a.u. (Figure 3.2a). To test the specificity of D-serine enhancement of this response similar experiments were performed using 100 μM NMDA (Figure 3.2c, d) or 50 μM kainate (Figure 3.2e, f) as the glutamate receptor agonist. NMDA alone caused a fura ratio increase of 0.07 ± 0.01 a.u. while coapplication with D-serine caused a significantly ($P < 0.0001$) larger increase to 0.28 ± 0.04 a.u. There was no significant difference ($P = 0.7081$) between kainate application alone (0.09 ± 0.02 a.u.) or when applied with D-serine (0.09 ± 0.03 a.u.). Taken together these results support the conclusion that D-serine is acting specifically at the NMDAR to enhance the glutamate-induced $[Ca^{2+}]_i$ increase.

To confirm that the enhancement by D-serine was due to its known role as an NMDAR coagonist we used two different compounds that also act at the NMDAR coagonist binding site (Figure 3.3). As above, the fura ratio increase in response to 10 μM glutamate alone was significantly enhanced ($P < 0.001$) by coapplication with 10 μM D-serine. This enhancement was completely and reversibly blocked following a 5 min exposure to the coagonist binding site antagonist 5,7-dichlorokynurenic acid (DCKA, 10 μM). However, at this concentration DCKA interfered with the 340 nm wavelength excitation of the fura 2 dye, due to its pale yellow color, as can be seen by the decreasing fura ratio baseline (arrow in Figure 3.3a). To ensure that the effect of DCKA was due to its pharmacological properties and not its colour in solution we also used the NMDAR coagonist binding site partial agonist 1-amino-cyclobutane-1-carboxylic acid (ACBC;

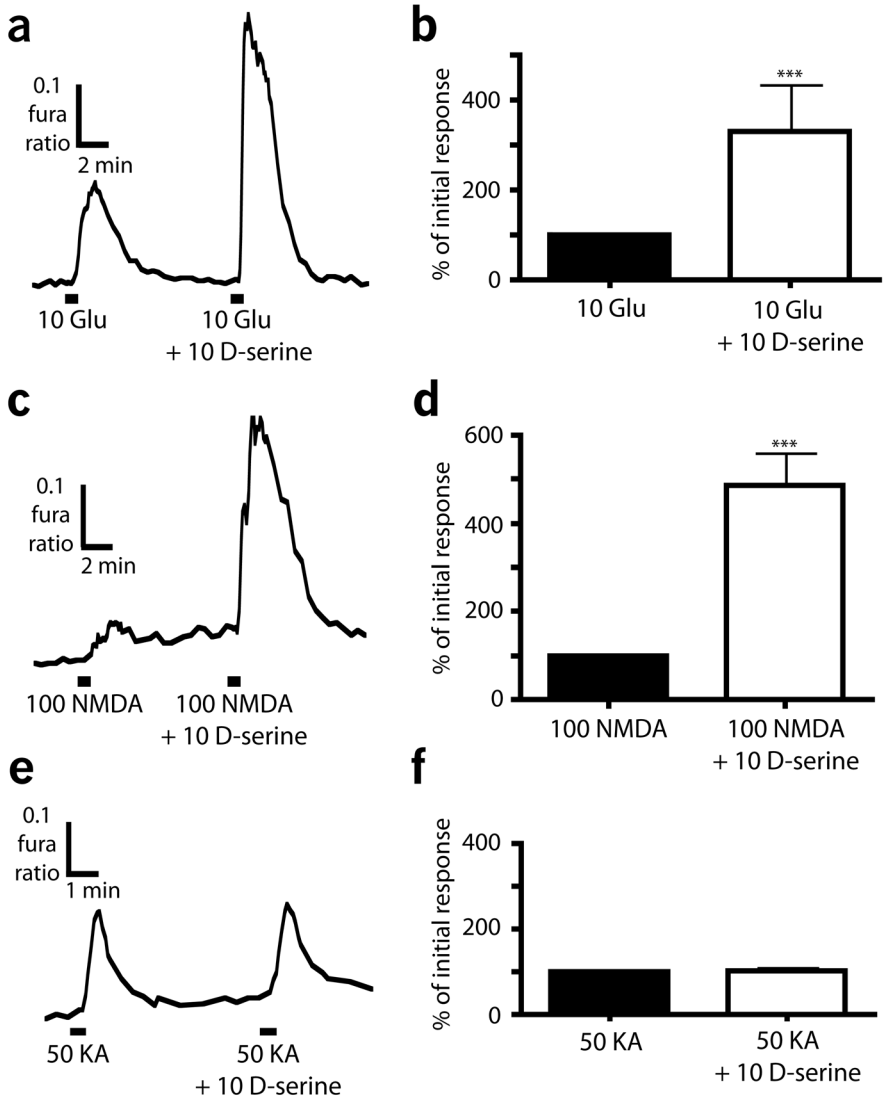

Figure 3.2 D-Serine enhances glutamate-induced $[Ca^{2+}]_i$ increases via NMDARs. (a, c, e) Example traces from 3 different cultured RGCs showing increased $[Ca^{2+}]_i$, in response to bath application of 10 μM glutamate (10 Glu), 100 μM NMDA and 50 μM kainate (50 KA). Following recovery to basal $[Ca^{2+}]_i$ D-serine was coapplied with each glutamate receptor agonist. (b, d, f) Normalized mean peak increases of fura-2 ratios in response to (b) glutamate (n=19 cells from 3 coverslips), (d) NMDA (n=20 cells from 4 coverslips) and (f) kainate (n=16 cells from 3 coverslips) with or without D-serine. (***$P < 0.001$, paired t-test; black bars indicate drug application).

100 μM) to compete with D-serine at the NMDAR (Figure 3.3c, d). A 5 min application of ACBC significantly ($P < 0.001$) reduced the effect of D-serine on glutamate-induced fura ratio increase, from 0.13 ± 0.02 to 0.07 ± 0.01 a.u., and the reduction was reversible (0.12 ± 0.02 a.u.). These findings confirmed that D-serine is acting specifically at the NMDAR coagonist binding site.

Comparison of D-serine and Glycine Enhancement of NMDAR-Mediated Ca^{2+} Increases *In Vitro*

D-Serine and glycine are NMDAR coagonists that are present endogenously in the CNS. There have been contradictory reports on their comparative efficacies as coagonists, which may depend on NMDAR subunit composition (Matsui *et al*., 1995; Priestley *et al*., 1995). Glycine acting at strychnine-sensitive glycine receptors is inhibitory and these receptors are expressed on most RGCs. We first tested whether the 30 sec glycine co-application with glutamate was sufficient to activate glycine receptors (Figure 3.4), thereby compromising any comparisons between D-serine and glycine acting at NMDARs. Glycine (10 μM) coapplied with 10 μM glutamate caused a Ca^{2+} response of 0.38 ± 0.31 a.u and there was no significant difference ($P = 0.22$) when compared to the same response in the presence of 5 μM strychnine (0.37 ± 0.29 a.u.). This supports the conclusion that 30 sec bath application of 10 μM glycine does not inhibit the glutamate- induced response. Nonetheless 5-10 μM strychnine was included in all solutions when glycine was used in the experiment as a precautionary measure. Dose response curves for RGCs were generated for D-serine and glycine (10 nM -1000 μM) coapplied with a 30 sec bath application of 10 μM glutamate (Figure 3.5a). The measured EC_{50} for D-serine was 3.31 μM and for glycine was 1.48 μM, however these

Figure 3.3 Glutamate-induced $[Ca^{2+}]_i$ increases are enhanced by D-serine acting at the NMDAR coagonist binding site. (a, c) Example fura-2 ratio traces showing increased $[Ca^{2+}]_i$ in response to 10 μM glutamate (10 Glu) alone and three subsequent coapplications with 10 μM D-serine (10 D-ser). Prior to the third peak (a) 10 μM DCKA or (c) 100 μM ACBC were washed in reducing the D-serine enhancement of the glutamate-induced Ca^{2+} response. The arrow indicates a change in baseline ratio due to DCKA reducing the fura-2 340 nm signal. (b) There was no significant difference (n.s.; repeated measures Tukey's one-way ANOVA; n=14 cells from 2 coverslips) between the mean peak response elicited by glutamate alone and when coapplied with D-serine in the presence of DCKA. D-Serine enhancement of the glutamate-induced Ca^{2+} response was completely recoverable (no significant difference between responses before and after DCKA application). (d) ACBC significantly reduced the effect of D-serine on the glutamate-induced Ca^{2+} response (Tukey's one-way ANOVA, n=30 cells from 5 coverslips) but did not completely block the effect (# $p<0.05$). The reduction of D-serine enhancement of the glutamate-induced Ca^{2+} response by ACBC was completely recovered following washout of ACBC. (***$P < 0.001$; black bars indicate drug application)

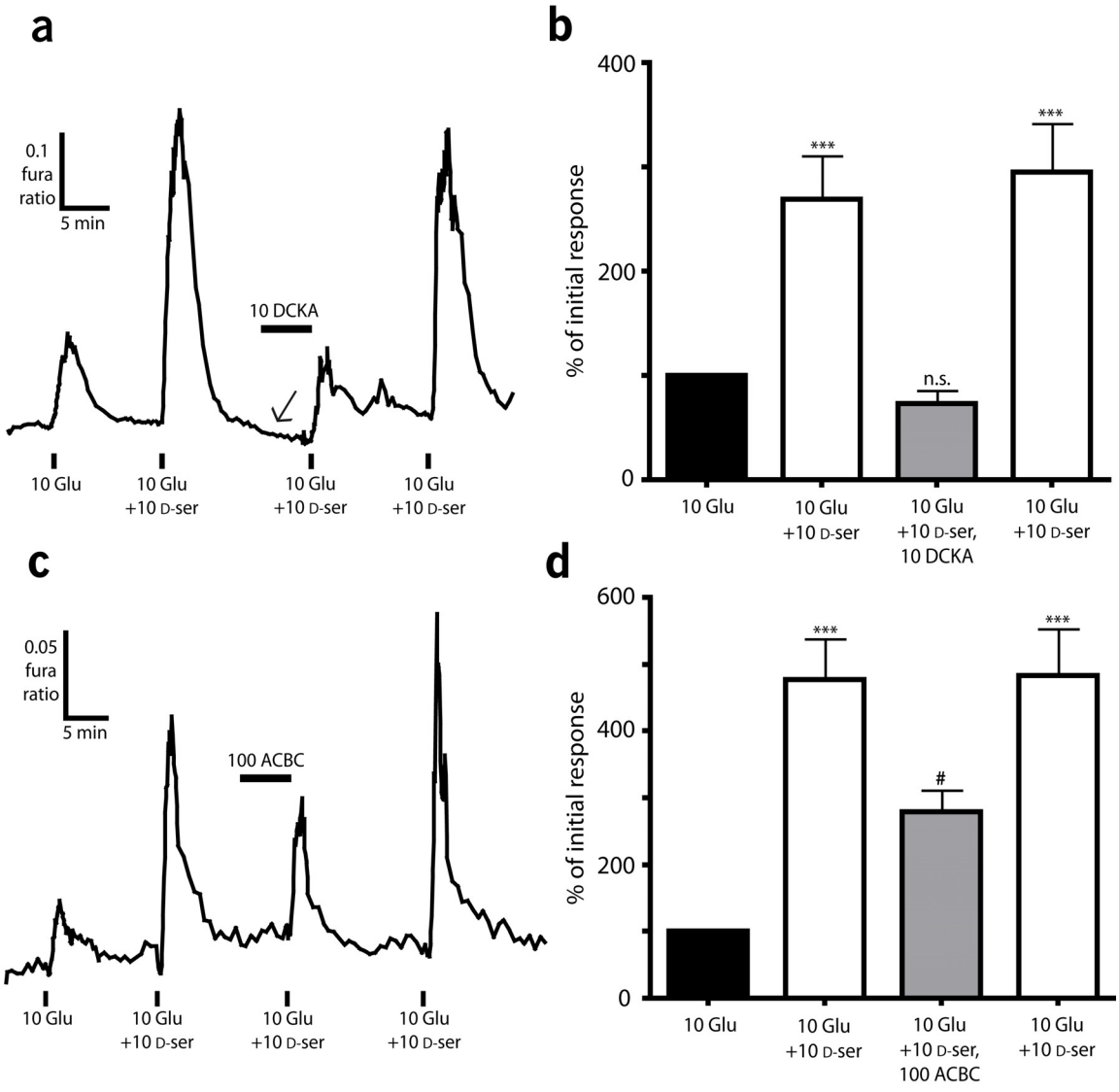
a
0.1
fura
ratio
5 min
10 DCKA
10 Glu
10 Glu
+10 D-ser
10 Glu
+10 D-ser
10 Glu
+10 D-ser
b
400
200
0
% of initial response
***
***
n.s.
10 Glu
10 Glu
+10 D-ser
10 Glu
+10 D-ser,
10 DCKA
10 Glu
+10 D-ser
c
0.05
fura
ratio
5 min
100 ACBC
10 Glu
10 Glu
+10 D-ser
10 Glu
+10 D-ser
10 Glu
+10 D-ser
d
600
400
200
0
% of initial response
***
***
#
10 Glu
10 Glu
+10 D-ser
10 Glu
+10 D-ser,
100 ACBC
10 Glu
+10 D-ser

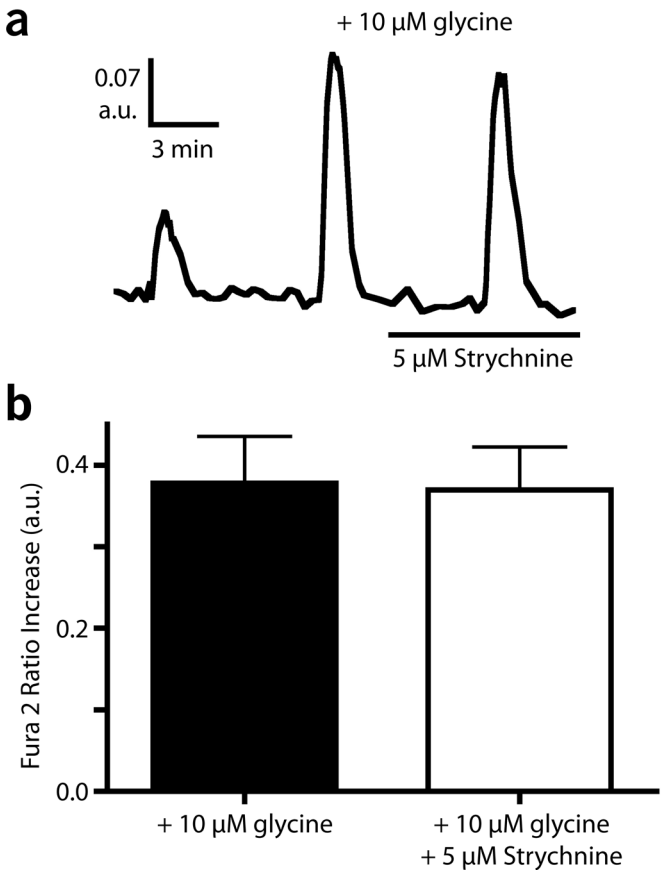

Figure 3.4 Glycine inhibition does not affect glutamate-induced Ca^{2+} responses. (a) Example trace of three consecutive 10 µM glutamate-induced (30 sec) Ca^{2+} responses. Glycine (10 µM) was coapplied with the second and third glutamate application and the third was performed in the presence of 5 µM strychnine. Mean ± SD glutamate plus glycine-induced Ca^{2+} responses in the absence (*left bar*) or presence (*right bar*) of strychnine and there was no significant difference between the two. Paired t-test, n=29 cells from 4 coverslips.

experiments did not allow for a direct, within-cell comparison of D-serine and glycine. Given the variability of the raw fura ratio response to 10 μM glutamate (~0.05 to 0.4 a.u.) we wanted to be certain that any observed differences were not due to a difference in the initial response. RGCs were exposed to 30 sec bath application of 10 μM glutamate followed by coapplication with 10 μM D-serine and then 10 μM glycine (or vice versa; Figure 3.5b). Both coagonists significantly ($P < 0.001$) enhanced the initial glutamate-induced fura ratio increase but there was no difference in their ability to do so (D-serine, 0.25 ± 0.04 a.u., glycine, 0.21 ± 0.03 a.u.). Similar results were obtained at 100 μM coagonist concentration (D-serine, 0.53 ± 0.05 a.u., glycine, 0.54 ± 0.05 a.u.). While the dose response curves indicated a difference between EC_{50} for D-serine and glycine there was no clear difference between the two coagonists when compared in the same RGCs.

We report a maximum effect at 100 μM for both coagonists (Figure 3.5b) but wondered if this was because the glutamate-induced response was saturated rather than coagonist saturation. To test this possibility the glutamate concentration was reduced from 10 to 5 μM and produced a fura ratio increase of 0.14 ± 0.02 a.u. when applied alone (Figure 3.6). This was followed by coapplication with 100 and 1000 μM D-serine that significantly ($P < 0.001$) enhanced the glutamate-induced response to 0.32 ± 0.03 and 0.29 ± 0.03 a.u., respectively. The same experiments were performed using 1 μM glutamate but it gave sporadic responses and was not consistently enhanced by coapplication with either coagonist up to 1000 μM. These findings confirm that 100 μM D-serine saturates the RGC NMDAR coagonist binding site.

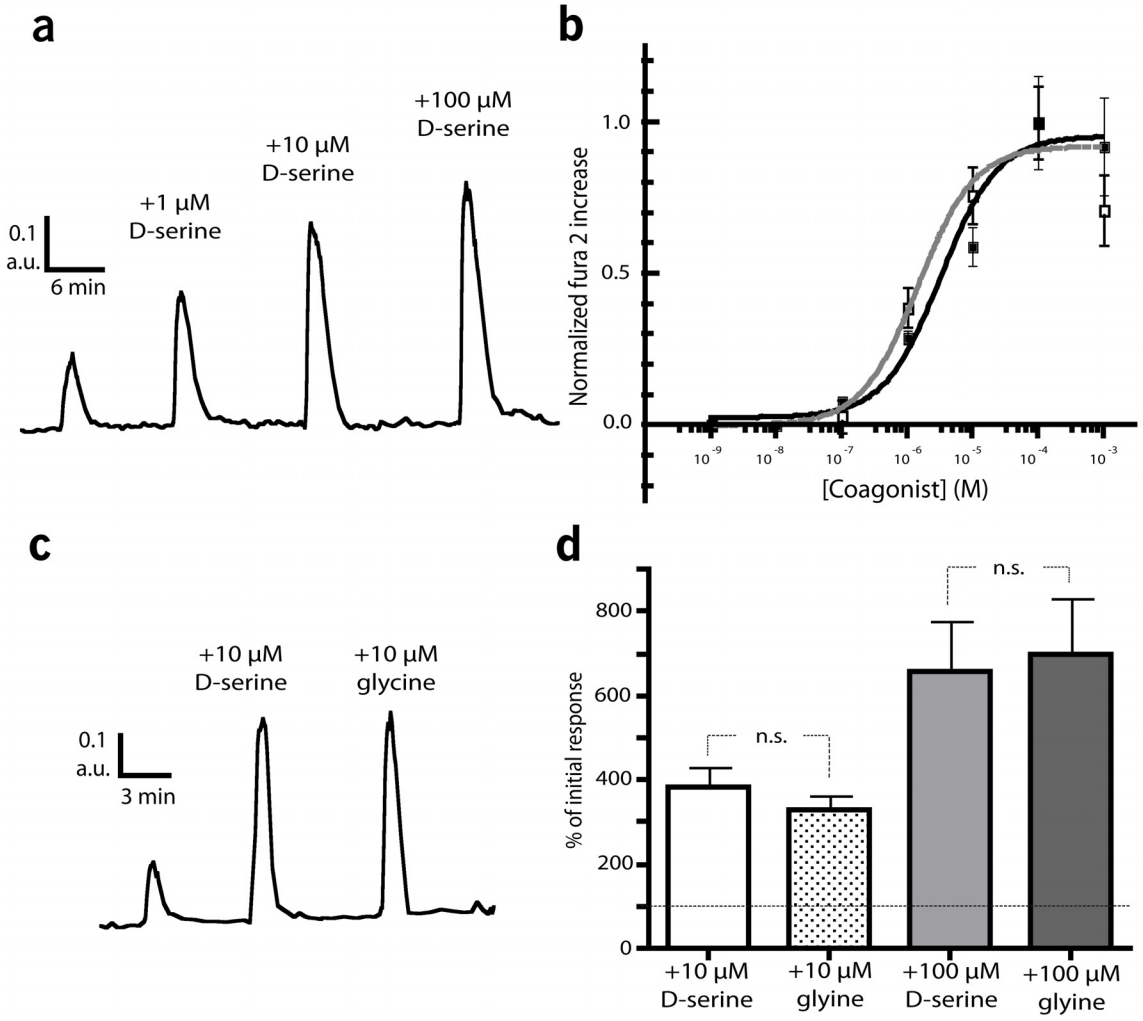

Figure 3.5 Comparison between D-serine and glycine as NMDAR coagonists. (a) Representative trace showing four consecutive Ca^{2+} responses to 30 sec 10 µM glutamate with increasing D-serine concentration (0-100 µM). (b) Dose-responses curves showing increasing $[Ca^{2+}]_i$ in response to glutamate plus increasing D-serine (black line) or glycine (grey line) concentrations. (c) Example trace comparing the effect of coapplication between 10 µM D-serine and glycine on glutamate responses in the same cell. (d) Mean normalized responses comparing D-serine and glycine in the same cells as coagonists at 10 µM (n=25 cells from 4 coverslips) and 100 µM (n=26 cells from 4 coverslips) when coapplied with glutamate. The dashed line indicates the initial glutamate response at 100%. n.s. not significant, repeat measures, one-way ANOVA.

Under similar experimental conditions the glutamate-induced calcium response has been shown to be predominated by NMDAR activation (Hartwick *et al*., 2008). However, we also compared the coagonists when coapplied with NMDA (Figure 3.7e) instead of glutamate to achieve a more 'pure' NMDAR-mediated response. D-Serine and glycine (10 μM) significantly ($P < 0.001$) enhanced the initial 100 μM NMDA-induced Ca^{2+} response from 0.017 ± 0.003 to 0.104 ± 0.025 and 0.104 ± 0.024 a.u., respectively, but there was no difference between this enhancement. Using expressions systems it has been shown that D-serine is a more potent NMDAR coagonist than glycine at GluN2A-containing NMDARs (Matsui *et al*., 1995; Priestley *et al* 1995). Therefore, we next sought to determine if a difference between D-serine and glycine could be identified by blocking the contribution of the GluN2B subunit. Consistent with our previous findings there was no difference between the ability of D-serine (0.065 ± 0.008 a.u.) and glycine (0.066 ± 0.009 a.u.) to enhance the initial NMDA-induced response (0.016 ± 0.002 a.u.; Fig. 4C) in the presence of ifenprodil (Figure 3.7d, f). Taken together this suggests that there is no preferential coagonist for GluN2B containing or non-containing NMDARs. Ifenprodil was also used to reveal a difference in the NMDAR subunit expression of cultured RGCs compared to GCL cells in the isolated retina. In cultured RGCs the initial NMDA Ca^{2+} response (0.17 ± 0.03 a.u.) was significantly ($P < 0.0001$) reduced by 77 ± 4 % following application of the specific GluN2B antagonist ifenprodil (3 μM, Figure 3.7a, b). This was a strong effect with relatively low variability indicating that the NMDAR-mediated Ca^{2+} responses in cultured RGCs was dominated by GluN2B. Alternatively, 6 μM ifenprodil application in the adult isolated retina resulted in a more varied effect as some cells exhibiting a strong, weak and no reduction (Figure 3.7c). The initial

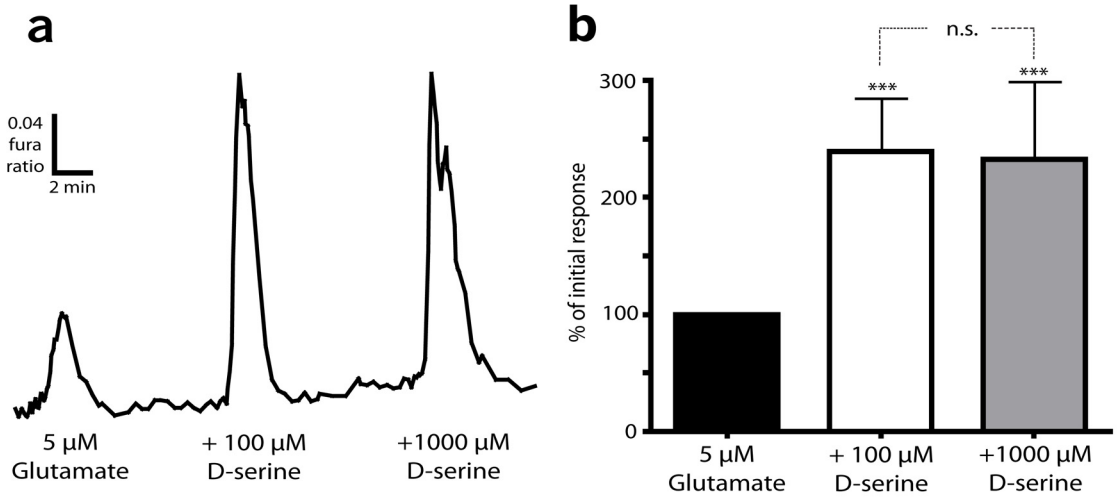

Figure 3.6 NMDAR coagonist binding site is saturated by 100 µM D-serine. (a) Example fura-2 ratio trace showing a similar enhancement of 5 µM glutamate Ca^{2+} response by 100 or 1000 µM D-serine. (B2) Mean normalized responses comparing 100 and 1000 µM D-serine (n=37 cells from 5 coverslips) coapplied with 5 µM glutamate. ***$P < 0.001$, n.s., not significant, repeated measures, Tukey's one way ANOVA

Figure 3.7 There is no coagonist selectivity for non-GluN2B containing NMDARs. (a) A fura-2 ratio trace of two responses to 100 μM NMDA (2 peaks) applications (30 sec) before (1st peak) and during (2nd peak) 3 μM ifenprodil application. (b) Mean normalized responses for effect of ifenprodil on the NMDA-induced Ca^{2+} response. (c) Scatter plots of the reduction of the NMDA-induced Ca^{2+} responses caused by infenprodil in cultured RGCs (left) and in cells from adult isolated retina (6 μM, right). Mean ± SD is indicated for each plot. (d) Representative trace showing similar enhancement of the NMDA-induced Ca^{2+} response by 10 μM glycine and D-serine in the presence of ifenprodil. Mean normalized responses comparing D-serine and glycine as coagonist when coapplied with NMDA in the (c) absence (n=19 cells from 3 coverslips) or (d) presence (n=45 cells from 6 coverslips) of ifenprodil. ***$P < 0.001$, n.s., not significant, repeated measures, Tukey's one way ANOVA.

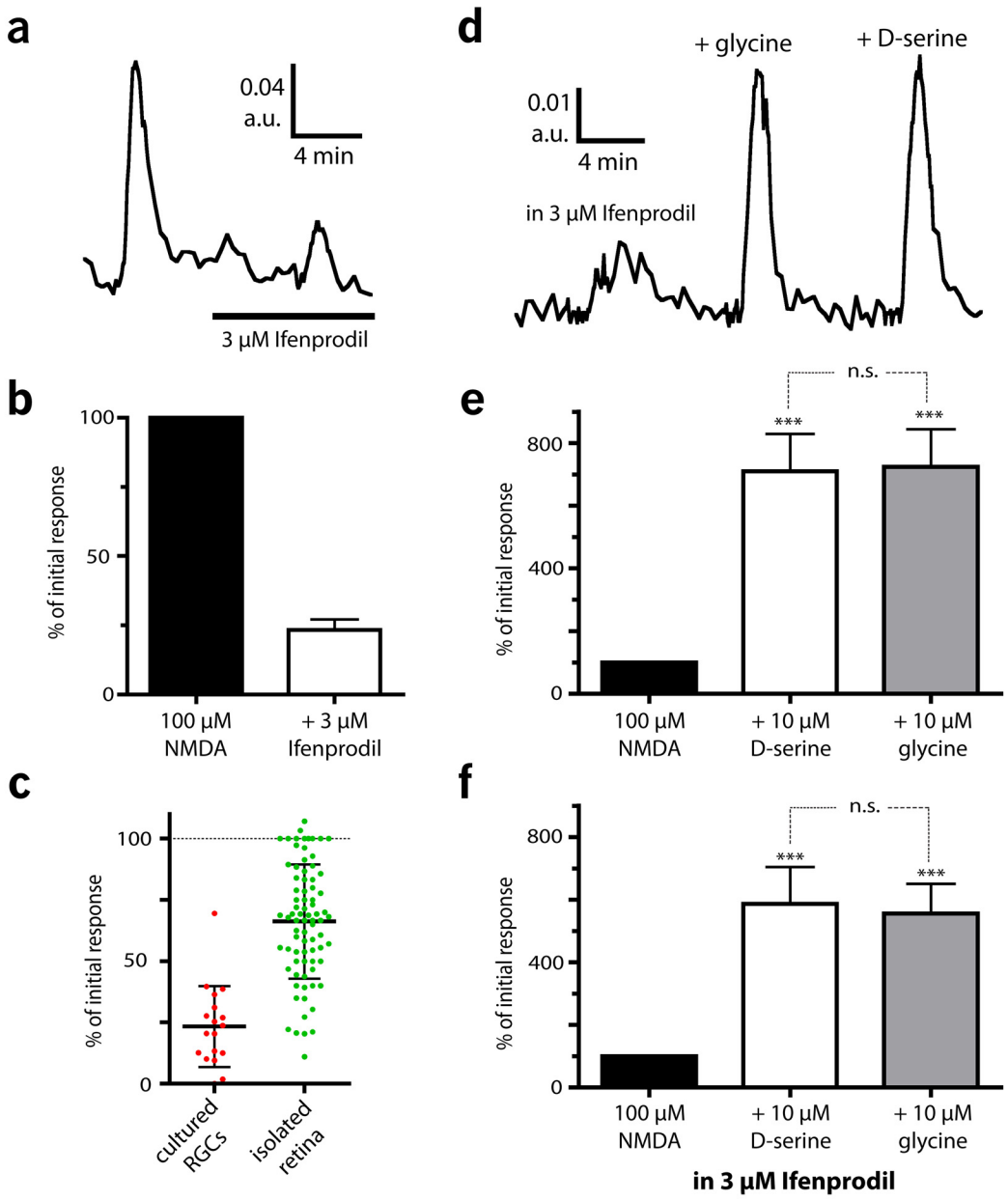
a
0.04
a.u.
4 min
3 µM Ifenprodil
d
+ glycine
+ D-serine
0.01
a.u.
4 min
in 3 µM Ifenprodil
b
% of initial response
100
50
0
100 µM NMDA
+ 3 µM Ifenprodil
e
n.s.
***
***
800
400
0
% of initial response
100 µM NMDA
+ 10 µM D-serine
+ 10 µM glycine
c
100
50
0
% of initial response
cultured RGCs
isolated retina
f
n.s.
***
***
800
400
0
% of initial response
100 µM NMDA
+ 10 µM D-serine
+ 10 µM glycine
in 3 µM Ifenprodil

NMDAR-mediated Ca^{2+} response (0.19 ± 10 a.u.) was significantly ($P < 0.001$) reduced by 32.6 ± 24.3% (n=81 cells from 5 retinas). Accordingly, this supports the varied expression of GluN subunits in the retina and suggests that cultured RGCs express GluN2B predominantly.

Endogenous D-serine in the Wholemount Retina

We next moved to the wholemount retina to investigate NMDAR coagonist binding site activation in a more physiological preparation. As glutamate is readily taken up by transporters in the retina, NMDA was used as NMDAR agonist. We first studied RGCs loaded with fura dextran (Figure 2.1). Bath application of 200 μM NMDA (60 sec) caused a peak increase in the fura ratio to 0.20 ± 0.04 a.u. that was significantly (P = 0.0011) enhanced to 0.26 ± 0.05 a.u. with a subsequent coapplication of 100 μM D-serine (Figure 3.8a *left trace*). However, under these conditions only 46% (17/37) of RGCs that responded to NMDA were enhanced by D-serine. Calcium responses were not saturated by 200 μM NMDA application alone because 500 μM NMDA consistently produced significantly ($P < 0.0001$) larger responses (233 ± 23.4%) and only 6% (3/54 from 5 retinas) of RGCs showed no change relative to the lower NMDA concentration. In a separate set of experiments GCL cells (including RGCs as identified by the presence of an axon) were loaded with pentapotassium fura-2 salt by electroporation (Figure 2.4). Two other drug application protocols were used that allowed for smaller, but repeatable, NMDA-induced increases in the fura ratio. Bath application of 200 μM NMDA (30 sec) caused a mean $[Ca^{2+}]_i$ increase of 0.15 ± 0.03 a.u. that was enhanced by the coapplication of 100 μM D-serine to 0.23 ± 0.04 a.u ($P < 0.001$) in 31/41 (76%) cells measured. Including Mg^{2+} in the superfusion solution limited NMDAR activation but reliable fura

ratio increases (0.10 ± 0.01 a.u.) were obtained with 500 μM NMDA and 46/53 (87%) cells exhibited an enhanced NMDA-induced fura ratio increase in the presence of 100 μM D-serine (0.22 ± 0.02 a.u., $P < 0.001$). These results indicate that D-serine enhanced the NMDA-induced fura ratio response in many but not all cells *in situ* and reducing the amplitude of the NMDA response increased the likelihood that D-serine would enhance the NMDA-mediated response.

To test the level of endogenous D-serine activation of the NMDAR coagonist binding site we specifically degraded D-serine using bath application of DAAO (Mothet *et al*., 2000; Stevens *et al*., 2003; Gustafson *et al*., 2007) to the wholemount retina. NMDA (200 μM) was bath applied for 60 sec causing a peak increase in the fura ratio of 0.30 ± 0.03 a.u. (Figure 3.8c). DAAO (400 μg/ml) was washed in for 10-15 minutes followed by another exposure to NMDA. In 20/32 RGCs the fura ratio response was significantly reduced to 0.17 ± 0.03 a.u. and was fully recovered by a subsequent coapplication of NMDA and 300 μM D-serine (0.31 ± 0.04 a.u.). In the other 12 cells DAAO caused a significant decrease in the NMDA-induced response that was not recovered by D-serine coapplication.

Discussion

The experiments presented here were designed to determine the impact of D-serine on NMDAR-mediated Ca^{2+} responses in RGCs activated by appropriate glutamate receptor agonists and to assess the level of NMDAR coagonist binding site saturation in the wholemount retina. Immunopurified RGCs were used to characterize the ability of

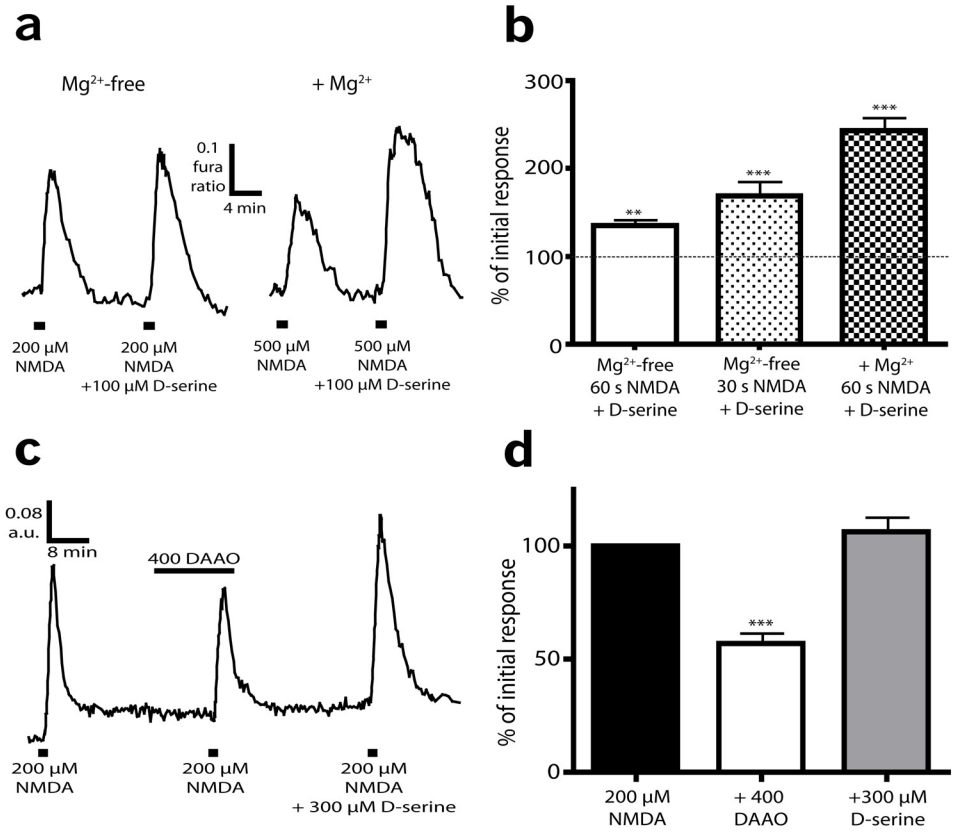

Figure 3.8. Effects of D-serine on RGC NMDA-induced Ca^{2+} responses in wholemount retina. (a) Example traces showing an increase in the fura-2 ratio in response to *left*, 200 µM NMDA (Mg^{2+}-free HBSS) or *right*, 500 µM NMDA (Mg^{2+}-containing HBSS) followed by a larger increase when coapplied with 100 µM D-serine. (b) Mean normalized responses from three separate experiments where D-serine was coapplied with NMDA following an initial NMDA-induced response (dashed line). NMDA (200 µM) was applied in Mg^{2+}-free HBSS for 60 (n=17 cells from 3 retinas) or 30 s (n=31 cells from 4 retinas) and in Mg^{2+}-containing HBSS for 60 s at 500 µM (n=46 cells from 5 retinas; paired t-test). (c) An example trace showing a smaller NMDA-induced fura ratio increase in the continued presence of 400 µg/ml DAAO (400 DAAO, second peak), compared to its absence (first peak), which was recovered by the coapplication of 300 µM D-serine (third peak). (d) Mean normalized responses for the initial NMDA-induced response, following DAAO application and with coapplication of D-serine. (n=20 cells from 4 retinas; repeated measures, Tukey's one way ANOVA). Black bars indicate drug application. $^{**}P < 0.01$, $^{***}P < 0.001$.

D-serine to influence NMDARs in a preparation free from synaptic and network influences with little contribution from natively produced NMDAR coagonists. Using this reduced preparation we demonstrated that D-serine produced a dose-dependent enhancement of glutamate-induced $[Ca^{2+}]_i$ increases in RGCs and specified this effect to its action as an NMDAR coagonist. In intact CNS, glycine is normally cleared from the extracellular space by glycine transporters, making it difficult to compare the actions of exogenously applied D-serine and glycine. Therefore, cultured RGCs were used to compare D-serine and glycine as NMDAR coagonists. When compared directly, there was no significant difference between the efficacy of D-serine and glycine as NMDAR coagonists. D-Serine was shown to enhance NMDA-induced Ca^{2+} responses in many but not all cells that were investigated in the wholemount retina. However, by reducing the Ca^{2+} response by decreasing NMDA application time or including Mg^{2+} in solutions, the number of cells that were responsive to D-serine coapplication was greatly increased. Finally, the specific degradation of endogenous D-serine in the retina by DAAO reduced the NMDA-induced $[Ca^{2+}]_i$ increase by ~45% and this was recovered fully in most cells by the subsequent coapplication of a saturating D-serine concentration.

Characterization of D-Serine Enhancement of NMDAR-Dependent Increases of RGC $[Ca^{2+}]_i$ *In Vitro*

There has been extensive characterization of coagonist enhancement of NMDAR channel currents (for example Johnson & Ascher, 1987; Kleckner & Dingledine, 1988; Matsui *et al.*, 1995; Curras & Pallotta, 1996; Mothet *et al.*, 2000; Gustafson *et al.*, 2007; Kalbaugh *et al.*, 2009), but only a few reports on its effects on NMDAR channel calcium influx (Wroblewski *et al.*, 1989; Baron *et al.*, 1990; Oliver *et al.*, 1990; Rabe & Tabakoff, 1990). To our knowledge this is the first study in RGCs to explore the specific effect of

D-serine on NMDA-induced calcium responses and to compare the efficacy of the two endogenous NMDAR coagonists. Previous studies have reported that NMDAR coagonists have a maximum effect at 30-100 μM (Kleckner & Dingledine, 1988; Bonhaus & McNamara, 1989; Mayer *et al.*, 1989; Mothet *et al.*, 2000). It has been suggested (Kleckner & Dingledine, 1988; Kessler *et al.*, 1989) that the observed range is due to variable background levels of glycine present in physiological solutions (Berger, 1995). This is also thought to account for why NMDAR activity can be seen with a glutamate receptor agonist alone when NMDAR function is thought to be absolutely dependent upon coactivation by D-serine or glycine (Kleckner & Dingledine, 1988). Like others we find that 100 μM D-serine is a saturating concentration at the coagonist binding site and therefore assume that our solutions have minimal glycine contamination.

NMDAR Coagonist Comparison

Two studies have used expression systems to compare D-serine and glycine as NMDAR coagonists (Matsui *et al*., 1995; Priestley *et al*., 1995) while also distinguishing their efficacy depending on NMDAR subunit composition using whole-cell recording. Matsui and colleagues (1995) expressed GluN1 with each individual GluN2 subunit (A-D) in *Xenopus* oocytes and found that D-serine had an ED_{50} at least 3 times lower than glycine for each subunit composition when coapplied with 10 μM glutamate. In similar experiments Priestley and colleagues (1995) reported that NR1 coexpressed with GluN2A or B in mouse fibroblast cells show a 2-fold greater affinity for D-serine (GluN2A) or a 3-fold greater affinity for glycine (GluN2B). A consistent finding in these studies is that both coagonists have a greater affinity for GluN1 when coexpressed with GluN2B rather than 2A. The expression of all NMDAR subunits has been demonstrated

in rodent RGCs with GluN1/2A and 2B predominating (Fletcher *et al.*, 2000; Sucher *et al.*, 2003; Zhang & Diamond, 2006; Jakobs *et al.*, 2007). Given the differences in Ca^{2+} influx due to subunit expression (see Cull-Candy *et al*., 2001), variability in NMDAR composition may account for the range of NMDA and glutamate-induced Ca^{2+} responses and that of the coagonist affinity seen in our experiments. The dose response curve experiments reported here revealed a slightly greater affinity for glycine over D-serine but they were performed on separate cells. When we compared D-serine and glycine (in the presence or absence of the GluN2B antagonist ifenprodil) within the same RGCs, thereby reducing the impact of response variability between cells, we found no difference in their efficacy as NMDAR coagonists.

D-Serine Modulation of NMDARs *In Situ*

It has been demonstrated that the coagonist binding site of RGC NMDARs is not saturated in intact retinal preparations (Lukasiewicz & Roeder, 1995; Stevens *et al.*, 2003; Gustafson *et al.*, 2007; Kalbaugh *et al.*, 2009). All of these studies used electrophysiology to measure changes in NMDAR activity, limiting the examination to one cell at a time. In our study exogenous D-serine application enhanced NMDA-induced calcium responses in many cells indicating that extracellular NMDAR coagonist concentration is sub-saturating for many GCL cells. However, calcium imaging affords the ability to measure NMDAR activity from multiple cells simultaneously (typically 5-10 cells per piece of retina) and in some cells the NMDA-induced response was not enhanced by D-serine. This is in direct contrast to our isolated RGCs where virtually every NMDAR-mediated $[Ca^{2+}]_i$ increase was enhanced by D-serine. We report that reducing NMDAR activity (smaller NMDA-induced fura ratio response) increased the

proportion of cells whose NMDA-induced calcium response was enhanced by D-serine. There are three plausible mechanisms that could account for this occurrence. (1) Bath application of NMDA (200 μM, 60 sec) alone may have saturated the calcium response of some cells even in the presence of sub-saturating endogenous coagonist concentration. By reducing NMDAR activation the number of cells with saturated NMDA-mediated calcium responses would be reduced allowing for enhancement by D-serine application. However, we do not believe this contributes significantly to our observations because 200 μM NMDA does not produce a saturating response as 500 μM consistently produces larger calcium responses under similar conditions (233 ± 23.4% greater response achieved with 500 μM NMDA). (2) There could be a reduction in the amount of NMDAR coagonist released endogenously as a result of the NMDA bath application. Kalbaugh and colleagues (2009) show that synaptically activated NMDARs can be saturated by the transient presumptive release of coagonist, similar to findings at the mossy fibre-granule cell synapse in the cerebellum (Billups & Attwell, 2003). Stimulation of glycinergic amacrine cells with bath applied NMDA could cause glycine release adding to the extracellular coagonist concentration. D-Serine is found in all, but predominantly Müller, glial cells in the retina (Stevens *et al*., 2003). NMDA could indirectly signal glial cells, which are known to release D-serine following non-NMDA glutamate receptor activation (Mothet *et al*., 2005). Recently, mRNA for the D-serine synthesizing enzyme, serine racemase, was identified in Müller cells as well as neurons throughout the GCL and inner nuclear layer (Takayasu *et al*., 2008) providing another potential source of releasable D-serine. (3) Cells that do not respond to exogenous coagonist coapplication may express NMDAR subunits with greater affinity for coagonist

as there is an increasing affinity for NMDAR coagonists from GluN2A to 2D expressing NMDAR channels. Our experiments were performed after loading fura dye into RGCs specifically (dextran) or GCL cells including RGCs (electroporation). It is possible that the increased percentage of cells responding to D-serine (from 46% to >75%) was due to the inclusion of other cell types (in particular amacrine cells) in the analysis and not simply the altered NMDA application protocol. The larger percentage of cells with NMDA-induced responses affected by D-serine could be due to differential NMDAR subunit expression by different cell types (Martina *et al*., 2003).

The results of many studies, including this one, are consistent with a role for endogenous D-serine in the retina. Enzymatic degradation of D-serine by DAAO has repeatedly been shown to reduce RGC NMDAR activity (Stevens *et al*., 2003; Gustafson *et al*., 2007; Kalbaugh *et al*., 2009). A lingering question concerns whether this is physiological or an artificial indication of ambient D-serine levels caused by the removal and preparation of the retina for experiments. NMDA-induced RGC death was significantly reduced by DCKA or DAAO *in vivo* (Hama *et al*., 2006) supporting the idea that NMDA coagonist levels are sufficient to influence NMDARs *in vivo*. Furthermore, since coapplication of either coagonist with NMDA significantly increased RGC death, their endogenous levels must be sub-saturating (Hama *et al*., 2006) indicating that retinal preparations (wholemount and slice) closely approximate extracellular NMDAR coagonist concentrations *in vivo*. However, it is unclear whether the implied sub-saturating extracellular coagonist concentration also reflects the level of coagonist saturation at synaptic NMDARs (versus extrasynaptic), which may vary considerably. D-Serine and glycine concentrations from rat vitreous samples have been measured to be

approximately 2 and 5 μM, respectively (Thongkhao-On *et al*., 2004). Based upon the NMDAR coagonists dose response curves such concentrations would contribute sub-maximal enhancement of NMDAR activity, but questions as to whether those measurements accurately reflect those within the retina and whether coagonist concentration fluctuates still remain.

Chapter 4: Functional Evidence for D-Serine Inhibition of Non-NMDA iGluRs

Preface

D-Serine has continued to receive much attention for its now well-established coagonist activity at NMDARs. For the last 5 years, in particular, it has been investigated as a stand alone therapeutic agent in disease states that involve NMDAR hypo- or hyperfunction, such as schizophrenia. Therefore any alternative actions that D-serine might have should be identified to better understand its physiological role and its specific actions as it pertains to drug therapy.

Three events led me to the pilot experiments that paved the way for the data presented in this chapter. (1) I observed that the 1000 μM D-serine enhancement of 10 μM glutamate-induced Ca^{2+} responses (Chapter 3) were sometimes, but not consistently, smaller than with 100 μM D-serine. (2) A paper published by Gong and colleagues (2007) showed that D-serine could inhibit AMPAR-mediated currents in primary cultured hippocampal neurons. (3) At the 2008 Canadian Association for Neuroscience meeting a poster (subsequently published, Faye *et al*., 2009) reported data that suggested the direct binding of D-serine to the kainate receptor glutamate binding site and that responses from GluK2-expressing HEK 293 cells were antagonized by D-serine. Taken together, these results suggested that D-serine could inhibit AMPA or kainate receptors.

Ultimately, I wanted to know whether D-serine inhibition of non-NMDA iGluRs could be physiologically relevant. My initial experiments were to determine the effects

of endogenous D-serine degradation in isolated retina on kainate-induced Ca^{2+} responses and exogenous D-serine application on responses in cultured RGCs. Both results were positive and I continued on with some imaging and patch clamp experiments in cultured cells, but the majority of data was collected from the isolated retina preparation. I next determined that D-serine inhibited bath-applied kainate-induced Ca^{2+} responses in the isolated retina in a concentration dependent manner. In order to ensure that the effect that I saw using Ca^{2+} imaging in the isolated retina was not biased by the methodology, I turned to 2 other techniques that examined synaptically activated iGluRs. An inhibitory effect of D-serine was evident in spontaneous EPSC recordings from RGCs in the isolated retina and light-evoked spiking recorded using isolated guinea pig retina using the multi electrode array (MEA). The MEA was a new piece of equipment obtained by Dr Francois Tremblay who kindly allowed me access to it and his MSc student, Leah Wood, introduced me to the technique. Their previous attempts with rats/mice were unsuccessful, as were mine, and I decided to use guinea pig retinas for these experiments even though all other experiments were from rat. In a timesaving effort, Leah kindly prepared retinas for the MEA recordings but all the experiments, data analysis and mistakes are mine. Lastly, I characterized the contribution of Ca^{2+}-permeable AMPARs to glutamatergic RGC Ca^{2+} responses and showed that the inhibitory effect of D-serine using imaging is predominantly mediated by these receptors.

A portion of this data was presented in abstract form at the 2009 European Retina Meeting in Oldenburg, Germany.

Introduction

D-Serine is a coagonist of *N*-methyl-D-aspartate receptors (NMDARs) (Johnson & Ascher, 1987) and coagonist binding is necessary for full NMDAR-gated channel activity (Kleckner & Dingledine, 1988; Nakanishi *et al.*, 1992; Curras & Pallotta, 1996). D-Amino acids were initially thought not to occur naturally in vertebrates, however, D-serine was eventually identified in the central nervous system (CNS: Hashimoto *et al.*, 1992; Hashimoto *et al.*, 1995; Hashimoto & Oka, 1997; Schell *et al.*, 1997) and then its synthesizing enzyme, serine racemase (SRR), was successfully identified and cloned (Wolosker *et al*., 1999a; Wolosker *et al*., 1999b), solidifying its acceptance as an endogenous substance. Over the past decade D-serine has been identified as an important endogenous coactivator of NMDARs throughout the CNS, including the retina. For example, in the cerebellum (Mothet *et al*., 2000) and retina (Stevens *et al.*, 2003; Kalbaugh *et al.*, 2009; Daniels & Baldridge, 2010) degradation of endogenous D-serine has clearly been shown to reduce NMDAR function.

Interestingly, a select few have reported results that imply that D-serine may have actions separate from its accepted role as an NMDAR coagonist. *In vivo* experiments in the rat thalamus showed that glycine and D-serine could inhibit kainate- and quisqualate-induced responses but only the effect of glycine was prevented by strychnine (Salt, 1989) suggesting that the effect of D-serine was independent of glycine receptors. Similarly, serendipitous results from the study of salamander retinal slices reported that D-serine greatly reduced light-evoked excitatory postsynaptic currents (EPSCs) in retinal ganglion cells (RGCs; Lukasiewicz & Roeder, 1995). D-(^{3}H)Serine binding in rat brain synaptosomes revealed a D-serine binding site that was insensitive to displacement by

5,7-dichlorokynurenic acid, a potent NMDAR coagonist binding site antagonist (Matoba *et al*., 1997). To our knowledge the identity of the non-NMDAR binding site is still unknown. Finally, Gong and colleagues (2007) showed that D-serine reduced non-NMDA ionotropic glutamate receptor (iGluR)-mediated currents in primary cultured hippocampal neurons and suggested that the effect was mediated by α-amino-3-hydroxy-5-methyl-4-isoxazoleproprionic acid receptor (AMPAR) inhibition. Taken together these studies support an inhibitory role for D-serine that is independent of its excitatory action at NMDARs.

In this study we first show that non-NMDA iGluR-mediated increases in intracellular calcium (Ca^{2+}) concentration ($[Ca^{2+}]_i$) and AMPA-evoked currents are reduced by D-serine in primary cultured RGCs. The remaining experiments were performed on acutely isolated wholemount retinas. Ratiometric Ca^{2+} imaging experiments revealed a reversible, concentration-dependent reduction of kainate-induced responses by D-serine but potassium (K^+)-induced responses were unaffected. These findings argue against a non-specific inhibitory action of D-serine and suggest it is specific to AMPA/KA receptors. D-Serine was also shown to reduce glutamatergic responses that were synaptically driven, from sEPSCs in RGCs and light-evoked spiking using the multi electrode array (MEA). Using the D-serine degrading enzyme D-amino acid oxidase (DAAO) we demonstrate that in our preparation a subpopulation of cells were inhibited by endogenous D-serine showing that D-serine can reach sufficient concentrations to affect non-NMDA iGluRs. Finally, we show that the effect of D-serine on Ca^{2+} responses was prevented by first blocking calcium-permeable AMPARs (CP-AMPARs).

Materials and Methods

Procedures were performed in accordance with the Dalhousie University Committee on Laboratory Animals. Chemicals were purchased from Sigma-Aldrich (Oakville, ON, Canada) unless otherwise stated. All external recording solutions included a standard cocktail of at least 10 μM strychnine, 50 μM picrotoxin and 20 μM MK-801 to block glycine, GABA and NMDA receptors, respectively.

Immunopurified RGC Cultures

Litters of Long-Evans rats (postnatal day 5-8; Charles River, Montreal, QC, Canada) were killed by overexposure to halothane vapor followed by decapitation. Retinas were dissected from 24 eyes, on average, in Hibernate-A culture medium (BrainBits, Springfield, IL, USA) with 2% B27 supplements (Invitrogen, Burlington, ON, Canada) and 10 μg/ml gentamicin. Retinas were incubated in 10 ml Ca^{2+}/Mg^{2+}-free Dulbecco's phosphate-buffered saline (DPBS; Invitrogen) with 165 units of papain (Worthington Biochemicals, Lakewood, NJ, USA), 1mM L-cysteine, and 0.004% DNase for 30 min at 37°C, and then mechanically triturated in an enzyme inhibitor DPBS solution (with Ca^{2+} and Mg^{2+}) containing 1.5 mg/ml ovomucoid (Roche Diagnostics, Laval, QC, Canada), 1.5 mg/ml bovine serum albumin (BSA), and 0.004% DNase. The cell suspension was centrifuged at 200 g for 11 min and then washed in DPBS containing 10 mg/ml ovomocoid and BSA. Cells were resuspended in DPBS with 0.2 mg/ml BSA and 5 μg/ml insulin before incubation on panning plates. Immunopurified RGC cultures were generated from dissociated retinal cell suspensions using a two-step Thy1.1-based

immunopanning procedure. Immunopanned RGCs were plated onto poly D-lysine/laminin coated coverslips at a density of 2.5 or 5.0 x 10^4. Cells were maintained in 600 µl of serum-free culture medium consisting of Neurobasal-A with 2% B27 supplements, 1 mM glutamine, 50 ng/ml brain-derived neurotrophic factor (BDNF; PeproTech, Rocky Hill, NJ, USA), 10 ng/ml ciliary neurotrophic factor (CNTF; PeproTech), 5 µM forskolin and 10 µg/ml gentamicin. Cell cultures were maintained at 37°C in humidified (~80%) 5% CO_2-air atmosphere. Full details have been described previously (Barres *et al*., 1988; Hartwick *et al*., 2004). Coverslips were incubated in 5 µM fura-2 AM (Invitrogen) with 0.1% pluronic acid (15 min) and subsequently washed for at least 10 min in preparation for Ca^{2+} imaging.

Rat Retinal Wholemount Preparation

Adult Long Evans rats (250-400 g) were killed with an intraperotineal injection of sodium pentobarbital (240 mg/ml, CDMV, Dartmouth, NS, Canada) and the eyes were removed quickly. For WCR experiments retinas were removed under dim light, placed directly in recording chamber and held in place by a harp (Warner Instruments, Hamden, CT, USA). For Ca^{2+} imaging experiments fura-2 pentapotassium salt (Invitrogen) solution was electroporated into the retina (Daniels & Baldridge, 2010) following a modified spinal cord protocol (Bonnot *et al*., 2005). Eyes were removed quickly and 4 µl of 22 mM fura-2 was injected into the vitreous through the optic nerve head. Tweezertrodes (BTX, Holliston, MA, USA) were positioned on the eye (anode on the anterior pole, cathode on the posterior pole) and five 40 V square wave pulses were applied for 50 ms at 1 Hz using the ECM 830 electroporation system (BTX). The retina was dissected out under red light in room temperature HBSS bubbled with 100% oxygen.

Each retina was cut into 2-4 pieces and mounted separately onto black filter paper (Millipore, Bedford, MA, USA) GCL up and left in oxygenated HBSS for at least 30 min, to allow for recovery from the procedure, before transfer to the superfusion chamber for calcium imaging.

Whole-Cell Patch Clamp Recordings

Voltage clamp WCR was used for all experiments using micropipettes (8-10 MΩ) filled with (in mM) 115 K-gluconate, 9.7 KCl, 5 NaCl, 1 $MgCl_2$, 0.5 $CaCl_2$, 10 HEPES and 1.5 EGTA (pH 7.3). The solution for wholemount experiments also included 2.5 mM Neurobiotin for subsequent cell identification. The extracellular solution contained (in mM) 137 NaCl, 5.4 KCl, 1.3 $CaCl_2$, 0.8 $MgSO_4$, 0.3 Na_2HPO_4, 0.4 KH_2PO_4, 5 glucose and 10 HEPES (pH 7.4) and was superfused (100% oxygenated) at 2 ml/min at ~23ºC. Recordings were performed using a Multiclamp 700A amplifier, Digidata 1322A digitizer and pClamp 8 software and analyzed off-line with Clampfit 10 (Molecular Devices Inc., Sunnyvale, CA, USA). Recordings were low pass filtered at 2-3 kHz, digitized and sampled at 10 kHz. A -10 mV step (250 ms) was consistently applied throughout each experiment to monitor input resistance. Series resistance was uncompensated. For pressure ejection (~0.05 psi) experiments micropipettes (4-5 MΩ), filled with 500 μM AMPA in external solution, were fitted to a modified fast perfusion system ($VC^3$4, ALA Scientific Instruments, Farmingdale, NY, USA) and the tip positioned within 15 μm of an RGC soma with a manual micromanipulator (Fine Science Tools, North Vancouver, BC, CAN).

Calcium Imaging

The recording chamber was superfused at ~2 ml/min with 100% oxygenated HBSS (10 mM HEPES, pH 7.4) at ~23ºC. Cultured RGCs (coverslips) or a piece of isolated retina (filter paper) was transferred to the chamber and allowed to equilibrate for 10-15 min. Ratiometric fura-2 dyes (K_d = 140 nM) were used and image pairs of 340 and 380 nm excitation were collected with an exposure of 400 ms each. Image pair was captured with a CCD camera (Sensicam, PCO) and recorded using Imaging Workbench 4 software (Molecular Devices) every 20 sec during baseline recordings and every 5 sec for 1 min prior to a response until >30 sec after the peak of the response. A response was measured by averaging the fura-2 ratio (340 nm/380 nm) for 5 image pairs prior to a response subtracted from the peak ratio of the response. Increases in the fura-2 ratio are indicative of an increase in $[Ca^{2+}]_i$, therefore we use the term Ca^{2+} response throughout.

MEA Recording from Guinea Pig Retina

Adult guinea pig retina were isolated and placed RGC side down on an 8 × 8 MEA (500 μm spacing, Multi Channel Systems, Reutlingen, Germany). Ames solution bubbled with carbogen (pH ~7.4, 35-36ºC) was continuously superfused (2 ml/min) over the preparation. A full-field flash was presented to the retina (LED 530nm, 500ms duration, 420 lx) every 2 sec. Data was digitized and sampled at 50 kHz and recorded with MC_Rack software (Multi Channel Systems) and spikes high pass filtered at 200 Hz. Baseline recordings were obtained over a 20-30 min period to ensure stability of the recordings. Spikes recorded on each electrode were sorted into individual cells off-line (MC_Rack) and then analyzed with Neuroexplorer software (Nex Technologies, Littleton, MA, USA). For each cell spikes were cumulated over 60 consecutive sweeps

(60 light flashes). The ON response consisted of all spikes during the 500 ms light flash and the OFF response consisted of all spikes for 700 ms following light offset. Cells were excluded if they did not fire at least 1 spike per sweep.

Data Analysis

All statistical analysis was performed with Prism 4 (GraphPad, La Jolla, CA, USA) using the raw values and data were normalized for presentation only for visual clarity due to variability in absolute response size between cells. Experiments always consisted of a control, treatment and washout allowing the use of paired or repeated measure statistics for within-retina or within-cell comparisons. For WCR from cultured RGCs peak amplitudes and 10-90% decay slopes were averaged from three AMPA-induced responses in each condition for every cell. The number of experiments (n) reported is from individual cells (WCRs) or retinas, pieces of retina and coverslips (Ca^{2+} imaging and MEA). If an experiment included multiple cells the total number per experiment is included in the figure legends. Data are expressed as mean ± SD.

Results

Effect of D-Serine on AMPA/Kainate Receptor-Mediated Responses in Cultured RGCs

We began our investigation using cultured RGCs, which are free of synaptic connections, to identify the effect of D-serine on kainate-induced Ca^{2+} responses. All experiments were performed in a standard cocktail of 15 μM strychnine and 50 μM picrotoxin to rule out the possibility of D-serine acting on glycine (Junjaud *et al*., 2006) or γ-aminobutyric acid (GABA) receptors, as well as in 20 μM MK-801 to avoid possible

NMDAR activation through tonic or evoked glutamate release. Kainate (100 μM) was bath applied for 15 sec causing a rise in the fura 2 ratio of 0.22 ± 0.11 a.u. (Figure 4.1a, b). Prior to a second kainate application, 500 μM D-serine was bath applied for 5 minutes and the resulting response was reduced significantly to 62.3 ± 13.2% of the initial response ($P < 0.01$). D-Serine application alone caused no significant change in basal $[Ca^{2+}]_i$. Following washout of D-serine and return to basal $[Ca^{2+}]_i$ a third kainate-induced response showed full recovery to 93.1 ± 18.4%. To determine the contribution of AMPARs to the reduced Ca^{2+} response caused by D-serine we repeated the same experiment in the presence of 15 μM GYKI 52466 to reduce AMPAR activation (Figure 4.1c, d). The initial kainate application caused a 0.12 ± 0.05 a.u. increase in the fura 2 ratio. Following a 5 min D-serine (500 μM) application the second kainate-induced calcium response was not significantly different than the first (98.2 ± 12.7%, $P = 0.98$). After washout of D-serine the third calcium response elicited was 101 ± 10.6% of the initial response. These results confirm that D-serine can reduce non-NMDAR iGluR-mediated activity and indicate that the effect on kainate-induced Ca^{2+} responses mostly involves AMPARs.

To compare the strong effect of D-serine detected with Ca^{2+} imaging seen in Figure 4.1, we also performed whole cell recordings (WCRs) from cultured RGCs held at -60 mV in response to pressure ejection of 500 μM AMPA (50 ms). This application of AMPA elicited a mean ± SD peak inward current of 47.7 ± 7.5 pA (Figure 4.2). D-Serine (500 μM) was bath applied for 5 min while recording AMPA-induced currents every 30 sec. Over the time course of D-serine superfusion the peak amplitude was significantly

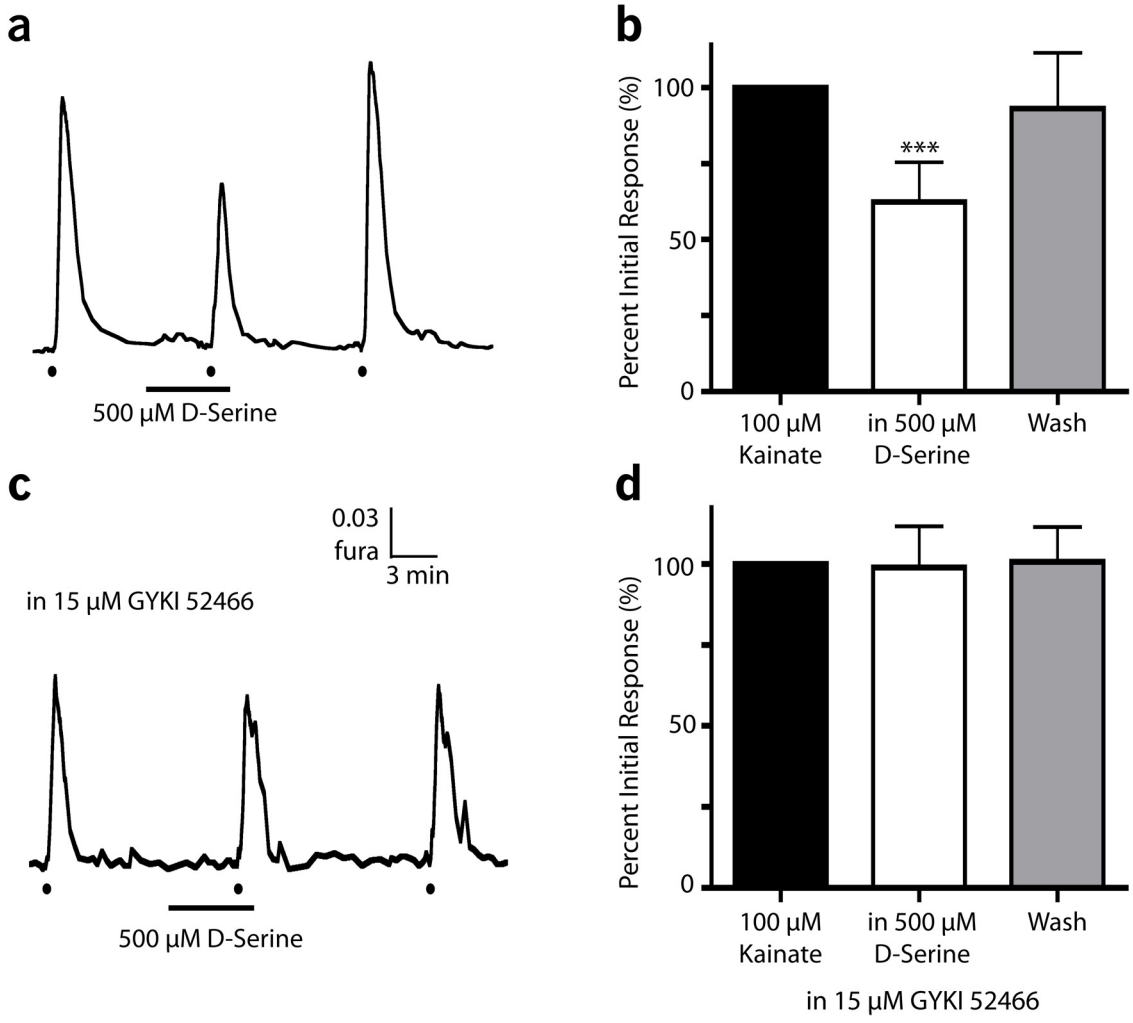

Figure 4.1 D-Serine reduces kainate-induced Ca^{2+} responses in cultured RGCs via AMPARs. (a) Representative trace showing three consecutive Ca^{2+} responses to 15 sec bath applications of 100 µM kainate (black circles). The second response is preceded by a 5 min bath application of 500 µM D-serine (black bar). (b) Mean ± SD normalized peak kainate-induced Ca^{2+} responses before, during, and following D-serine application (n = 7, from 70 cells). (c) Representative trace of three responses elicited by bath application of kainate in the presence of the selective AMPAR inhibitor GYKI 52466 (15 µM). The second kainate application was preceded by 5 min exposure to D-serine and the third response occurred following washout. (d) Mean normalized peak Ca^{2+} responses for the experiment outlined in panel C (n = 6, from 40 cells). ***$P < 0.001$, repeated measures Tukey's one-way ANOVA.

reduced to 88.2 ± 3.9% and recovered to 100 ± 7.3% of the initial response after a 5 min washout ($P < 0.01$). Although modest, the effect of D-serine under these conditions was similar to an earlier electrophysiological study of cultured hippocampal neurons (Dong *et al*., 2007). However, we also found that the decay slope (10-90%) was increased by 28 ± 22% ($P < 0.05$, Figure 4.2c, d) indicating that the recovery rate from the AMPA-induced response was significantly faster. Both the amplitude and shape of the response were changed and this could potentially account for the larger percent reduction observed with Ca^{2+} imaging experiments.

Exogenous D-Serine Application and Ca^{2+} Responses in the Isolated Retina

To date no reports have specifically investigated D-serine inhibition of non-NMDA iGluR-mediated responses in intact tissue. To this end we moved to the isolated wholemount retina preparation to see if the inhibitory effect of D-serine remained. Experiments were performed using three different extracellular solutions while testing the effect of 1000 μM D-serine on the Ca^{2+} response to 50 μM kainate bath application (20 sec, Figure 4.3). In control HBSS the mean ± SD response to kainate in the presence of D-serine was 98.2 ± 35.5% relative to the intial response to kainate alone. The response were variable and could be sorted into three types; 40% of cells showed no change (≤ 10% of initial response), 21.3% of cells had an enhanced response (> 10% increase of initial response) and 38.7% of cells showed a reduced response (> 10% decrease of initial response) in the presence of D-serine (Figure 4.3b). In addition to the cells under investigation, D-serine could be acting at presynaptic cells potentially resulting in net positive or negative modulation or no net change at all. To account for the majority of

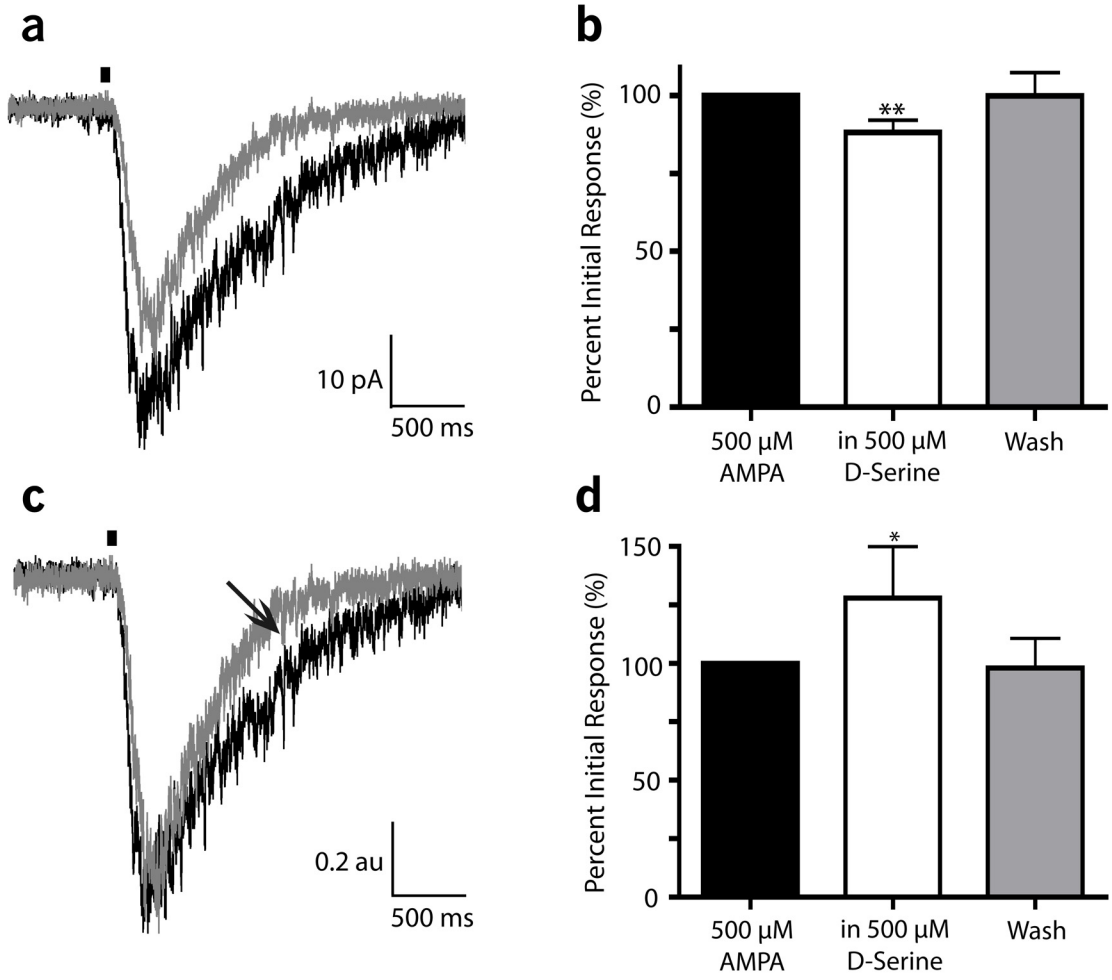

Figure 4.2 Amplitude and decay kinetics of AMPA-induced currents in cultured RGCs are affected by D-serine. (a) Representative WCRs showing inward current elicited by pressure ejection of 500 µM AMPA (black bar, -60 mV holding potential) before and during 5 min application of 500 µM D-serine (black and grey trace, respectively). (b) Mean ± SD normalized peak AMPA-induced currents before (left bar), during (middle bar) and following washout of D-serine (right bar, n = 6). (c) The same traces in panel *a* normalized to have equal peak amplitudes. Arrow indicates the change in the decay slope in the presence of D-serine. (d) Mean ± SD normalized 10-90% decay slope before (left) during (middle) and following washout (right) of 500 µM D-serine (n = 6). $*P < 0.05$, $**P < 0.01$, repeated measures, Tukey's one-way ANOVA.

inhibitory input in the GCL strychnine (15 μM) and picrotoxin (50 μM) were included in the extracellular HBSS. Under these conditions the kainate-induced Ca^{2+} response in the presence of 1000 μM D-serine was 72.9 ± 30.1 relative to the initial response to kainate alone. Again the effect was variable, but now shifted in favour of a reduction of the kainate-induced Ca^{2+} response caused by D-serine. Now 29.6% of cells showed no change, 12.7% showed an enhancement and 57.7% showed a reduction of the initial kainate-induced response in the presence of 1000 μM D-serine (Figure 4.3c). It was possible that the D-serine-dependent enhancement of the kainate response was due to D-serine acting at NMDARs thereby enhancing a contribution of tonic or kainate-evoked glutamate release. To test this 20 μm MK-801 was added to the extracellular HBSS with strychnine and picrotoxin resulting in a reduction to 60.5 ± 18.9% of the intial kainate-induced Ca^{2+} response in the presence of D-serine. In 11.9% of cells there was no change, no cells showed an enhancement and 88.1% of cells showed a reduction of the kainate-induced Ca^{2+} response in the presence of 1000 μM D-serine (Figure 4.3d). These findings support an inhibitory action of D-serine on non-NMDA iGluR-mediated Ca^{2+} responses that is independent of NMDA, glycine and GABA receptor binding.

Next, a dose-response curve for the inhibitory effect of D-serine on 50 μM kainate-induced Ca^{2+} response in isolated retina was generated using six different concentrations of D-serine (0, 100, 300, 500, 1000 and 3000 μM) that were tested independently (Figure 4.4). Given the results presented in Figure 4.3, all experiments were performed in the standard cocktail (strychnine, picrotoxin and MK-801). Each experiment consisted of three consecutive kainate-induced Ca^{2+} responses and the second was preceded by a 6

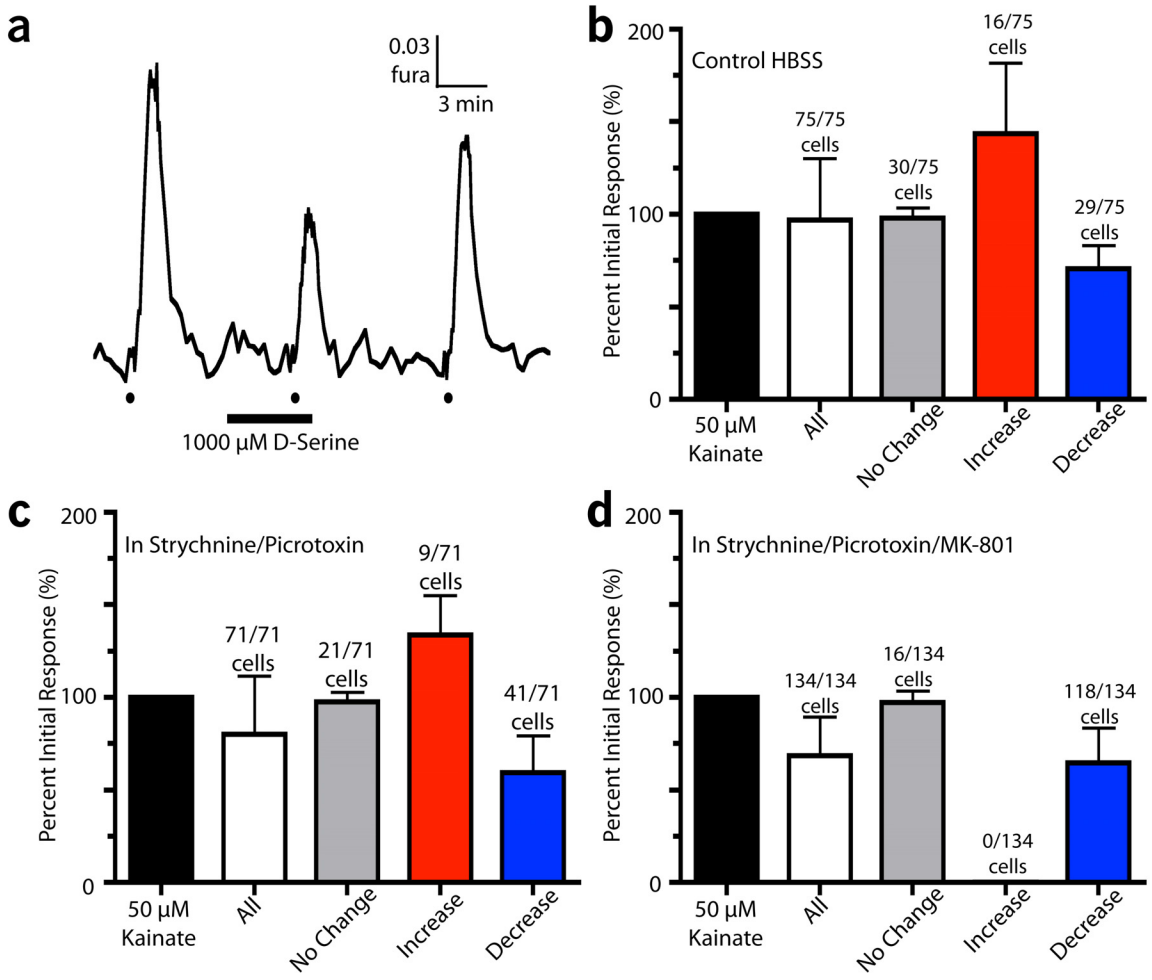

Figure 4.3 Network influences on D-serine reduction of kainate Ca^{2+} responses in isolated retina. (a) Example trace showing three 50 µM kainate-induced (20 sec, black dots) Ca^{2+} responses. The second application was preceded by 6 min bath exposure of 1000 µM D-serine (grey bar). Mean ± SD normalized response showing the effect of 1000 µM D-serine in (b) control (c) 15 µM strychnine/ 50 µM picrotoxin and (d) 15 µM strychnine/ 50 µM/ 20 µM MK-801-containing HBSS. Individual cell responses were grouped together (All) or separated based on whether the percent change was ≤ 10% (no change), > 10% increase or > 10% decrease relative to the initial kainatae-induced Ca^{2+} response. Data was collected from 5 retinas for each condition

min bath application of D-serine. Concentrations > 300 μM D-serine showed a significant reduction in the Ca^{2+} response ($P < 0.001$) and even the effect of 300 μM was approaching significance ($P = 0.059$). The dose-response curve yielded an IC_{50} of 280 μM (95% confidence 240-328 μM). Washout (at least 7 min) of all D-serine concentrations showed significant ($P < 0.001$) but incomplete recovery because the initial kainate-induced response was different ($P < 0.05$) from the final response.

To strengthen the argument that the inhibitory effect of D-serine is specific to AMPA/KA receptor activation we tested the effect of D-serine on K^+-induced Ca^{2+} responses in the presence 15 μM NBQX to block AMPA/KA receptors in addition to the standard cocktail (Figure 4.5). Two consecutive Ca^{2+} responses were elicited by 40 mM K^+ (20 sec bath application), the second was preceded by a 6 min application of 1000 μM D-serine. The initial K^+-induced Ca^{2+} response of 0.21 ± 0.09 a.u. was not significantly different than the initial kainate-induced Ca^{2+} response (0.18 ± 0.05, $P = 0.44$, two-tailed, T-test) and amplitude of the second K^+-induced response, obtained in the presence of 1000 μM D-serine, was 101 ± 6.7% of the initial ($P = 0.47$). Activation of voltage gated sodium (Na^+) and Ca^{2+} channels would contribute to the K^+-induced Ca^{2+} response, therefore our findings suggest that the effect of D-serine does not involve inhibition of either of these channels.

D-serine Reduces Synaptically-Activated Non-NMDAR iGluR-Mediated Electrophysiological Responses

In order to study the effect of D-serine on endogenous activation of non-NMDAR iGluRs by glutamate release we used 2 electrophysiological techniques. First, sEPSCs were recorded from RGCs held at -60 mV in isolated rat retina. To reduce the potential

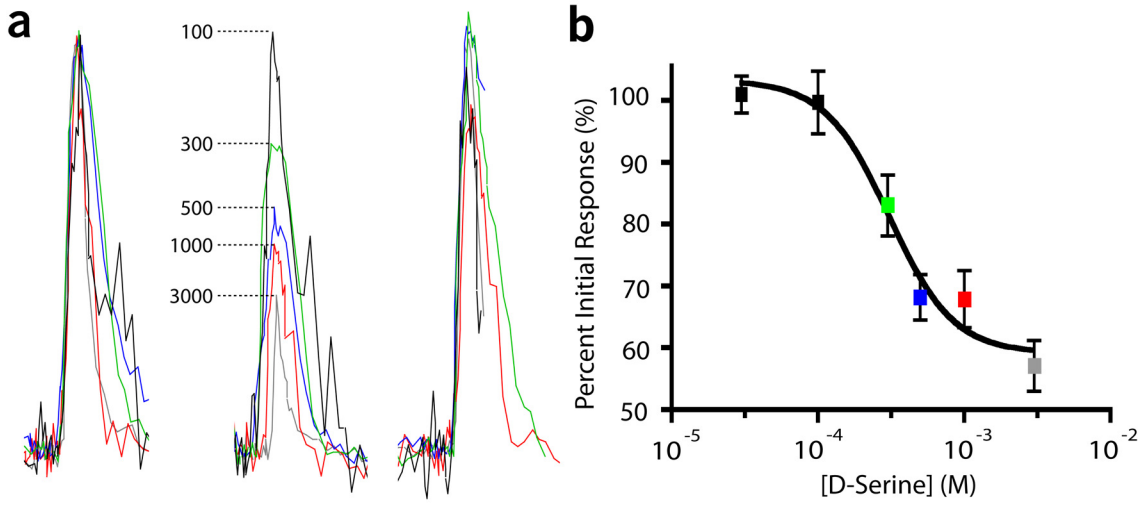

Figure 4.4 D-Serine concentration-dependent reduction in kainate-induced Ca^{2+} responses in GCL cells. (a) Representative colour-coded fura-2 traces, normalized to the initial 50 µM kainate-induced Ca^{2+} response, from individual cells from separate experiments. The second kainate application is preceded by a 6 min application of D-serine. The concentration (in µM) is noted to the left of the peak of each trace. The third kainate response was obtained after washout of D-serine. All peak responses are normalized to the initial responses to emphasize the effect of D-serine. (b) Dose-response curve for D-serine inhibition of 50 µM kainate-induced Ca^{2+} responses (mean ± SEM). Each concentration (colour-coded to panel *a*) was tested in separate experiments with subsequent washout (i.e., third peak in panel a; n = 5-9, from 102-195 cells per concentration). For graphing purposes $10^{-4.5}$ M was used as the 0 M concentration and the data was fit with a variable slope sigmoidal dose response function, r^2=0.9663.

network effects from synaptically driven input, all recordings were obtained in the standard cocktail (strychnine, picrotoxin and MK-801). Under these conditions the sEPSCs recorded from RGCs were mediated primarily by non-NMDAR iGluRs as determined by the effect of the potent AMPA/kainate receptor antagonist NBQX (Figure 4.6). The mean ± SD sEPSC amplitude of 10.1 ± 6.9 pA (the average amplitude over 2 sec was taken for each cell and mean ± SD indicates between cell variability) was significantly reduced to 21.7 ± 25.2% during a 90 sec bath application of 5 μM NBQX. Because of the small initial amplitude and a limit on the smallest acceptable response (sEPSC threshold set at 2 SD) the change in amplitude was not as representative as the change in sEPSC frequency since very few events were recorded in the presence of NBQX. On average (± SD) the initial frequency was 52.9 ± 27.2 Hz (in the presence of strychnine and picrotoxin) and was significantly reduced in the presence of NBQX to 4.4 ± 7.6%. Recovery from NBQX was inconsistent (returned to 29 ± 26.4%). We next sought to determine the effect of D-serine on the non-NMDA iGluR predominant sEPSCs recordings. The mean peak response amplitude (averaged for each cell) of 10.7 ± 6.8 pA was significantly reduced to 73.9 ± 15.4% during a 5-8 min bath application of 1000 μM D-serine ($P < 0.01$) and was recovered fully (93.1 ± 8.9%), following a 6 min washout with control solution (Figure 4.7c). While the amplitude was significantly decreased there was no significant change in the frequency of events (63.1 ± 38.8% of initial frequency, $P = 0.14$, Figure 4.8a). In 3/6 RGCs there was an obvious decrease in the frequency of events during D-serine application (> 50% reduction) but this was probably

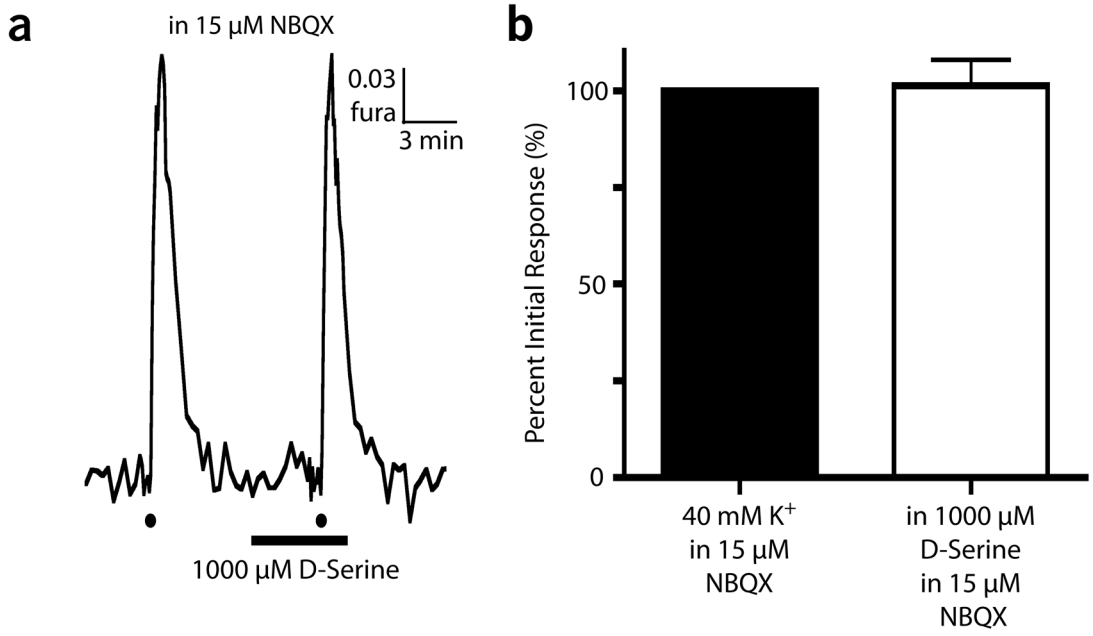

Figure 4.5 Potassium-evoked Ca^{2+} responses are not affected by D-serine in GCL cells. Example trace of consecutive 40 mM K^+-induced (black dots) responses. The second K^+ application was preceded by 6 min exposure of 1000 µM D-serine (black bar). (D) Mean ± SD normalized peak data showing the lack of effect of 1000 µM D-serine on the K^+-induced Ca^{2+} response (n = 5, from 138 cells, $P = 0.47$, paired t-test). Experiments were performed in 15 µM NBQX and the standard inhibitory cocktail of 15 µM strychnine, 50 µM picrotoxin and 20 µM MK-801.

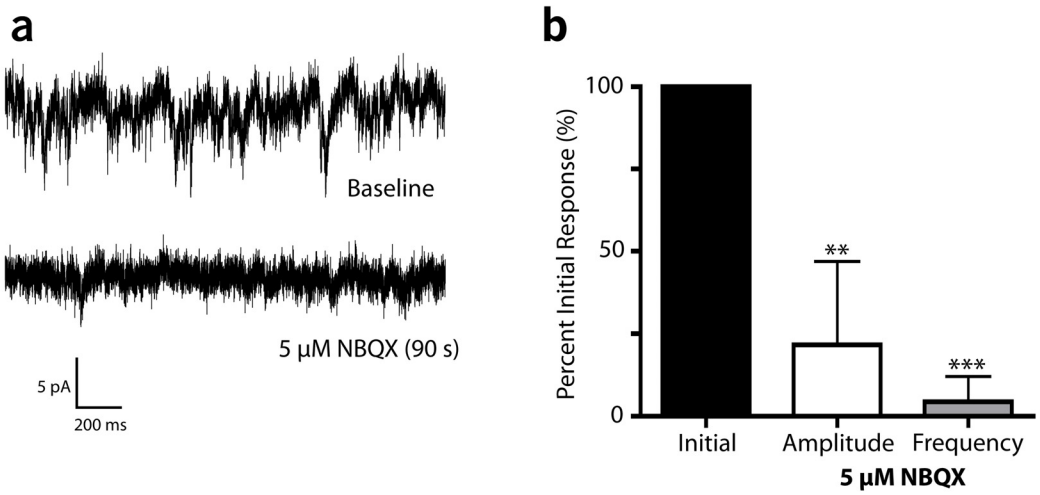

Figure 4.6 NBQX reduces sEPSCs in RGCs in the isolated retina. (a) Representative raw, unfiltered trace from an RGC held at -60 mV showing the sEPSCs before (baseline, *top*) and during (*bottom*) 90 sec bath application of 5 µM NBQX. (b) Mean ± SD normalized peak amplitude (*middle bar*) and sEPSCs frequency (*right bar*) reduction following application of NBQX (n=4). $^{**}P<0.01$, $^{***}P<0.001$. Paired t-test.

due to sEPSC amplitudes falling below the detection threshold of 2 SD because these cells had the lowest signal-to-noise ratios. This accounts for the low mean and large deviation in regards to the effect of D-serine on event frequency. Indeed, changing the response threshold from 2SD to 1SD results in a frequency of 85.9 ± 27.2% in the presence of 1000 μM D-serine. To determine whether D-serine might influence the recordings by changing membrane resistance and/or an unidentified conductance, cell input resistance and current-voltage relationships (I/V curve) were measured frequently during the course of an experiment (Figure 4.8b, c, d). There was no change in the input resistance when comparing before, during and following washout of 1000 μM D-serine application. The absolute peak currents measured on the I/V curves decreased significantly from 1900 ± 278 pA to 1274 ± 443 pA (example at 40 mV, $P = 0.027$), but not the steady-state current (1143 ± 274 pA to 1048 ± 239, $P=0.082$) from the start to the end of an experiment. The normalized I/V curves were almost identical before, during and after washout of 1000 μM D-serine application (only normalized peak I/V curves shown in Figure 4.8d). Together these results support an inhibitory role for D-serine that influence kainate/AMPAR activity and suggest that it is acting post- but not pre-synaptically.

Secondly, we employed the MEA to record light-evoked spiking from GCL cells in the guinea pig retina and determine the effect of D-serine on this activity. A 500 ms full-field flash of light elicited both and ON and OFF response in most cells and either ON or OFF responses in a small number of cells, hence we chose to group ON and OFF responses separately (Figure 4.9b). All experiments were performed in the presence of the standard inhibitory cocktail (strychnine, pictrotoxin and MK-801). Bath application

of 20 μM NBQX nearly abolished all remaining ON and OFF responses (Figure 4.9c). Next, we tested whether D-serine could reduce the light evoked spiking that, under these conditions, was predominated by non-NMDA iGluR activation. A 10 min bath application of 1000 μM D-serine reduced the ON response to 83.4 ± 13.9% of the initial response that recovered to 101 ± 16.1% after a 10 min washout ($P < 0.05$, Figure 4.10b *left*). Similarly, D-serine reduced the OFF response to 73 ± 10% of the initial response and was recovered to 102 ± 6% after washout ($P < 0.01$, Figure 4.10c *left*). Interestingly, not all cells behaved the same because a significant proportion of ON and OFF responses were not affected by D-serine application (as indicated by ≤ 10% change in initial response). Excluding the cells that showed no change in the initial response D-serine application caused a reduction to 68 ± 9.7% (recovered to 97.1 ± 21.9%) of the initial ON response ($P < 0.001$, Figure 4.10b *right*) and to 62.2 ± 10.6% (recovered to 99.8 ± 6.3%) of the OFF response ($P < 0.001$, Figure 4.10c *left*). Furthermore, there was a significant difference ($P = 0.046$, paired T-test) between the cells with ON (50.7 ± 22.3%) versus OFF responses (73.3 ± 9.5%) that showed > 10% decrease due to D-serine application.

Endogenous D-Serine Degradation Relieves Non-NMDA iGluR Inhibtion

In order to assess the effect of endogenous D-serine on AMPA/KA receptors we used the specific D-serine degrading enzyme DAAO (0.25 mg/ml) in standard cocktail (Figure 4.11). Three consecutive kainate-induced (20 sec, 50 μM) Ca^{2+} responses were compared in the wholemount rat retina and the initial response was followed by 10-12 min bath application of 0.25 mg/ml DAAO (Figure 4.11a). The subsequent kainate application caused a Ca^{2+} increase of 118.2 ± 29.2% and the third (washout) response

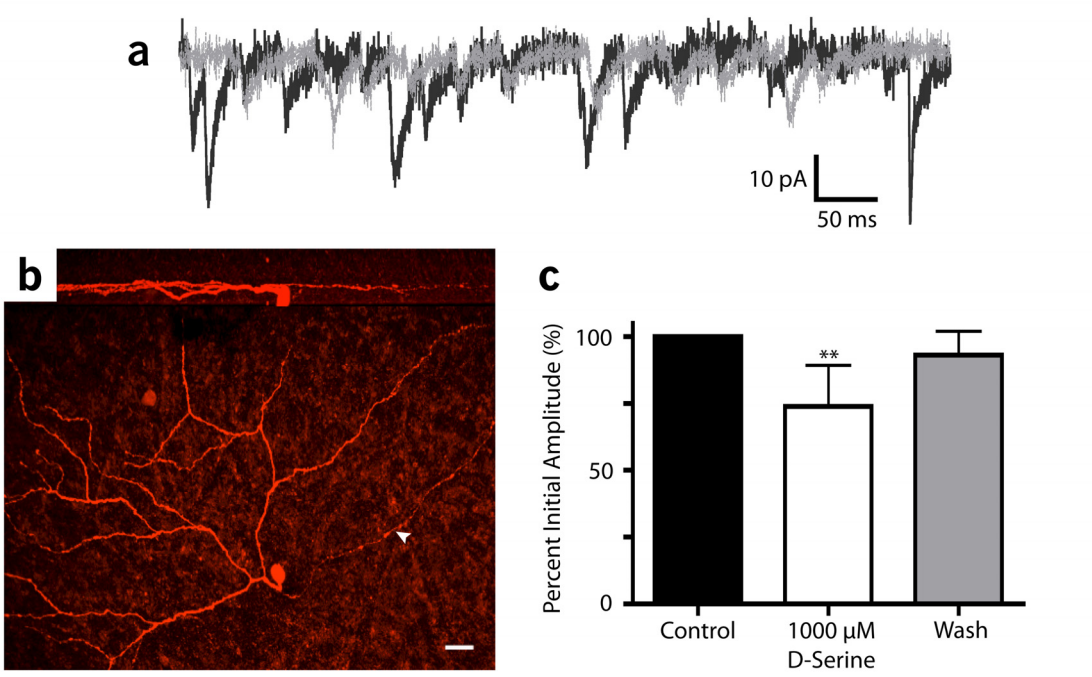

Figure 4.7 AMPA/KA receptor-mediated RGC sEPSC amplitude is reduced by D-serine in isolated retina. (a) Representative WCR of sEPSCs from a RGC before (black trace) and during (grey trace) 1000 µM D-serine application. (b) An example of an RGC filled with neurobiotin from the microeclectrode during the recording. The axon is indicated by the arrowhead and an orthogonal view is presented *above* (scale bar = 20 µm). (c) Mean ± SD normalized peak amplitude of sEPSCs before (left bar), during (middle bar) and after (right bar) 1000 µM D-serine application (n = 6). $^{**}P < 0.01$, repeated measures, Tukey's one-way ANOVA

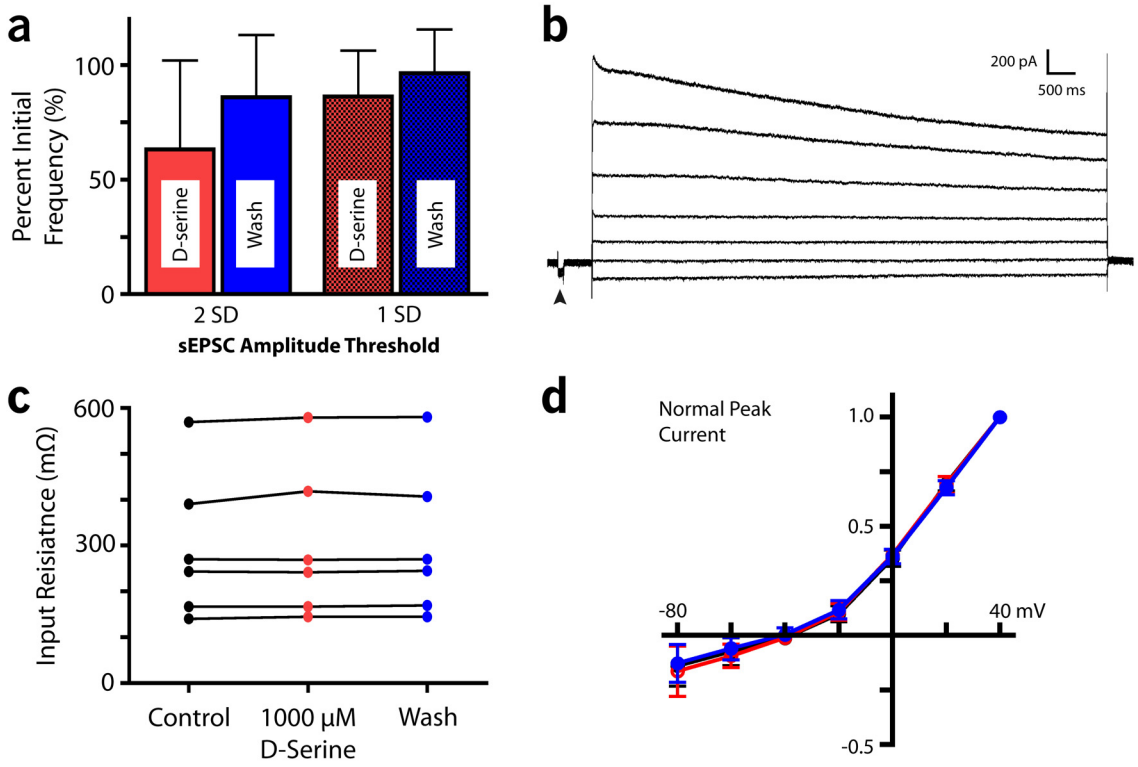

Figure 4.8 The effect of D-serine on other RGC electrophysiological parameters in isolated retina. (a) Mean ± SD frequency of sEPSC events during 1000 µM D-serine application (*red*) and after it is washed out (*blue*) relative to the normalized initial frequency (100%). The *left* set of bars is the frequency when the sEPSCs threshold is set to 2SD from baseline (no events) vs 1SD (*right*). There is no significant difference when D-serine is present. (b) A representative current recording of the voltage-step protocol used before, during and after washout of 1000 µM D-serine (-60 mV holding, steps from -80 to 40 by 20 mV). The arrowhead shows the resultant current to a 10 mV step used to calculate (c) each cells input resistance that was measured throughout the experiment. There was no change in input resistance for the six RGCs from before (control), during and after washout of 1000 µM D-serine. (d) Mean ± SD normalized (to the peak absolute current) currents plotted against the respective voltage before (black), during (red) and following (blue) 1000 µM D-serine application (n=4). Raw data analyzed with repeated measures, one way ANOVA.

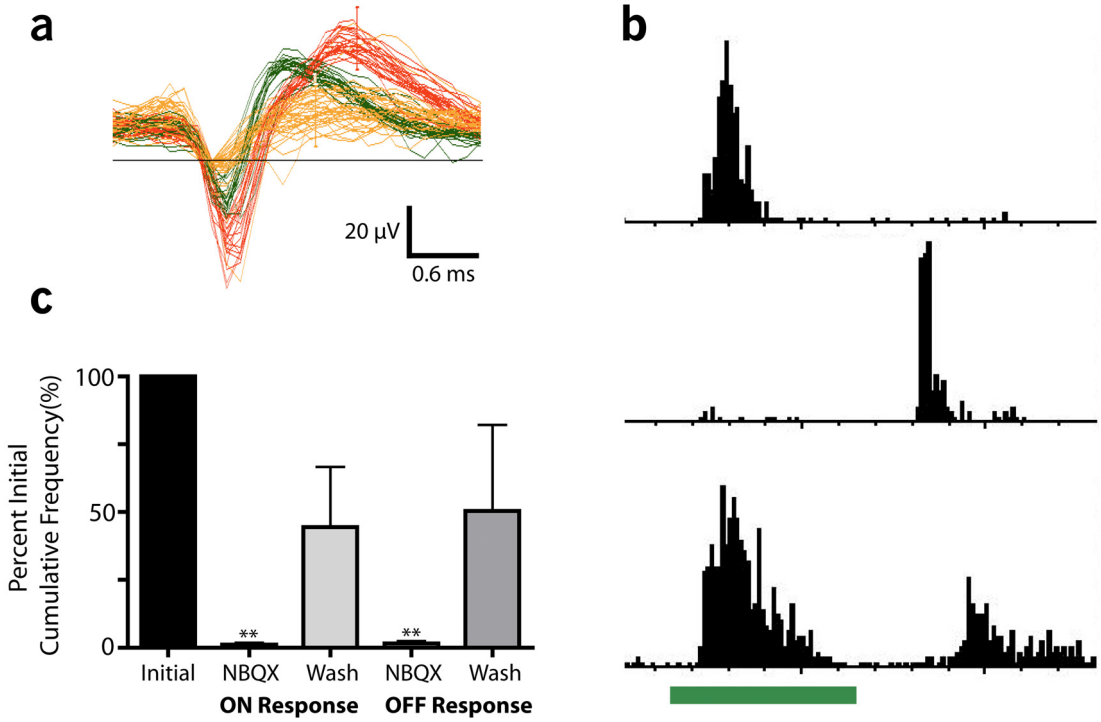

Figure 4.9 Light-evoked MEA recordings and the effect of NBQX. (a) Example of off-line spike sorting from a single MEA electrode. Three neurons are separated and colour-coded based on waveform similarity. (b) Cumulative frequency histograms (10 ms bins for 60 sweeps) from the three cells in *a* demonstrate the three basic response profiles from the spiking neurons to a 500 ms flash of light (green bar). The *top* trace shows an ON cell, the *middle* an OFF cell and the *bottom* an ON-OFF cell. ON and OFF responses were analyzed separately regardless of whether the response came from a pure ON or OFF cell or an ON-OFF cell. (c) Experiments were performed in the standard inhibitory cocktail (strychnine/ picrotoxin/ MK-801) and the bath application of 20 µM NBQX (2 min) significantly reduced light-evoked spiking. Some recovery was achieved after a washout period of 10-60 min. (n=4 from 183 ON responding cells, and 182 OFF responding cells). Data expressed as mean ± SD and analyzed with repeated measures, Tukey's one way ANOVA.

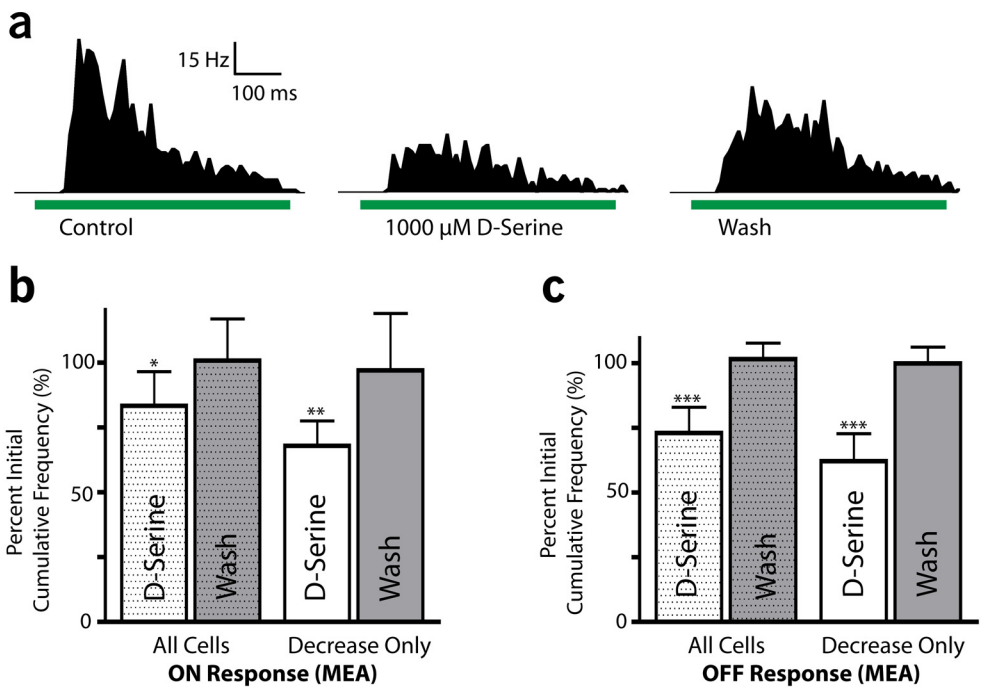

Figure 4.10 D-serine reduction of light-evoked MEA spiking from the isolated guinea pig retina. (a) Frequency histograms (10 ms bins) of the spike rate of an RGC in response (ON response) to a 500 ms full-field flash of light (green bar) before (*left*), during (*middle*) and upon washout (*right*) of 1000 µM D-serine recorded from guinea pig retina on a MEA. Mean ± SD normalized cumulative spikes for all (b) ON and (c) OFF responding neurons (first two bars of each graph) during and upon washout of 1000 µM D-serine (n = 5, from 194 ON and 163 OFF responses). Mean ± SD normalized cumulative spikes only for cells showing a >10 % decrease in ON and OFF responses (last two bars of each graph) resulting from D-serine application (n = 5, from 89 ON and 124 OFF responding cells). ON and OFF responses were cumulated over the 500 ms of light stimulus and 700 ms post-stimulus, respectively. $*P < 0.05$, $**P < 0.01$, $***P < 0.001$, repeated measures Tukey's one-way ANOVA.

was 99.6 ± 16.2% of the initial response and there was no significant difference between these responses ($P = 0.28$, Figure 4.10b *left*). However, a subset of the cells (42.5 ± 25.3%) showed an increase > 10% of the initial response, while all other cells were within ± 10%. Analysis of these cells showed that DAAO caused a significant increase in the second response, relative to the first, to 149.9 ± 29.9 % and the washout response was 112.6 ± 25.7% ($P < 0.01$, Figure 4.11b *right*). To determine if the effect of DAAO was due to its enzymatic activity, the enzyme in solution was placed in boiling water for at least 10 min. The use of the heat inactivated DAAO caused an enhanced kainate-induced Ca^{2+} response in 1/57 cells (n = 3 retinas) with mean ± SD second response that was 97.9 ± 5.4% of the initial response. Light-evoked MEA recordings showed similar results with the active enzyme because when all cells were analyzed together (separated into ON and OFF responses) a 10-15 min DAAO application had no significant effect on spiking activity ($P > 0.05$, Figure 4.11d *left*). Excluding cells that showed an increase < 10% in activity left 29.3 ± 9.5% of ON and 44.5 ± 24% of OFF responses (no significant difference between the number of remaining cells). In these cells DAAO caused an increase to 144.9 ± 19.4% for ON responses and 161 ± 22.6% for OFF responses ($P < 0.01$, Figure 4.11d *right*). Recovery recordings, up to 30 min of DAAO washout, were 134.2 ± 26.6% for ON responses and 130.6 ± 22.9% for OFF responses and only OFF responses significantly, but incompletely, recovered.

Calcium-Permeable AMPARs and their Contribution to the Inhibitory Effect D-Serine

Our data show a comparatively large effect of D-serine on kainate-induced Ca^{2+} responses versus its effect on electrophysiological recordings. The results that D-serine reduces AMPA-induced currents and increases the rate of recovery (Figure 4.2) could

account for this difference. In cultured cells the effect of D-serine on kainate-induced Ca^{2+} responses was largely mediated by AMPARs as shown in Figure 4.1. Most cultured cells show a significant contribution of CP-AMPAR activation to the AMPA-induced Ca^{2+} response because the specific CP-AMPAR antagonist IEM 1460 reduces the initial response to 48.8 ± 7.3% (Figure 4.12a, b). The AMPA-induced (100 μM, 30 sec) Ca^{2+} response was unchanged in 6/46 cells in this data set. When glutamate (10 μM for 30 sec) was used as the agonist there was no significant difference in the Ca^{2+} response in the presence of IEM 1460 (66 ± 19.5% of the intial glutamate-induced response) when all cell were analyzed. In 12/32 there was no change in the Ca^{2+} response elicited by glutamate in the presence of IEM but the remaining cells did show a significant decrease (44.9 ± 13% of the initial response). Data collected using AMPA and glutamate as the agonist indicate that the cultured RCGs may be separable into CP-AMPAR-containing and non-containing cells.

We next tested the involvement of CP-AMPARs activation in the kainate-induced Ca^{2+} response in the isolated retina. Because kainate-induced increases in $[Ca^{2+}]_i$ could involve direct influx through CP-AMPA/KA receptors and indirect influx through VGCCs resulting from depolarization we used a cocktail including 0.5 μM TTX, 100 μM $NiCl_2$, 1 μM ω-conotoxin and 10 μM nimodipine to separate the two components (Figure 2.13). All solutions also contained 15 μM strychnine, 50 μM picrotoxin and 20 μM MK-801. The initial mean ± SD kainate-induced Ca^{2+} response of 0.06 ± 0.02 a.u. was reduced to 47.3 ± 6% by the TTX/ VGCC blocker cocktail (Figure 2.13b). Addition of 100 μM IEM 1460 to block CP-AMPARs caused a further reduction in the third response to 24.4 ± 1.7%. Similarly, the reciprocal experiment where the second kainate-induced

Figure 4.11 Degradation of endogenous D-serine enhances kainate-induced Ca^{2+} responses and light-evoked MEA activity in some GCL cells. (a) Example trace of three kainate-induced (black circles) Ca^{2+} responses (50 μM for 20 sec), the second response is preceded by 10 min application of DAAO (0.25 mg/ml). (b) Mean ± SD normalized peak kainate-induced Ca^{2+} response of (*left bars*) all cells during and after washout of DAAO and (*right bars*) only those that showed a >10% increase relative to the initial response (n = 5, from 94 cells). (c) Frequency histograms (10 ms bins) of the spike rate (MEA recording) from a cell showing an ON response during 500 ms light flash (*green bar*) and a subsequent OFF response before (*top*) and directly following (*bottom*) a 10 min DAAO application (0.25 mg/ml). (D) Mean ± SD normalized cumulative spikes for (*left bars*) all ON (top, n = 5, from 299 cells) and OFF (bottom, n = 5, from 224 cells) responses during and upon washout of DAAO relative to each cells initial response (100%). The *right bars* are data only for cells that showed a >10% increase of the initial response due to DAAO application. ON and OFF responses were cumulated over the 500 ms of light stimulus and 700 ms post-stimulus, respectively. $^{n.s.}$ $P > 0.05$, ** $P < 0.01$, repeated measures, Tukey's one-way ANOVA.

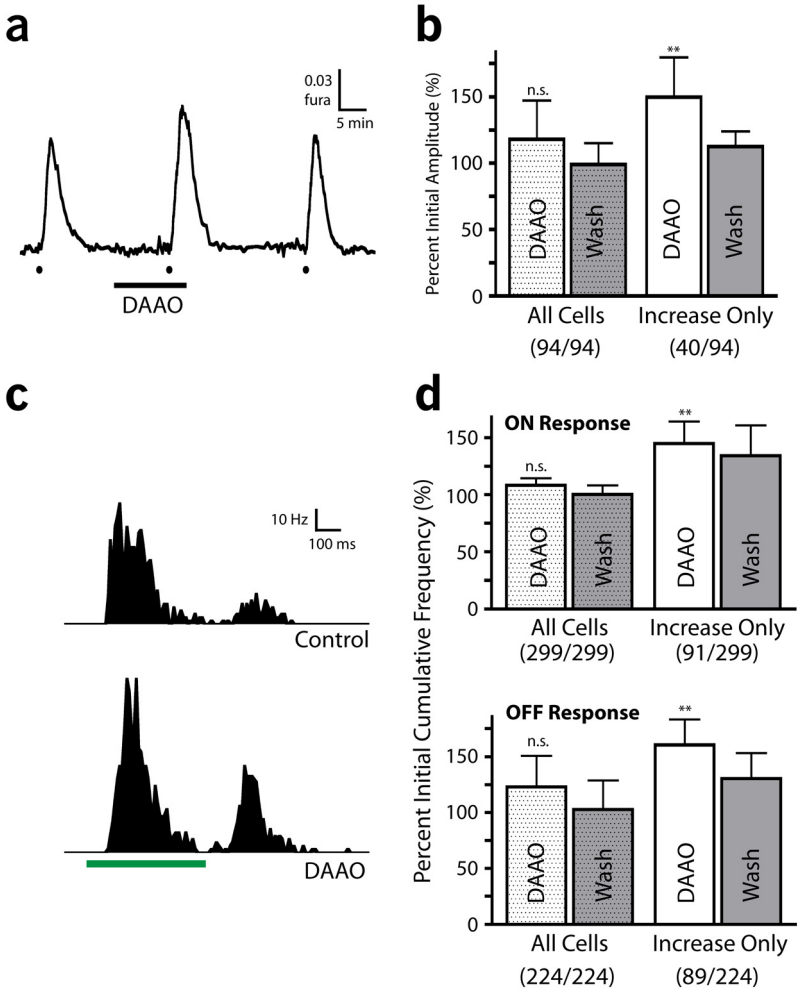
a
0.03
fura
5 min
DAAO
b
Percent Initial Amplitude (%)
n.s.
**
DAAO
Wash
DAAO
Wash
All Cells
(94/94)
Increase Only
(40/94)
c
10 Hz
100 ms
Control
DAAO
d
ON Response
n.s.
**
DAAO
Wash
DAAO
Wash
All Cells
(299/299)
Increase Only
(91/299)
OFF Response
n.s.
**
DAAO
Wash
DAAO
Wash
All Cells
(224/224)
Increase Only
(89/224)
Percent Initial Cumulative Frequency (%)

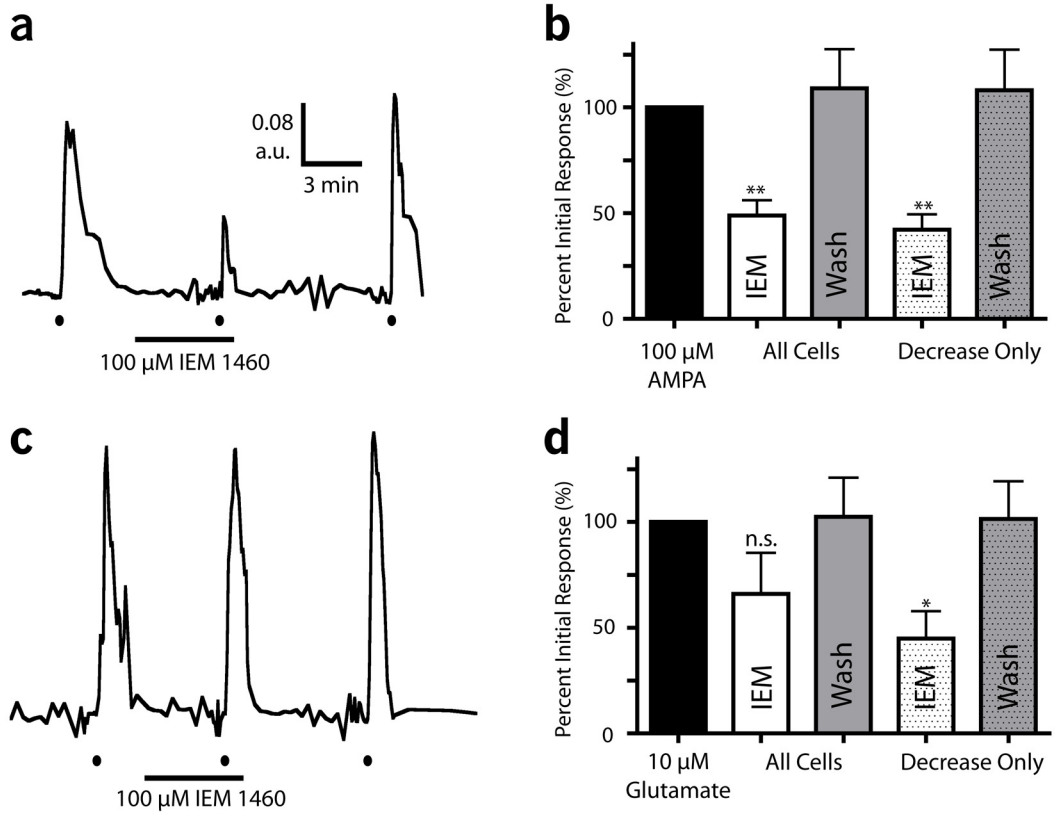

Figure 4.12 Contribution of Ca^{2+}-permeable AMPARs to AMPA- and glutamate-mediated Ca^{2+} responses in cultured RGCs. Example fura-2 ratio traces of three consecutive (a) 100 µM AMPA-induced and (c) 10 µM glutamate-induced Ca^{2+} responses (30 sec bath application indicated by black circles) from cultured RGCs. The second application is preceeded by a 5 min application of the specific CP-AMPAR antagonist 100 µM IEM 1460 (*black bar*). Mean ± SD normalized peak Ca^{2+} responses induced by (b) AMPA and (d) glutamate. Most cells show a >10% reduction in the agonist-induced response in the presence of IEM 1460 relative to the initial response to the agonist alone, but some cells show no change (≤10% change). Using AMPA as the agonist 6/46 cells from five experiments show no change in the presence of IEM 1460 and 12/32 from five experiments show no change when glutamate was used. $^{n.s.}P > 0.05$, $^{*}P < 0.05$, $^{**}P < 0.01$, repeated measures, Tukey's one way ANOVA.

Ca^{2+} response was obtained in the presence of IEM alone and the third in the presence of IEM plus the cocktail caused a decrease of the initial response (0.15 ± 0.09 a.u.) to 48.1 ± 4% and further decrease to 17.7 ± 5.4%, respectively (Figure 2.13c). In both sets of experiments a fourth response obtained after a 10-20 min washout of IEM and the TTX/ VGCC blocker cocktail showed variable recovery (to 38.8 ± 5.7% and 20 ± 12.4%, respectively). Also, there was a significant ($P < 0.05$) difference between the kainate-induced Ca^{2+} responses in the presence of either drug alone compared to when combined. This clearly demonstrates that Ca^{2+} influx through CP-AMPARs and due to depolarization are additive, although there is likely some overlap between CP-AMPAR activation and subsequent depolarization-dependent Ca^{2+} influx.

Given the significant contribution of CP-AMPARs to the kainate-induced Ca^{2+} response and that AMPAR inhibition blocked the inhibitory effect of D-serine in cultured RGCs (Figure 4.1), we hypothesized that the large effect of D-serine in Ca^{2+} imaging experiments was due to CP-AMPAR inhibition. Since a large component of the Ca^{2+} response elicited by kainate was due to influx through VGCCs we first confirmed previous results (Figure 4.5) that D-serine inhibition does not involve voltage gated Na^{+} and Ca^{2+} channels. Kainate caused an initial Ca^{2+} response of 0.052 ± 0.016 a.u. and a second response was reduced to 51.1 ± 15.3% by the presence of the TTX/ VGCC blocker cocktail (Figure 4.14). A third response obtained in the presence of the cocktail plus 3000 μM D-serine caused a further reduction to 27.8 ± 11.5% and some recovery was achieved with a fourth kainate-induced Ca^{2+} response following a 10-15 min washout of D-serine and the cocktail (returned to 67.4 ± 5.9% of initial response). There was a significant difference between Ca^{2+} responses obtained in the presence of the TTX/

VGCC blocker cocktail alone and when coapplied with 3000 μM D-serine, thus supporting the conclusion that voltage gated Na^+ and Ca^{2+} channels are not directly involved in D-serine inhibition. Finally, in isolated retinas IEM alone reduced the initial kainate-induced Ca^{2+} response (0.19 ± 0.1 a.u.) to 48.6 ± 10.1% and subsequent coapplication with 3000 μM D-serine did not have any further effect (43.4 ± 9.1% P = 0.4, Figure 4.15b). After washout of IEM and D-serine the fourth kainate-induce Ca^{2+} response returned to 76.7 ± 10% of the initial (Figure 4.15c). In the reciprocal experiment the initial Ca^{2+} response (0.17 ± 0.12 a.u.) was reduced to 58.1 ± 12.6% in the presence of 3000 μM D-serine. The third response obtained in the presence of D-serine with IEM caused a further reduction to 47.6 ± 8.6% and the final response recovered to 81.6 ± 19.1% after ≥ 10 min washout. Although not significant, P = 0.06 when kainate-induced Ca^{2+} responses were compared in the presence of D-serine alone and when coapplied with IEM. Altogether, these findings demonstrate that CP-AMPARs can have a large contribution to the glutamatergic-induced $[Ca^{2+}]_i$ increase and strongly suggest that a primary target of D-serine in the Ca^{2+} imaging experiments was CP-AMPARs.

Discussion

The results from this study emphasize that D-serine is capable of inhibiting AMPA/KA receptor-mediated responses, particularly Ca^{2+} increases mediated by CP-AMPAR activation. Furthermore, using DAAO, we demonstrated that endogenous D-serine within the retina can reach concentrations sufficient for AMPA/KA receptor inhibition. Calcium imaging and whole cell recording from cultured RGCs showed that

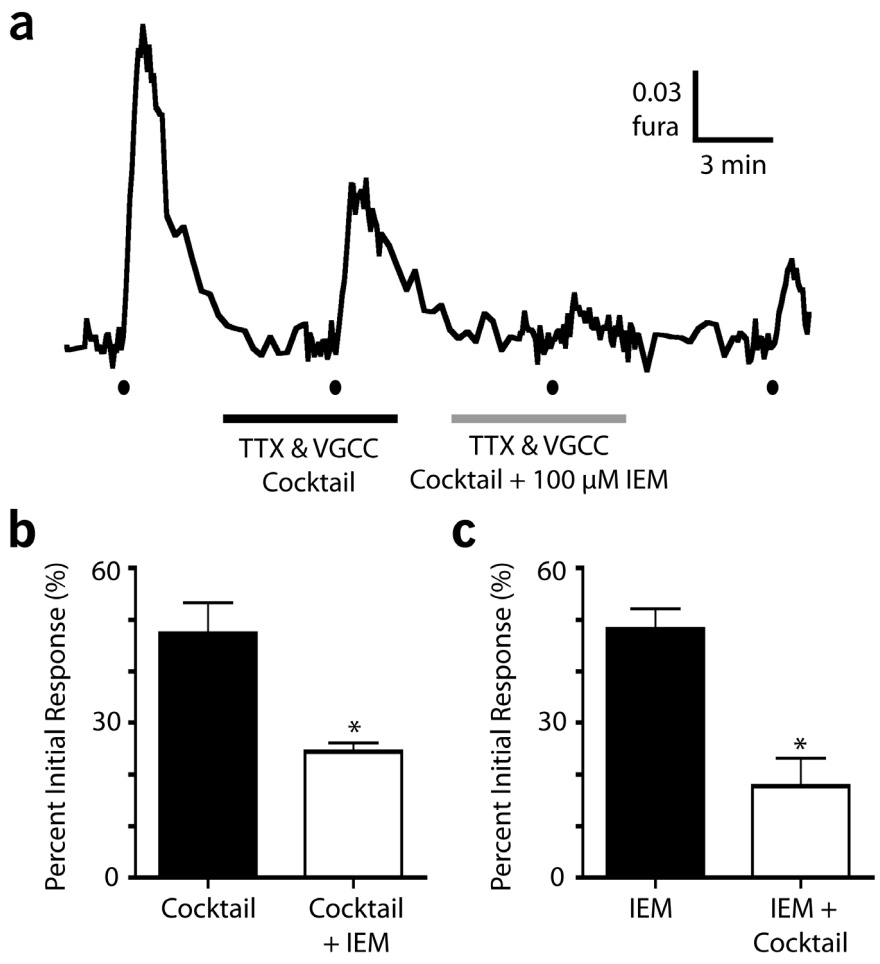

Figure 4.13 Contribution of voltage-gated Na^+ and Ca^{2+} channels and CP-AMPARs to kainate-induced Ca^{2+} response in isolated retina. (a) A representative trace showing four Ca^{2+} increases elicited by bath application of 50 µM kaniate for 20 sec (black circles). The second peak is obtained in the presence of (in µM) 0.5 TTX, 100 $NiCl_2$, 1 ω-conotoxin, 10 nimodipine (TTX & VGCC cocktail, *black bar*). In addition to the cocktail 100 µM IEM 1460 was also present during the third response (*grey bar*). Bar graphs show mean ± SD normalized peak responses (second and third only) for reciprocal experiments where either (b) the cocktail (n = 3, from 88 cells) or (c) IEM (n = 5, from 131 cells) was present alone during the second response and both were present for the third response. *$P < 0.05$, two-tailed, paired T-test.

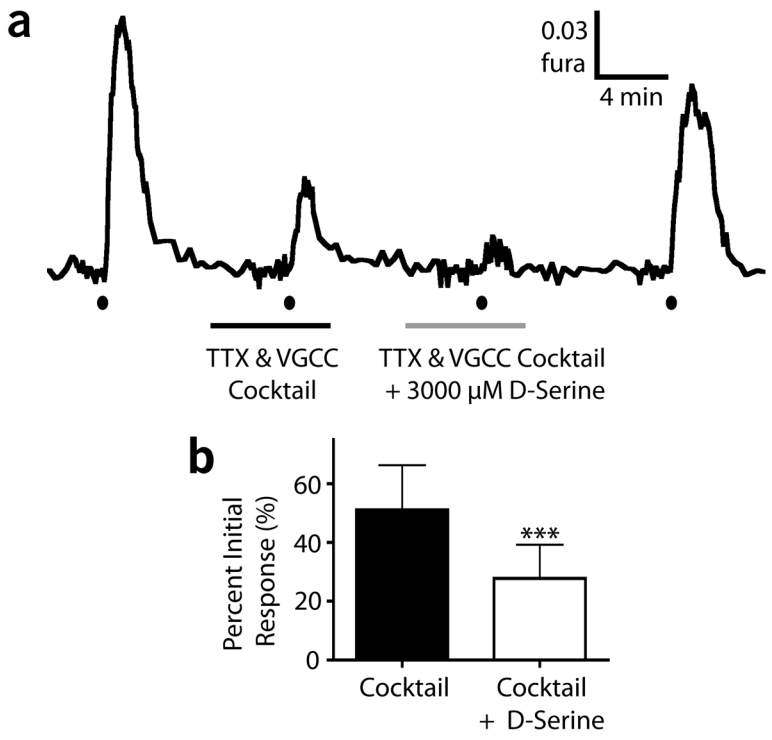

Figure 4.14 D-Serine inhibition of the kainate-induced Ca^{2+} response is not prevented by TTX and VGCC inhibition. (a) A representative trace showing four Ca^{2+} increases elicited by bath application of 50 µM kaniate (20 sec, *black circles*). The second response is obtained in the presence of (in µM) 0.5 TTX, 100 $NiCl_2$, 1 ω-conotoxin, 10 nimodipine (TTX & VGCC cocktail, *black bar*) and the third in the presence of the cocktail and 3000 µM D-serine (*grey bar*). (b) Mean ± SD normalized peak responses comparing the second and third response from the experiment in *a* (n = 6, from 153 cells). ***$P < 0.001$, two-tailed, paired T-test.

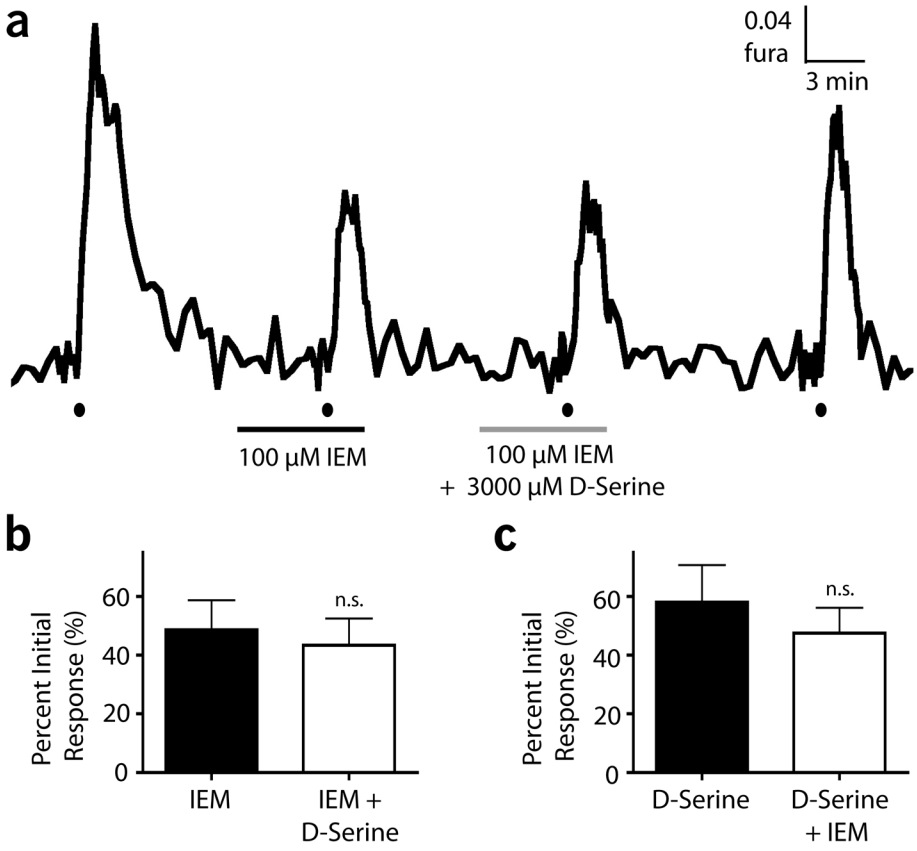

Figure 4.15 The CP-AMPAR antagonist IEM 1460 prevents the inhibitory effect of D-serine in isolated retina. (a) A representative trace showing four Ca^{2+} increases elicited by bath application of 50 µM kaniate (20 sec, *black circles*). The second response is obtained in the presence of 100 µM IEM 1460 (*black bar*) and the third in the presence of IEM and 3000 µM D-serine (*grey bar*). Bar graphs show mean ± SD normalized peak responses (second and third only) for reciprocal experiments where either (b) IEM 1460 (n = 8, from 191 cells) or (c) D-serine (n = 5, from 110 cells) alone was present during the second response and both were present during the third response. $^{n.s.}$ $P > 0.05$, two-tailed, paired T-test.

D-serine can reversibly inhibit non-NMDA iGluR-mediated responses and does so primarily by acting on the AMPAR pathway because it could be prevented in imaging experiments by reducing AMPAR activation. Similarly, kainate-induced Ca^{2+} increases in GCL cells in isolated retina were reduced by D-serine in a concentration-dependent fashion, but K^+-induced responses were unaffected, suggesting that voltage-gated Na^+ and Ca^{2+} channel inhibition was not involved. Synaptically-activated non-NMDA iGluR-mediated responses were also inhibited by D-serine, as revealed by WCR and MEA recordings in the isolated retina. We show that under our experimental conditions a significant proportion of cells are inhibited by endogenously produced D-serine. Lastly, the effect of D-serine in imaging experiments could be prevented by blocking CP-AMPARs indicating that D-serine inhibition of kainate-induced Ca^{2+} responses occurred largely via these receptors.

Potential Mechanisms for D-Serine Inhibition

Remaining questions linger about the precise mechanism of D-serine inhibition and whether it is caused by a direct effect on AMPA/KA receptors or an indirect effect that targets some other aspect of receptor activity. Also, while the results presented here and by Gong and colleagues (Gong *et al*., 2007) strongly suggest that D-serine is acting on AMPARs (directly or indirectly), it is not possible to unequivocally exclude KARs. Addressing both of these issues is a previous study that identified D-serine, amongst other amino acids, as a partial agonist of GluK2 receptors expressed in the human embryonic kidney 293 cell line (Fay *et al*., 2009). As a partial agonist of KARs, and potentially AMPARs, D-serine would compete for GluR binding sites thereby reducing the efficacy of full agonists such as kainate and glutamate. This could also account for

the relatively high (> 300 μM) concentrations of D-serine required to produce an effect on AMPA/KA receptor-mediated responses. Related are reports that D-serine can inhibit spontaneous currents of GluRδ2 (with the *lurcher* mutation) by acting at the agonist binding domain (Naur *et al*., 2007; Hansen *et al*., 2009). This is noteworthy because it provides other evidence that D-serine can bind directly to non-NMDA iGluRs.

An alternative mechanism for D-serine inhibition of AMPA/KARs involves the potential down-regulation of AMPARs. Prolonged exposure (96 h) of D-serine administered intraperitoneally resulted in increased gene expression of 17 specific genes in the rat forebrain (i.e, AP2B1- adapter-related protein 2 beta subunit 1) related to endocytosis and vesicle-mediated transport (Davidson *et al*., 2009). Non-discriminate up-regulation of these genes could result in a plethora of effects serving to modulate non-NMDA iGluRs. The findings of Davidson *et al*. (2009) could potentially result from enhanced NMDAR activation leading to AMPAR internalization (Lee *et al*., 2002; Biou *et al*., 2008) but this would not explain our results, as all of our external solutions included MK-801 to block NMDAR activation. Even if NMDARs were not completely blocked, the time frame for recovery from AMPAR internalization is too long to account for the recovery from D-serine inhibition in our experiments since NMDA-induced AMPAR internalization leads predominantly to degradation, not recycling (Lee *et al*., 2004). While this may prove to be yet another mechanism that D-serine can influence glutamatergic neurotransmission it is unlikely that it is involved in the effects reported here.

Inhibition of Kainate/AMPARs by Endogenous D-Serine

Surprisingly, the results of our studies with DAAO suggest that endogenous D-serine concentrations in wholemount retina are ≥ 500 μM (based on Fig. 2B) in some areas inhibiting 30-45% of cells under investigation. However, previous studies in the retina demonstrated that D-serine concentrations within the retina are sub-saturating for NMDAR (< 100 μM) because exogenous D-serine application enhanced NMDAR-mediated responses (Stevens *et al*., 2003; Gustafson *et al*., 2007; Kalbaugh *et al*., 2009; Reed *et al*., 2009). Our own study (Chapter 3; Daniels & Baldridge, 2010), using Ca^{2+} imaging techniques and retinal preparations identical to those used here, confirmed these results suggesting that this apparent discrepancy is not due to the preparation. Importantly, we show in Chapter 3 that some cells appear to be saturated since exogenous D-serine does not enhance their NMDA-induced response (Figure 3.8). Since < 50% of cells show an increased response upon degradation of D-serine it is possible that these may represent a specific cell type, or express a specific non-NMDA iGluR subunit, that is more susceptible to D-serine inhibition. In addition, it is possible that D-serine concentrations are not constant throughout the retina and may reach levels sufficient for AMPA/KA receptor inhibition in some areas but not others. Indeed Kalbaugh and colleagues (2009) showed that D-serine (and glycine) can transiently saturate the bipolar cell-RGC synapse while Stevens and colleagues (2003) showed that extrasynaptic NMDARs, activated by NMDA pressure ejection, were not saturated. Nonetheless, our findings strongly suggest that the retina can produce D-serine concentrations capable of influencing AMPA/KA receptors.

Could D-Serine Serve as a Negative Feedback Mechanism for iGluRs?

We hypothesize that D-serine inhibition of AMPA/KA receptor-mediated responses could serve as a feedback mechanism to regulate NMDAR activation in 2 distinct ways. This is plausible since D-serine reduces AMPA/KA receptor activity at concentrations in excess of that required for NMDAR coagonist binding site saturation. First, it is well characterized that cells must be depolarized sufficiently in order to relieve the Mg^{2+} block (Nowak *et al*., 1984) that prevents a full NMDAR-mediated response. Elevated D-serine could act to reduce depolarization by non-NMDA iGluR and in turn reduce NMDAR activation. Second, both production (Kim *et al*., 2005) and release (Schell *et al*., 1995; Mothet *et al*., 2005) of D-serine have been linked to AMPAR activation suggesting that AMPAR inhibition could target both of these processes resulting in less available D-serine for NMDAR activation. Interestingly, NMDAR activation itself has been shown to reduce SRR production of D-serine by causing SRR translocation to the membrane (Balan *et al*., 2009), therefore AMPA/KA receptor inhibition may provide an alternative feedback mechanism that is independent of NMDAR activation. Lastly, elevated D-serine may simply serve as a feedback mechanism for AMPA/KA receptors irrespective of NMDARs. A schematic diagram outlining this proposed mechanism is shown in Figure 5.2.

Summary

It is increasingly common that a single neurotransmitter or neuromodulator can act in an excitatory and inhibitory fashion typically depending on the receptor upon which it acts. The "original" NMDAR coagonist, glycine, is a prime example of this. It was first identified as an inhibitory neurotransmitter acting on glycine receptors and

subsequently found to bind NMDARs (Bristow *et al.*, 1986; Johnson & Ascher, 1987). Glutamate, the primary excitatory neurotransmitter in the CNS, inhibits ON bipolar cells in the retina by acting at mGluR6 and has recently been shown to enhance glycinergic inhibitory currents in these cells (Liu *et al*., 2010) presumably by allosteric modulation. The findings presented here and by Gong *et al*. (2007) argue that D-serine can inhibit non-NMDAR iGluRs, opposing its well-documented excitatory effect on glutamatergic neurotransmission. For all three of these neuroactive substances it is becoming increasingly important to determine the intricacies that govern the balance between excitation and inhibition.

Chapter 5: Discussion

Thesis Summary

This work began with the development of a new method to load Ca^{2+} indicator dye into GCL cells in the isolated retina preparation using electroporation. The electroporation method was deemed advantageous, compared to other methods, because cells could be loaded quickly and retinas studied almost immediately following isolation. This technique was employed for almost all of the Ca^{2+} imaging experiments using isolated retinas reported here.

The major theme of the research described in this thesis concerns the ability of the amino acid D-serine to influence NMDARs and non-NMDA iGluRs. Using cultured RGCs I demonstrated that D-serine and glycine enhanced NMDAR-mediated $[Ca^{2+}]_i$ increases in a concentration-dependent manner with maximal enhancement achieved at 100 μM. Comparatively, the two NMDAR coagonists were equally effective at enhancing NMDAR-mediated Ca^{2+} responses over a range of concentrations. Calcium imaging from GCL cells in the isolated retina allowed for a functional assessment of ambient D-serine levels in the retina. Exogenous application of D-serine could enhance NMDA-induced Ca^{2+} responses indicating that extracellular coagonist concentrations must be sub-saturating (i.e., < 100 μM based on my work in cultured cells and other reports in the literature). The use of DAAO to degrade endogenous D-serine demonstrated that D-serine contributes to ambient coagonist concentrations since NMDAR-mediate Ca^{2+} responses were reduced after its application.

Calcium imaging and patch clamp electrophysiology, of cultured RGCs and isolated retinas, and light-evoked MEA recordings, from isolated retinas, were used to obtain functional evidence of inhibition of non-NMDA iGluRs by D-serine. At concentrations of D-serine that would be saturating for NMDARs, kainate-induced $[Ca^{2+}]_i$ increases were reduced in a concentration dependent manner in cultured RGCs and from GCL cells in the isolated retina. The effect of D-serine on endogenous glutamate activation of AMPA/kainate receptors was assessed by measuring sEPSCs and light-evoked spiking in isolated retinas. D-Serine was clearly shown to reduce these responses, supporting a potential role for D-serine as an inhibitor of AMPA/kainate receptor activity, providing that D-serine concentrations could reach sufficient levels endogenously. To that end DAAO was again used to degrade endogenous D-serine resulting in enhanced AMPA/kainate receptor mediated responses in some GCL cells indicating that D-serine did reach sufficient levels endogenously to inhibit non-NMDA iGluR activity. Importantly, these findings were shown in the presence of antagonists that ruled out the possibility of D-serine acting via NMDARs to increase inhibition or by affecting GABA or glycine receptors. D-Serine did not affect K^+-induced Ca^{2+} responses and significantly decreased kainate-induced responses in the presence of TTX and VGCC blockers suggesting that it was not acting to reduce voltage-gated Ca^{2+} and Na^+ channel activity. Using specific AMPAR antagonists in cultured cells and isolated retina I showed that the inhibitory effect of D-serine on kainate-induced Ca^{2+} responses could be abolished suggesting that D-serine primarily targets AMPAR activity.

Discussion sections have been included in Chapters 2-4. The following general discussion will encompass more global issues and in some cases elaborate upon ideas that originated in previous sections.

Using Calcium Imaging to Study Neurophysiology

The predominant technique used in this study was calcium imaging from cultured RGCs and GCL cells in the isolated retina. The focus of this work has not been on intracellular Ca^{2+} dynamics *per se*; rather I have taken advantage of the fact that GluR activation leads directly and indirectly to increased intracellular $[Ca^{2+}]_i$. Calcium imaging allows for the relatively non-invasive study of many cells simultaneously, which permits simultaneous comparisons between the cells under investigation. Several reports provide extensive reviews of Ca^{2+} imaging and its applications (for example Kao *et al.*, 2010), but here I provide a brief outline of their history and properties and address key issues regarding the use of fura-2 in this thesis.

The seminal work of Nobel Laureate Roger Tsien enabled the study of intracellular Ca^{2+} with high specificity through the development of Ca^{2+}-sensitive fluorescent dyes. Ethylene glycol tetraacetic acid (EGTA) is a Ca^{2+} chelator that is one of the most widely used Ca^{2+} buffers in the study of biological systems. Tsien modified EGTA and produced the lower affinity, less pH sensitive Ca^{2+} chelator BAPTA that was the basis for one of the initial fluorescent calcium indicator dyes, Quin 2 (Tsien, 1980). A second generation of indicators were subsequently synthesized, resulting in one of the most widely used Ca^{2+} indicator dyes in neuroscience, fura-2 (Grynkiewicz *et al.*, 1985) which is used throughout this thesis. Fura-2 is a ratiometric dye whose excitation spectrum shifts towards shorter wavelengths with increased Ca^{2+} binding (Fig. 1.2).

Within the relevant range of $[Ca^{2+}]_i$ (K_d = 140 or 244 nM depending on $[Mg^{2+}]$), fura-2 has two peak excitation wavelengths, 340 and 380 nm on either side of the isobestic point (~360 nm). Collecting image pairs at 340 and 380 nm excitation allows the calculation of a ratio that accounts for uncertainties (differential dye loading, changing level of focus, dye bleaching, etc.) due to changes in dye concentration (Grynkiewicz *et al*., 1985). This is not possible when non-ratiometric dyes (e.g. Fluo-4, X-rhodamine-1) are used as these depend on absolute changes in fluorescence and measurements are susceptible to changes in intracellular dye concentration independent of $[Ca^{2+}]_i$. I have used fura-2 exclusively in this thesis, and in wholemount retinas, most cells show relatively normal baseline $[Ca^{2+}]_i$ (~50-100 nM) for neurons, as estimated from calibration experiments in cultured RGCs previously performed in our lab (Hartwick *et al*., 2004). However, some cells had elevated basal $[Ca^{2+}]_i$ as identified by ratiometric imaging and discussed in Chapter 2. This dichotomy did not exist with cultured RGCs suggesting that it was due either to the normal physiology or pathology of the isolated retina preparation. While both groups of cells showed increases in the fura-2 ratio in response to bath application of kainate, NMDA or K^+, only those cells with a low basal $[Ca^{2+}]_i$ (< 0.75 fura ratio) were included in the data analysis. This was due to concerns that peak responses from these cells would saturate the high affinity fura-2 leading to changes in the ratio that were not proportional to changes in $[Ca^{2+}]_i$. In order to truly assess the normalcy of Ca^{2+} responses from those cells with elevated basal $[Ca^{2+}]_i$ a low affinity ratiometric dye, such as fura-4F (K_d = 770 nM), would be better suited, although this could also make it difficult to discern the two populations of cells (low and high basal $[Ca^{2+}]_i$) clearly.

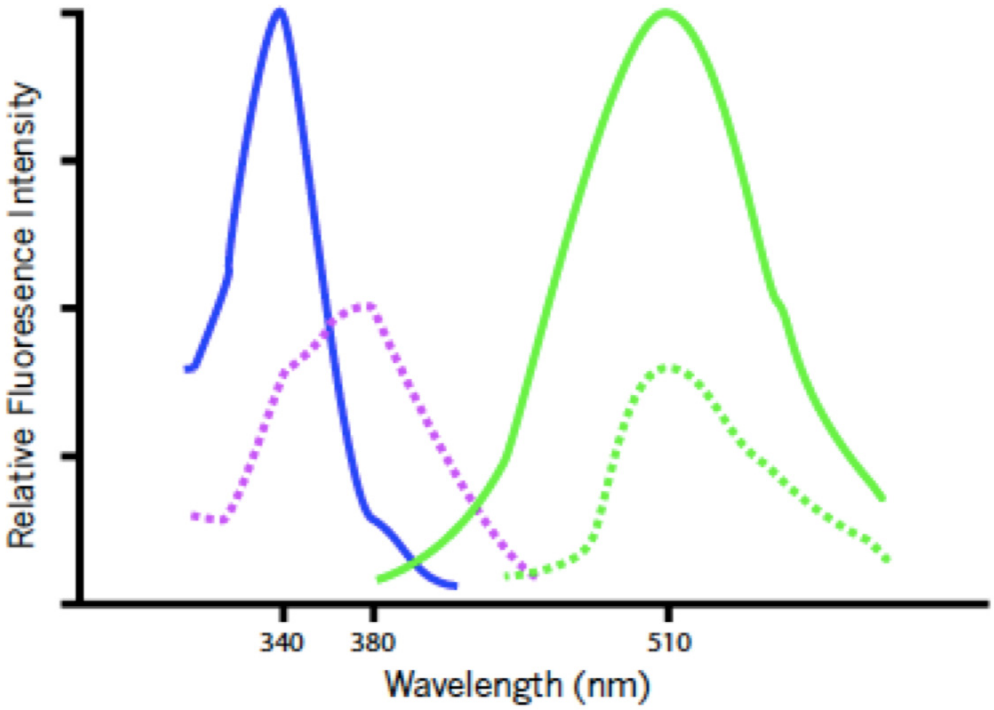

Figure 5.1 Fura-2 spectra schematic. The solid blue line represents the excitation spectrum for fura-2 in a high calcium solution while the dashed purple line is the excitation spectrum in zero calcium. The corresponding emission spectra are indicated in green (solid compared to dashed). At approximately 360 nm the excitation spectra are identical, known as the isobestic point. Notice that from high to zero calcium the peak excitation fluorescence shifts from 340 nm to 380 nm and the peak emission fluorescence is unchanged.

The development of the electroporation technique for loading Ca^{2+} indicator dye into the retina allowed for extensive loading of fura-2 throughout the GCL but some labeled cells were excluded from the data analysis for the following reasons. (1) Presumptive neurons were identified by size and shape criteria (outlined in Chapter 2) and presumptive glia were not included. (2) Cells with a fura-2 ratio ≥ 0.75 were excluded as mentioned above. (3) Retinal wholemounts are seldom completely flat and some areas within a given FOV were out of focus. Ratiometric imaging accounts for small changes in focus during the course of an experiment (Grynkiewicz *et al*., 1985) but cells with large deviations or cells that were initially extremely out of focus were not used. (4) There can be significant variability in the raw fluoresence between cells (see Figure 2.1) and retinas. Care was taken to limit photobleacing by adjusting the excitation exposure and intensity, while maintaining the ratio of 340 nm to 380 nm, through the use of neutral density filters. In some cells the resulting excitation intensity was too low or high for at least one excitation wavelength and therefore unusable because the ratio would not reflect relative difference between basal $[Ca^{2+}]_i$. (5) Some cells did not show a Ca^{2+} response to the initial treatment (kainate, NMDA, K^+). The working concentrations used throughout the thesis were determined based on the ability to achieve small, robust, repeatable responses in the majority of cells. Higher concentrations resulted in more cells responding but also larger responses in others cells thus risking saturation of the indicator dye and of the response. Alternatively, lower concentrations resulted in fewer cells responding and less consistent responses. (6) The majority of the experiments in this thesis consisted of an initial Ca^{2+} response, a second response in the presence of a treatment that might change the response and a third recovery response. While some

experiments had variable recovery, especially with the use of TTX and DAAO, most had very successful recovery. Cells that did not recover at all (uncommon, but where the recovery response was ≤ the response amplitude during the treatment) were excluded from analysis. We rationalized that this 'rundown' could be due to factors other than the drug treatment and would artificially influence the results. (7) Finally, some cells exhibited spontaneous changes in $[Ca^{2+}]_i$, in absence of any treatment and they were excluded from analysis if it interfered with the evoked Ca^{2+} response.

A clear downside of ratiometric imaging (with two excitation wavelengths) is the limited temporal resolution due to the need to excite with two wavelengths for any given ratio image. Calcium responses presented in this thesis were obtained by 15-60 sec bath applications of GluR agonists (or K^+) resulting in slow responses (tens to hundreds of seconds) and therefore the low temporal resolution was not a concern. However, in principle the fura-2 ratio could have been used to first report relative basal $[Ca^{2+}]_i$, and subsequently a single wavelength (380 nm excitation) used for more frequent image sampling. Other ratiometric dyes are available that have a single wavelength excitation but two peak emissions, such as Asante Calcium Red (Teflabs, Austin, TX, USA). Using two photomultiplier tubes the two emission channels could be separated and simultaneously captured allowing for ratiometric measurements with the temporal resolution of a non-ratiometric dye.

The Ca^{2+} responses elicited by bath application of GluR agonists and K^+ throughout this work do not recapitulate physiological responses. Typically, GluR activation is due to the activation of postsynaptic GluRs confined to the synapse and 'extra' glutamate is actively removed from the extracellular space by high affinity

transporters resulting in responses that last only a few milliseconds. Even prolonged glutamate release, such as volume transmission (glutamate spillover), is constricted to a localized region and results in responses that last tens of milliseconds and usually only involve high affinity NMDARs and mGluRs (Okubo & Iino, 2010). To some extent our drug delivery method is more representative of excitotoxic conditions where glutamate concentrations are elevated globally for prolonged periods (Leist & Nicotera, 1998). Nonetheless, we chose this method to explore GluR activity because we could reliably activate a population of cells simultaneously with the same agonist concentration at all cells. Alternative methods, such pressure ejection and other fast drug applications, may be more representative of synaptic input but are better suited for single-cell analysis. While surrounding cells can also respond to agonist application by pressure ejection the concentration and length of exposure would change as a function of time and space. Glutamate receptors have different agonist affinities depending on type and subunit expression (Hollmann & Heinemann, 1994), therefore, ensuring that the concentration is relatively equal for all cells under investigation eliminates this as a potential reason for differences in response amplitude and treatment effect between cells. In Chapter 3 we were specifically interested in the effect of D-serine on NMDAR-mediated [Ca^{2+}] increases and Ca^{2+} imaging was used exclusively. However, in Chapter 4 we were more broadly concerned with the influence of D-serine on non-NMDA iGluRs. Although confident in the results obtained using bath application of kainate (and K^{+}) to elicit Ca^{2+} responses, I performed WCR patch clamp and MEA experiments to strengthen the data since these recordings involved synaptic activation of GluRs by endogenous glutamate.

In our experiments Ca^{2+} response and treatment effect size variability was likely due, at least in part, to differential GluR and subunit expression. This was particularly evident in CP-AMPAR experiments in cultured RGCs where there was clear distinction between IEM-sensitive and insensitive cells (see Figure 4.12). However, most responses and treatment effects were graded as opposed to having distinct populations. For example, in isolated retina there was a wide spectrum of NMDA-induced Ca^{2+} response inhibition by the GluN2B antagonist ifenprodil (see Figure 3.7). To sufficiently test the hypothesis that specific receptor expression and cell type account for differences in agonist-induced Ca^{2+} responses and treatment effectiveness, cells could be targeted for morphological (neurobiotin injections; Perez De Sevilla Muller *et al.*, 2007) or molecular (single cell RT-PCR; Li *et al.*, 2004) identification based on their Ca^{2+} response profile.

D-Serine Release, Extracellular Concentration and Function

There is now a large body of knowledge pertaining to the potential physiological and pathophysiological consequences of D-serine in the CNS. However, there is not a clear understanding of how and when D-serine is released, the extent of extracellular concentration regulation and ultimately what its physiological role is.

Throughout the CNS D-serine and its synthesizing enzyme, serine racemase, have been localized to neurons and glia, but D-serine is generally considered to be a 'gliotransmitter'. In the brain the majority of serine racemase expression in glial cells is in protoplasmic astrocytes (Schell *et al.*, 1995; Schell *et al.*, 1997; Wolosker *et al.*, 1999a), which predominate amongst neurons, but it is also found in fibrous astrocytes of white matter tracts (Williams *et al.*, 2006) and microglia (Wu *et al*., 2004). Similarly,

retinal astrocytes contain D-serine and serine racemase, however, they are much more abundant in Müller cells (Stevens *et al.*, 2003; Williams *et al.*, 2006; Diaz *et al.*, 2007; Dun *et al.*, 2007b; Kalbaugh *et al.*, 2009). Of course the term gliotransmitter suggests that there is a level of control over the 'release' of D-serine and there is evidence that non-NMDA iGluR activation seems to be involved. The first report demonstrating this showed that cultured cortical astrocytes preloaded with D-[^{3}H]serine had greatly enhanced efflux of D-serine upon administration of kainate, AMPA, or glutamate but not K^+ or NMDA (Schell *et al.*, 1995). Furthermore, AMPAR activation, in concert with one of its binding partners, glutamate receptor interacting protein (GRIP), in C6 glioma cells (an immortalized astrocyte cell line) led to a three times greater efflux of D-serine compared to basal conditions (Kim *et al.*, 2005). Notably, in both studies there was significant basal D-serine efflux without any stimulation. Recently, the ability of glutamate to cause D-serine release in hippocampal slices was shown to involve the synaptic elements ephrinBs and their associated receptors located on glia, suggesting that it could be due to ephrin receptor interaction with GRIP (Zhuang *et al.*, 2010). In apparent contrast, an *in vivo* microdialysis study showed that kainate or NMDA application caused a significant decrease in extracellular D-serine (Hashimoto *et al.*, 2000). While the authors suggest that this might be due to increased uptake by glia, they do not attempt to explain a mechanism by which this decrease could be caused by iGluR activation. Conventional microdialysis studies require a sufficient amount of dialysate to provide accurate measurements and therefore were collected over 20 min intervals in this study (Hashimoto *et al*., 2000). Given this time period it is possible that the reported reduction in free D-serine was secondary to a transient increase in D-serine efflux. The

proposed D-serine increase might have then been counteracted by increased transport (discussed below) due to the altered concentration gradient and account for the reduction in free D-serine. In the retina AMPAR activation was shown to increase extracellular D-serine in wildtype and DAAO knockout mice (Sullivan & Miller, 2010). Furthermore, disruption of glial cell function by the glial-toxin α -aminoadipic acid prevented this effect in the knockout mice supporting AMPAR-mediated D-serine efflux from Müller cells and/or astrocytes.

Mechanistically, there are two non-competing views on how D-serine is released from glia. Most appealing, in light of the aforementioned relationship with non-NMDA iGluR activation, is the possible vesicular release of D-serine (from glia) like classical transmitter release from neurons. Using a DAAO-linked bioassay to monitor D-serine efflux from primary cultured cortical astrocytes or C6 glioma cells Mothet and colleagues (2005) confirmed that glutamate-induced D-serine efflux could be greatly reduced by blocking non-NMDA iGluRs and nearly abolished by also inhibiting group I/II mGluRs. In addition these authors showed for the first time that the efflux of D-serine from astrocytes was dependent on increased $[Ca^{2+}]_i$ (influx and stores release), and involved vesicular SNARE proteins (VAMP2 and VAMP3), necessary for exoxytosis of synaptic vesicles (Mothet *et al*., 2005). Accordingly, astrocytic D-serine has been identified in presumptive vesicles (Williams *et al.*, 2006) and colocalized with VAMP2 (Mothet *et al.*, 2005; Martineau *et al.*, 2008) and VAMP3 but not proteins associated with lysosomes and endosomes (Martineau *et al*., 2008). While most supporting data has been obtained using cultured astrocytes or cell lines, D-serine release from astrocytes in hippocampal slices can be prevented by clamping astrocytic $[Ca^{2+}]_i$ (Henneberger *et al*., 2010). This

was assessed functionally by the induction of LTP by D-serine in CA1 pyramidal neurons and the Ca^{2+} dependency supports the vesicular release of D-serine (Henneberger *et al.*, 2010). To my knowledge there is no evidence supporting or refuting the vesicular release of D-serine in the retina. While Williams and colleagues (2006) identified presumptive vesicularization of D-serine in pituitary astrocytes using electron microscopy, Müller cell cytoplasm was too electron-dense to make a firm conclusion about its localization in these cells.

The second mode of D-serine efflux has been identified in the retina as well as in other CNS areas. Salamander retinas incubated with 5-10 μM D-serine showed significant uptake over the course of 1-2 hrs that was Na^{+} dependent and thus consistent with ASCT transport (O'Brien *et al.*, 2005). The ASCT transporters (ASCT-1 and ASCT-2) are heteroexchangers of small neutral amino acids (alanine, serine, cysteine), exchanging at a 1:1 ratio (Zerangue & Kavanaugh, 1996) and have 40% sequence homology with glutamate transporters (Arriza *et al.*, 1993; Kanai *et al.*, 1993). Since ASC system involves exchange and not strictly uptake, like glutamate transporters, D-serine influx (O'Brien *et al*., 2005) or efflux could occur depending on the transmembrane concentration gradient. In support of previous findings (above) ACST-2 immunoreactivity was identified in mouse retinal sections and ASCT-1 and ASCT-2 were identified in primary cultured Müller cells and a Müller cell line (Dun *et al.*, 2007b). Furthermore, the authors provide evidence that ASCT-mediated D-serine uptake was performed primarily by ASCT-2 because glutamine and asparagine inhibited D-[^{3}H]serine uptake and ASCT-2, but not ASCT-1, accepts these amino acids as substrates. In ASCT-2 expressing oocytes D-[^{3}H]serine efflux was significantly enhanced by (25

mM) L-alanine > L-glutamine but not glutamate (Dun *et al.*, 2007b) supporting ASCT transport as an effective means of D-serine efflux that, importantly, is not influenced by extracellular glutamate concentrations. In cultured cortical astrocytes presumptive ASCT transport was shown to be more selective for the influx of neutral L-amino acids, in particular L-serine, and the L-serine-induced efflux of D-serine was greater than that caused by AMPA/KA receptor activation (Ribeiro *et al.*, 2002). This evidence suggests that glial cells preferentially support the efflux of D-serine compared to its influx. Furthermore, GluR- and transport-mediated efflux of D-serine can exist simultaneously, but transport is preferred. However, the importance of the transmembrane amino acid concentration gradient must be taken into consideration when interpreting these results. The effectiveness of L-serine vs. D-serine in inhibition of D-[^{3}H]serine uptake is concentration dependent with L-serine >> D-serine on 0.1 μM D-[^{3}H]serine uptake in glial cell cultures (Rutter *et al.*, 2007), L-serine > D-serine on 20 μM D-[^{3}H]serine uptake in cultured astrocytes (Ribeiro *et al*., 2002) and L-serine = D-serine on ≥1 mM D-[^{3}H]serine in C6 glioma cells (Sikka *et al.*, 2010). In total these studies reflect the majority of evidence pertaining to the glial release of D-serine and while it is likely that they both are physiologically relevant, the relative importance of AMPA/KA receptor- versus transport-mediated efflux and the delicate balance between transport-mediated D-serine influx/efflux is unclear.

Less well characterized is the synthesis and release of neuronal D-serine. Several studies have shown D-serine and serine racemase localization to neurons (Kartvelishvily *et al.*, 2006; Williams *et al.*, 2006; Dun *et al.*, 2007a; Miya *et al.*, 2008; Takayasu *et al.*, 2008), although D-serine was originally thought to be produced solely in glia

(Matsui *et al.*, 1995; Wolosker *et al.*, 1999a; Ribeiro *et al.*, 2002; Stevens *et al.*, 2003; Mustafa *et al.*, 2004). So far a single study has demonstrated D-serine release from neurons including release from primary cultured cortical neurons, cortical slices and from cortex *in vivo* (Rosenberg *et al.*, 2010). In this elegant study, the authors show that cultured neurons can release pre-loaded D-[^{3}H]serine by AMPAR activation or depolarization by veratridine but not via NMDARs. Since veratridine opens Na^+ channels it caused D-serine release from neurons selectively and not glia, as opposed to non-discriminate AMPA or K^+, allowing its use in slices and in the striatum, *in vivo*, to achieve endogenous neuronal D-release. Furthermore, veratridine-induced D-serine, but not glutamate, release in cortical slices was Ca^{2+}-independent suggesting that there was no significant vesicular release of neuronal D-serine (Rosenberg *et al.*, 2010). Lastly, they provide evidence that neuronal D-serine release occurs via the Na^+-independent Asc-1 transporter, which is thought to be restricted to neurons. Interestingly, the use of Asc-1 knockout mice has indicated that this transporter accounts for ~75% of D-serine transport in the brain but Asc-1 has also been identified in glia (Rutter *et al.*, 2007). As mentioned previously D-serine uptake in the retina is Na^+-dependent (O'Brien *et al.*, 2005; Dun *et al.*, 2007b) and therefore this may represent a major difference in the regulation of D-serine when compared to the brain.

The work presented in this thesis involved bath application of D-serine and GluR agonists that could potentially influence D-serine efflux. Particularly in the isolated retina preparation the likelihood and consequences of this must be considered. In Chapter 3, 100 μM D-serine was shown to enhance NMDA-induced Ca^{2+} responses in the majority of cells. There is general consensus that AMPA/KA receptor but not

NMDAR activation causes measurable D-serine release (Schell *et al.*, 1995; Rosenberg *et al.*, 2010; Sullivan & Miller, 2010) and therefore, this protocol should not have influenced the endogenous extracellular D-serine concentration. The bath application of D-serine could potentially drive ASCT-2 transport to increase D-serine uptake due to the change in concentration gradient. This could lead to a functional reduction in the amount of D-serine available to NMDARs suggesting that, if anything, our results may underestimate the extent of the enhancement of the NMDA-induced Ca^{2+} response. In Chapter 4 kainate was predominantly used to elicit Ca^{2+} responses and this could cause the efflux of D-serine from glial cells (Sullivan & Miller, 2010). In cortical slices and retina AMPAR activation caused a ≤ 2 fold net increase in extracellular D-serine concentration after application of 50-100 μM AMPA plus 50 μM cyclothiazide (Rosenberg *et al.*, 2010; Sullivan & Miller, 2010, respectively). Rat vitreous humor D-serine concentration were measured to be ~2 μM (Thongkhao-On *et al.*, 2004) however, in the restricted extracellular spaces of the retina concentrations may be significantly higher than can be measured from the vitreous or from perfusate. Therefore, in the isolated retina Ca^{2+} imaging experiments exogenous D-serine application might be supplemented by AMPAR-mediated D-serine efflux. Concentrations of exogenous D-serine application in Chapter 4 ranged from 100-3000 μM potentially causing a large D-serine transmembrane concentration gradient to drive D-serine influx. If D-serine itself truly inhibits AMPA/kainate receptors then transport would reduce its extracellular availability for the same reasons as argued above. An alternative concern arises from the fact that D-serine influx would be counteracted by efflux of another small neutral amino acid. The most likely candidate would be L-serine (Ribeiro *et al.*, 2002) that in turn

might induce the inhibitory effect that we have shown. However, in cultured hippocampal cells L-serine had no effect on the kainate-induced whole cell current supporting a specific effect of the D-isomer (Gong *et al*., 2007). In this thesis D-serine inhibited AMPAR-mediated currents and kainate-induced Ca^{2+} responses from cultured RGCs, in the absence of glial cell transport, strengthening the argument that D-serine is acting specifically and not via a transport or breakdown product.

The ambient extracellular D-serine concentration is of extreme importance because of its impact on iGluR-mediated cellular communication. Direct measurements of extracellular fluids from several CNS regions in tissue preparations or *in vivo* provide values ranging from 1-10 μM (Hashimoto *et al.*, 1995; Hashimoto & Oka, 1997; Thongkhao-On *et al.*, 2004; Ciriacks & Bowser, 2006; O'Brien & Bowser, 2006). Coincident with these reports are measurements of extracellular glutamate of 1-5 μM (Lerma *et al.*, 1986; Hashimoto *et al.*, 1995; Thongkhao-On *et al.*, 2004; Ciriacks & Bowser, 2006; Nyitrai *et al.*, 2006). Given the confined extracellular space at and surrounding the synapse and the presence of clearance mechanisms, these values are not necessarily reflective of the true concentrations, as they pertain to physiological function. However, it is impossible to measure this directly. Estimates of basal glutamate at the synapse are considerable lower (~25 nM) than those measured directly (Herman & Jahr, 2007). High affinity uptake by glutamate transporters located near the synapse drastically lower glutamate levels at the synapse (Chen & Diamond, 2002; Herman & Jahr, 2007) effectively reducing inappropriate activation and receptor desensitization. Similarly, direct measurements of glutamate release (up to 100 μM; Hashimoto *et al.*, 2000) are

substantially different than estimated synaptic concentrations (9-12 mM; Wadiche & Jahr, 2001). Ambient extracellular NMDAR coagonists would keep NMDARs primed for activation upon glutamate binding. However, extracellular measurements of D-serine and glycine are between 1-10 μM each. This is greater than the EC_{50} for both coagonists, would likely produce opposing effects to receptor priming by reducing glutamate binding efficacy (Kemp & Priestley, 1991; Lester *et al.*, 1993) and causing NMDAR internalization (Nong *et al.*, 2003). Therefore, like glutamate, NMDAR coagonist are probably kept at lower concentrations at the synapse by transport mechanisms than direct measurements from extracellular fluid indicate.

A functional difference in the extracellular coagonist concentration available to synaptic and extrasynaptic NMDARs is apparent. Recordings from pyramidal neurons from hippocampal cultures showed that EPSCs were not enhanced by 100 μM D-serine because the NMDAR coagonist binding site was saturated with endogenously produced D-serine (Mothet *et al.*, 2000). Alternatively, NMDA-evoked currents, which would be primarily mediated by extrasynaptic NMDARs, were ~2 times larger in the presence of D-serine. Recordings from hypothalamic slices showed that endogenous D-serine, and not glycine, had a higher coagonist binding site occupancy at synaptic relative to extrasynaptic NMDARs (Panatier *et al.*, 2006). In cerebellar vermis slices NMDA-mediated EPSCs were saturated with D-serine and/or glycine (Billups & Attwell, 2003). The authors of all of these studies suggest active release of saturating coagonist levels during synaptic activation, as it would be efficient to transiently release them in coordination with glutamate. A study in the retina showed that D-serine could enhance NMDAR-mediated synaptic responses only in the presence of NBQX suggesting non-

NMDA iGluR-induced coagonist release that saturated synaptic NMDARs (Kalbaugh *et al*., 2009). On the other hand, light-evoked responses from RGCs were enhanced by exogenous application of 100 μM D-serine in salamander and mouse indicating that the coagonist site was not saturated by coagonist release (Gustafson *et al.*, 2007; Reed *et al.*, 2009). The reason for this discrepancy has not been identified but it is possible that greater extrasynaptic NMDAR recruitment occurred during the light-evoked responses (Reed *et al*., 2009) than during simulated ON-responses with CPPG (Kalbaugh *et al*., 2009). One could test this by determining the relationship between glutamate transport and D-serine efficacy. Reducing glutamate transport would enhance extrasynaptic NMDAR activation that might then uncover a D-serine sensitive enhancment of CPPG-evoked responses from RGCs. A balance of the effect of glutamate on extrasynaptic NMDAR recruitment and iGluR-mediated coagonist release likely governs the coagonist site occupancy. Therefore, probing coagonist site occupancy over a range of input intensities could determine what the precise relationship is. A schematic diagram depicting the proposed role of D-serine at low (< 100 μM) and high (≥ 300 μM) concentrations on NMDARs and non-NMDA iGluRs is shown in Figure 5.2.

The determination that D-serine specifically has an active physiological role at NMDARs is largely based on the effects caused by its enzymatic degradation. In particular the use of DAAO has been shown to selectively degrade D-serine, and not L-serine, glycine, glutamate, D-aspartate (Mothet *et al.*, 2000; Gustafson *et al.*, 2007) causing a significant reduction in NMDAR activity in several different preparations (Stevens *et al.*, 2003; Yang *et al.*, 2003; Panatier *et al.*, 2006). Controls clearly

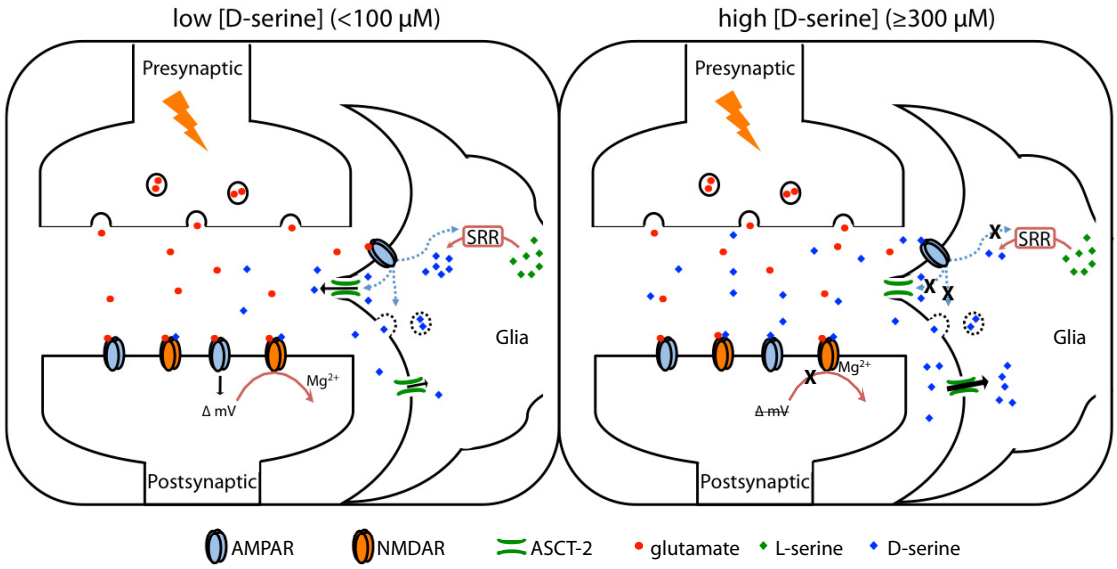

Figure 5.2 Schematic diagram of the influence of low and high D-serine concentrations at the synapse. Glutamate (●) is released from the presynaptic neuron and binds to AMPARs and NMDARs of the postsynaptic neuron. AMPAR-induced depolarization (Δ mV) facilitates the removal of the Mg^{2+} block on NMDARs. NMDARs require the coagonist D-serine (♦) to bind in concert with glutamate. Basal D-serine concentrations are maintained by influx/efflux via ASCT-2 located on the glial cell. Glutamate also acts on AMPARs on the glial cell that can increase the conversion of L-serine (♦) to D-serine by serine racemase (SRR) and enhance D-serine efflux by ASCT-2 transport or presumptive (dashed vesicles) exocytosis. At concentrations that are sub-saturating for NMDARs (low, < 100 µM) D-serine binds only to NMDARs enhancing activity of the postsynaptic cell. At elevated concentrations that would saturate NMDARs (high, ≥ 300 µM) D-serine can also inhibit AMPAR activity. On the postsynaptic neuron decreased AMPAR activity would decrease depolarization and lessen the relief of the Mg^{2+} block on NMDARs. Glial cell AMPAR inhibition would act to reduce D-serine production and efflux. High extracellular D-serine concentration would drive increased uptake via ASCT-2. Functionally, elevated D-serine causes the reduction of D-serine production and aims to reduce extracellular concentrations to keep the postsynaptic cell activity in a 'normal' range.

demonstrate that enzymatic activity (heat inactivation) and tissue with measurable D-serine concentrations (Mothet *et al.*, 2000) are necessary for DAAO to reduce NMDAR activity and that DAAO does not directly affect NMDAR activity (Lamas *et al.*, 2007). Although DAAO is highly specific for D-serine it degrades several other D-amino acids, alanine > leucine > proline (Krebs, 1935; Khoronenkova & Tishkov, 2008). Of particular consequence may be D-alanine because it is elevated ubiquitously throughout the CNS in mice lacking DAAO (Morikawa *et al.*, 2001) and can act as an NMDAR coagonist (Johnson & Ascher, 1987; Bonhaus *et al.*, 1989; Vyklicky *et al.*, 1990). Subsequent experiments have used DsDa to enzymatically degrade D-serine, with little effect on any other amino acids, confirming that D-serine, not D-alanine, is a major endogenous coagonist (Shleper *et al.*, 2005; Kartvelishvily *et al.*, 2006; Gustafson *et al.*, 2007).

In Chapters 3 and 4 DAAO was used to assess endogenous D-serine concentrations in the retina as they pertain to NMDAR and non-NMDA iGluR function, respectively. NMDA-induced Ca^{2+} responses were significantly reduced in all cells after DAAO application indicating an ambient coagonist concentration sufficient to influence NMDAR function. Consistent with other studies in the retina (Gustafson *et al.*, 2007; Kalbaugh *et al.*, 2009; Stevens *et al.*, 2010) we are confident that this reflects degradation of D-serine instead of other amino acids. Light-evoked spiking activity recorded using the MEA and kainate-induced Ca^{2+} responses were enhanced in 30-45% of cells following DAAO application (Figure 4.11). Accordingly heat inactivation of DAAO prior to its application resulted in no effect on kainate-induced Ca^{2+} responses suggesting that the enzymatic activity of DAAO relieved some endogenous inhibition of AMPA/kainate receptors. Experiments with exogenously applied D-serine (Figure 4.4;

Gong *et al*., 2007) indicate that ≥ 300 μM extracellular D-serine would be necessary to achieve AMPA/kainate receptor inhibition. Figure 3.8 showed that exogenous D-serine enhances NMDA-induced Ca^{2+} responses in most, but not all, cells (50-90% of cells depending on the NMDA concentration). D-Serine concentrations could be localized differentially, as has been shown in cultured hippocampal cultures (Mothet *et al.*, 2000), and therefore the majority, but not all, of cells are exposed to sub-saturating (< 100 μM) extracellular D-serine. Additionally, kainate (imaging) or light (MEA) could cause D-serine release from glia sufficient to inhibit AMPA/kainate receptors that is uncovered with degradation using DAAO. The specificity of DAAO is of concern in light of its known action on D-alanine (above). Racemic alanine concentrations are similar to D-serine measurements from the vitreous (Thongkhao-On *et al.*, 2004) and D-alanine can also inhibit AMPA/kainate receptors (Gong *et al*., 2007) but iGluR-mediated release has not been reported. To clarify this ambiguity regarding the effect of DAAO, experiments with DsDa , which degrades D-serine with higher specificity, would be useful. Unfortunately, it was not commercially available, we did not have the resources to make it ourselves and attempts to obtain it from other laboratories proved unsuccessful. Regardless, an inhibitory effect on non-NMDA iGluR responses was clearly uncovered by DAAO enzymatic activity that probably involved D-serine but a potential contribution from D-alanine cannot be ruled out.

Conclusion

The work presented here, and by others, support the idea that modulation of D-serine production, release and clearance can influence NMDAR activity independent of

glutamate. Another layer of complexity is now added with further evidence that D-serine can reduce AMPA/kainate receptor activity independent of NMDARs and the first report that native concentrations may be sufficient to do so endogenously. I feel that the results presented here are strengthened by the multiple approaches used to address specific questions (i.e., cultured cells, isolated retinas, Ca^{2+} imaging, patch clamp and MEA recordings). As a whole this body of work adds significantly to the fields of Ca^{2+} imaging, glutamate receptor, retinal physiology and D-serine research.

Appendix: Copyright Permissions

JOHN WILEY AND SONS LICENSE TERMS AND CONDITIONS

Oct 18, 2010

This is a License Agreement between Bryan A Daniels ("You") and John Wiley and Sons ("John Wiley and Sons") provided by Copyright Clearance Center ("CCC"). The license consists of your order details, the terms and conditions provided by John Wiley and Sons, and the payment terms and conditions.

All payments must be made in full to CCC. For payment instructions, please see information listed at the bottom of this form.

License Number	2532260783533
License date	Oct 18, 2010
Licensed content publisher	John Wiley and Sons
Licensed content publication	Journal of Neurochemistry
Licensed content title	d-Serine enhancement of NMDA receptor-mediated calcium increases in rat retinal ganglion cells
Licensed content author	Bryan A. Daniels,William H. Baldridge
Licensed content date	Mar 1, 2010
Start page	1180
End page	1189
Type of use	Dissertation/Thesis
Requestor type	Author of this Wiley article
Format	Print and electronic
Portion	Full article
Will you be translating?	No
Order reference number	
Total	0.00 USD

Terms and Conditions

TERMS AND CONDITIONS

Request for Permission to Reproduce Previously Published Material

(please save this file to your desktop, fill out, save again, and e-mail to permissions@the-aps.org)

Your Name: Bryan A. Daniels E-mail: badaniel@dal.ca

Affiliation: Dalhousie University

University Address (for PhD students): Killam College 6th , 14th floor Tupper Medical Bldg, Halifax, NS, CAN, B3H 1X5

Description of APS material to be reproduced (check all that apply):

- ☑ Figure
- ☐ Table
- ☑ Partial Article
- ☐ Full Article
- ☐ Abstract
- ☐ Book Chapter

Other (please describe):

Are you an author of the APS material to be reproduced? ◉ Yes ○ No

Please provide all applicable information about the APS material you wish to use:

Author(s): Jianing Yu, Bryan A. Daniels, William H. Baldridge

Article or Chapter Title: Slow Excitation of cultured rat retinal ganglion cells by Activating Group I metabo

Journal or Book Title: Journal of Neurophysiology

Volume: 102 Page No(s): 3728-38 Figure No(s): 1 Table No(s):

Year: 2009 DOI: 10.1152/jn.00880.2009

(If you are reproducing figures or tables from more than one article, please fill out and send a separate form for each citation.)

Please provide all applicable information about where the APS material will be used:

How will the APS material be used? (please select from drop-down list) Dissertation

If "other," please describe:

Title of publication or meeting where APS material will be used (if used in an article or book chapter, please provide the journal name or book title as well as the article/chapter title):

Publisher (if journal or book):

URL (if website):

Date of Meeting or Publication:

Will readers be charged for the material: ○ Yes ◉ No

Additional Information:

APPROVED
By Penny Ripka at 12:04 pm, Nov 16, 2010

THE AMERICAN PHYSIOLOGICAL SOCIETY
9650 Rockville Pike, Bethesda, MD 20814-3991

Permission is granted for use of the material specified above, provided the publication is credited as the source, including the words "used with permission."

Publications Manager & Executive Editor

References

AGUDO, M., PEREZ-MARIN, M. C., LONNGREN, U., SOBRADO, P., CONESA, A., CANOVAS, I., SALINAS-NAVARRO, M., MIRALLES-IMPERIAL, J., HALLBOOK, F. & VIDAL-SANZ, M. (2008). Time course profiling of the retinal transcriptome after optic nerve transection and optic nerve crush. *Mol Vis* 14, 1050-1063.

AGUDO, M., PEREZ-MARIN, M. C., SOBRADO-CALVO, P., LONNGREN, U., SALINAS-NAVARRO, M., CANOVAS, I., NADAL-NICOLAS, F. M., MIRALLES-IMPERIAL, J., HALLBOOK, F. & VIDAL-SANZ, M. (2009). Immediate upregulation of proteins belonging to different branches of the apoptotic cascade in the retina after optic nerve transection and optic nerve crush. *Invest Ophthalmol Vis Sci* 50, 424-431.

AIZENMAN, E., FROSCH, M. P. & LIPTON, S. A. (1988). Responses mediated by excitatory amino acid receptors in solitary retinal ganglion cells from rat. *J Physiol* 396, 75-91.

ANSON, L. C., CHEN, P. E., WYLLIE, D. J., COLQUHOUN, D. & SCHOEPFER, R. (1998). Identification of amino acid residues of the NR2A subunit that control glutamate potency in recombinant NR1/NR2A NMDA receptors. *J Neurosci* 18, 581-589.

ANSON, L. C., SCHOEPFER, R., COLQUHOUN, D. & WYLLIE, D. J. (2000). Single-channel analysis of an NMDA receptor possessing a mutation in the region of the glutamate binding site. *J Physiol* 527 Pt 2, 225-237.

ARRIZA, J. L., KAVANAUGH, M. P., FAIRMAN, W. A., WU, Y. N., MURDOCH, G. H., NORTH, R. A. & AMARA, S. G. (1993). Cloning and expression of a human neutral amino acid transporter with structural similarity to the glutamate transporter gene family. *J Biol Chem* 268, 15329-15332.

AWATRAMANI, G. B. & SLAUGHTER, M. M. (2001). Intensity-dependent, rapid activation of presynaptic metabotropic glutamate receptors at a central synapse. *J Neurosci* 21, 741-749.

AWOBULUYI, M., YANG, J., YE, Y., CHATTERTON, J. E., GODZIK, A., LIPTON, S. A. & ZHANG, D. (2007). Subunit-specific roles of glycine-binding domains in activation of NR1/NR3 N-methyl-D-aspartate receptors. *Mol Pharmacol* 71, 112-122.

BALAN, L., FOLTYN, V. N., ZEHL, M., DUMIN, E., DIKOPOLTSEV, E., KNOH, D., OHNO, Y., KIHARA, A., JENSEN, O. N., RADZISHEVSKY, I. S. & WOLOSKER, H. (2009). Feedback inactivation of D-serine synthesis by NMDA receptor-elicited translocation of serine racemase to the membrane. *Proc Natl Acad Sci U S A* 106, 7589-7594.

BALDRIDGE, W. H. (1996). Optical recordings of the effects of cholinergic ligands on neurons in the ganglion cell layer of mammalian retina. *J Neurosci* 16, 5060-5072.

BANSAL, A., SINGER, J. H., HWANG, B. J., XU, W., BEAUDET, A. & FELLER, M. B. (2000). Mice lacking specific nicotinic acetylcholine receptor subunits exhibit dramatically altered spontaneous activity patterns and reveal a limited role for retinal waves in forming ON and OFF circuits in the inner retina. *J Neurosci* 20, 7672-7681.

BARNETT, N. L. & POW, D. V. (2000). Antisense knockdown of GLAST, a glial glutamate transporter, compromises retinal function. *Invest Ophthalmol Vis Sci* 41, 585-591.

BARNETT, N. L., POW, D. V. & ROBINSON, S. R. (2000). Inhibition of Muller cell glutamine synthetase rapidly impairs the retinal response to light. *Glia* 30, 64-73.

BARON, B. M., HARRISON, B. L., MILLER, F. P., MCDONALD, I. A., SALITURO, F. G., SCHMIDT, C. J., SORENSEN, S. M., WHITE, H. S. & PALFREYMAN, M. G. (1990). Activity of 5,7-dichlorokynurenic acid, a potent antagonist at the N-methyl-D-aspartate receptor-associated glycine binding site. *Mol Pharmacol* 38, 554-561.

BARRES, B. A., SILVERSTEIN, B. E., COREY, D. P. & CHUN, L. L. (1988). Immunological, morphological, and electrophysiological variation among retinal ganglion cells purified by panning. *Neuron* 1, 791-803.

BEARD, M. E., DAVIES, T., HOLLOWAY, M. & HOLTZMAN, E. (1988). Peroxisomes in pigment epithelium and Muller cells of amphibian retina possess D-amino acid oxidase as well as catalase. *Exp Eye Res* 47, 795-806.

BEHREND, M. R., AHUJA, A. K., HUMAYUN, M. S., WEILAND, J. D. & CHOW, R. H. (2009). Selective labelling of retinal ganglion cells with calcium indicators by retrograde loading in vitro. *J Neurosci Methods* 179, 166-172.

BELCHER, S. M. & HOWE, J. R. (1997). Characterization of RNA editing of the glutamate-receptor subunits GluR5 and GluR6 in granule cells during cerebellar development. *Brain Res Mol Brain Res* 52, 130-138.

BENVENISTE, M., CLEMENTS, J., VYKLICKY, L., JR. & MAYER, M. L. (1990). A kinetic analysis of the modulation of N-methyl-D-aspartic acid receptors by glycine in mouse cultured hippocampal neurones. *J Physiol* 428, 333-357.

BERGER, M. L. (1995). On the true affinity of glycine for its binding site at the NMDA receptor complex. *J Pharmacol Toxicol Methods* 34, 79-88.

BERNARD, A., FERHAT, L., DESSI, F., CHARTON, G., REPRESA, A., BEN-ARI, Y. & KHRESTCHATISKY, M. (1999). Q/R editing of the rat GluR5 and GluR6 kainate receptors in vivo and in vitro: evidence for independent developmental, pathological and cellular regulation. *Eur J Neurosci* 11, 604-616.

BERRIDGE, M. J. (1998). Neuronal calcium signaling. *Neuron* 21, 13-26.

BILLUPS, D. & ATTWELL, D. (2003). Active release of glycine or D-serine saturates the glycine site of NMDA receptors at the cerebellar mossy fibre to granule cell synapse. *Eur J Neurosci* 18, 2975-2980.

BIOU, V., BHATTACHARYYA, S. & MALENKA, R. C. (2008). Endocytosis and recycling of AMPA receptors lacking GluR2/3. *Proc Natl Acad Sci U S A* 105, 1038-1043.

BLANKENSHIP, A. G., FORD, K. J., JOHNSON, J., SEAL, R. P., EDWARDS, R. H., COPENHAGEN, D. R. & FELLER, M. B. (2009). Synaptic and extrasynaptic factors governing glutamatergic retinal waves. *Neuron* 62, 230-241.

BONHAUS, D. W. & MCNAMARA, J. O. (1989). TCP binding: a tool for studying NMDA receptor-mediated neurotransmission in kindling. *Neurosci Biobehav Rev* 13, 261-267.

BONHAUS, D. W., YEH, G. C., SKARYAK, L. & MCNAMARA, J. O. (1989). Glycine regulation of the N-methyl-D-aspartate receptor-gated ion channel in hippocampal membranes. *Mol Pharmacol* 36, 273-279.

BONNOT, A., MENTIS, G. Z., SKOCH, J. & O'DONOVAN, M. J. (2005). Electroporation loading of calcium-sensitive dyes into the CNS. *J Neurophysiol* 93, 1793-1808.

BRANDSTATTER, J. H., KOULEN, P. & WASSLE, H. (1997). Selective synaptic distribution of kainate receptor subunits in the two plexiform layers of the rat retina. *J Neurosci* 17, 9298-9307.

BRISTOW, D. R., BOWERY, N. G. & WOODRUFF, G. N. (1986). Light microscopic autoradiographic localisation of [3H]glycine and [3H]strychnine binding sites in rat brain. *Eur J Pharmacol* 126, 303-307.

BUI, B. V., HU, R. G., ACOSTA, M. L., DONALDSON, P., VINGRYS, A. J. & KALLONIATIS, M. (2009). Glutamate metabolic pathways and retinal function. *J Neurochem* 111, 589-599.

BUREAU, I., DIEUDONNE, S., COUSSEN, F. & MULLE, C. (2000). Kainate receptor-mediated synaptic currents in cerebellar Golgi cells are not shaped by diffusion of glutamate. *Proc Natl Acad Sci U S A* 97, 6838-6843.

BURNASHEV, N., SCHOEPFER, R., MONYER, H., RUPPERSBERG, J. P., GUNTHER, W., SEEBURG, P. H. & SAKMANN, B. (1992). Control by asparagine residues of calcium permeability and magnesium blockade in the NMDA receptor. *Science* 257, 1415-1419.

CASTILLO, P. E., MALENKA, R. C. & NICOLL, R. A. (1997). Kainate receptors mediate a slow postsynaptic current in hippocampal CA3 neurons. *Nature* 388, 182-186.

CHATTERTON, J. E., AWOBULUYI, M., PREMKUMAR, L. S., TAKAHASHI, H., TALANTOVA, M., SHIN, Y., CUI, J., TU, S., SEVARINO, K. A., NAKANISHI, N., TONG, G., LIPTON, S. A. & ZHANG, D. (2002). Excitatory glycine receptors containing the NR3 family of NMDA receptor subunits. *Nature* 415, 793-798.

CHAVEZ, A. E., GRIMES, W. N. & DIAMOND, J. S. (2010). Mechanisms underlying lateral GABAergic feedback onto rod bipolar cells in rat retina. *J Neurosci* 30, 2330-2339.

CHAVEZ, A. E., SINGER, J. H. & DIAMOND, J. S. (2006). Fast neurotransmitter release triggered by Ca influx through AMPA-type glutamate receptors. *Nature* 443, 705-708.

CHEN, S. & DIAMOND, J. S. (2002). Synaptically released glutamate activates extrasynaptic NMDA receptors on cells in the ganglion cell layer of rat retina. *J Neurosci* 22, 2165-2173.

CHERGUI, K., BOURON, A., NORMAND, E. & MULLE, C. (2000). Functional GluR6 kainate receptors in the striatum: indirect downregulation of synaptic transmission. *J Neurosci* 20, 2175-2182.

CHOI, D. W. (1985). Glutamate neurotoxicity in cortical cell culture is calcium dependent. *Neurosci Lett* 58, 293-297.

CHOI, D. W. (1988). Glutamate neurotoxicity and diseases of the nervous system. *Neuron* 1, 623-634.

CHRISTENSEN, J. K., PATERNAIN, A. V., SELAK, S., AHRING, P. K. & LERMA, J. (2004). A mosaic of functional kainate receptors in hippocampal interneurons. *J Neurosci* 24, 8986-8993.

CHRISTENSEN, K. V., DAI, W. M., LAMBERT, J. D. & EGEBJERG, J. (2000). Larger intercellular variation in (Q/R) editing of GluR6 than GluR5 revealed by single cell RT-PCR. *Neuroreport* 11, 3577-3582.

CIABARRA, A. M., SULLIVAN, J. M., GAHN, L. G., PECHT, G., HEINEMANN, S. & SEVARINO, K. A. (1995). Cloning and characterization of chi-1: a developmentally regulated member of a novel class of the ionotropic glutamate receptor family. *J Neurosci* 15, 6498-6508.

CIRIACKS, C. M. & BOWSER, M. T. (2006). Measuring the effect of glutamate receptor agonists on extracellular D-serine concentrations in the rat striatum using online microdialysis-capillary electrophoresis. *Neurosci Lett* 393, 200-205.

COLLINGRIDGE, G. L., OLSEN, R. W., PETERS, J. & SPEDDING, M. (2009). A nomenclature for ligand-gated ion channels. *Neuropharmacology* 56, 2-5.

CONN, P. J. & PIN, J. P. (1997). Pharmacology and functions of metabotropic glutamate receptors. *Annu Rev Pharmacol Toxicol* 37, 205-237.

CONSTANTINE-PATON, M. & CLINE, H. T. (1998). LTP and activity-dependent synaptogenesis: the more alike they are, the more different they become. *Curr Opin Neurobiol* 8, 139-148.

CULL-CANDY, S., BRICKLEY, S. & FARRANT, M. (2001). NMDA receptor subunits: diversity, development and disease. *Curr Opin Neurobiol* 11, 327-335.

CURRAS, M. C. & PALLOTTA, B. S. (1996). Single-channel evidence for glycine and NMDA requirement in NMDA receptor activation. *Brain Res* 740, 27-40.

DANIELS, B. A. & BALDRIDGE, W. H. (2010). d-Serine enhancement of NMDA receptor-mediated calcium increases in rat retinal ganglion cells. *J Neurochem* 112, 1180-1189.

DAS, S., SASAKI, Y. F., ROTHE, T., PREMKUMAR, L. S., TAKASU, M., CRANDALL, J. E., DIKKES, P., CONNER, D. A., RAYUDU, P. V., CHEUNG, W., CHEN, H. S., LIPTON, S. A. & NAKANISHI, N. (1998). Increased NMDA current and spine density in mice lacking the NMDA receptor subunit NR3A. *Nature* 393, 377-381.

DAVIDSON, M. E., KEREPESI, L. A., SOTO, A. & CHAN, V. T. (2009). D-Serine exposure resulted in gene expression changes implicated in neurodegenerative disorders and neuronal dysfunction in male Fischer 344 rats. *Arch Toxicol* 83, 747-762.

DEROUICHE, A. & RAUEN, T. (1995). Coincidence of L-glutamate/L-aspartate transporter (GLAST) and glutamine synthetase (GS) immunoreactions in retinal glia: evidence for coupling of GLAST and GS in transmitter clearance. *J Neurosci Res* 42, 131-143.

DEVRIES, S. H. (2000). Bipolar cells use kainate and AMPA receptors to filter visual information into separate channels. *Neuron* 28, 847-856.

DIAMOND, J. S. & COPENHAGEN, D. R. (1993). The contribution of NMDA and non-NMDA receptors to the light-evoked input-output characteristics of retinal ganglion cells. *Neuron* 11, 725-738.

DIAZ, C. M., MACNAB, L. T., WILLIAMS, S. M., SULLIVAN, R. K. & POW, D. V. (2007). EAAT1 and D-serine expression are early features of human retinal development. *Exp Eye Res* 84, 876-885.

DING, X., MA, N., NAGAHAMA, M., YAMADA, K. & SEMBA, R. (2010). Localization of D: -serine and serine racemase in neurons and neuroglias in mouse brain. *Neurol Sci*, DOI: 10.1007/s10072-10010-10422-10072.

DINGLEDINE, R., BORGES, K., BOWIE, D. & TRAYNELIS, S. F. (1999). The glutamate receptor ion channels. *Pharmacol Rev* 51, 7-61.

DONOVAN, S. L. & DYER, M. A. (2006). Preparation and square wave electroporation of retinal explant cultures. *Nat Protoc* 1, 2710-2718.

DUN, Y., DUPLANTIER, J., ROON, P., MARTIN, P. M., GANAPATHY, V. & SMITH, S. B. (2007a). Serine racemase expression and d-serine content are developmentally regulated in neuronal ganglion cells of the retina. *J Neurochem*.

DUN, Y., MYSONA, B., ITAGAKI, S., MARTIN-STUDDARD, A., GANAPATHY, V. & SMITH, S. B. (2007b). Functional and molecular analysis of D-serine transport in retinal Muller cells. *Exp Eye Res* 84, 191-199.

DUNLOP, D. S., NEIDLE, A., MCHALE, D., DUNLOP, D. M. & LAJTHA, A. (1986). The presence of free D-aspartic acid in rodents and man. *Biochem Biophys Res Commun* 141, 27-32.

FARRELL, S. R., RAYMOND, I. D., FOOTE, M., BRECHA, N. C. & BARNES, S. (2010). Modulation of voltage-gated ion channels in rat retinal ganglion cells mediated by somatostatin receptor subtype 4. *J Neurophysiol* 104, 1347-1354.

FAY, A. M., CORBEIL, C. R., BROWN, P., MOITESSIER, N. & BOWIE, D. (2009). Functional characterization and in silico docking of full and partial GluK2 kainate receptor agonists. *Mol Pharmacol* 75, 1096-1107.

FLETCHER, E. L., HACK, I., BRANDSTATTER, J. H. & WASSLE, H. (2000). Synaptic localization of NMDA receptor subunits in the rat retina. *J Comp Neurol* 420, 98-112.

FONNUM, F. (1984). Glutamate: a neurotransmitter in mammalian brain. *J Neurochem* 42, 1-11.

FRITZSCH, B. & WILM, C. (1990). Dextran amines in neuronal tracing. *Trends Neurosci* 13, 14.

FUJIYAMA, F., HIOKI, H., TOMIOKA, R., TAKI, K., TAMAMAKI, N., NOMURA, S., OKAMOTO, K. & KANEKO, T. (2003). Changes of immunocytochemical localization of vesicular glutamate transporters in the rat visual system after the retinofugal denervation. *J Comp Neurol* 465, 234-249.

GANONG, A. H. & COTMAN, C. W. (1986). Kynurenic acid and quinolinic acid act at N-methyl-D-aspartate receptors in the rat hippocampus. *J Pharmacol Exp Ther* 236, 293-299.

GANONG, A. H., LANTHORN, T. H. & COTMAN, C. W. (1983). Kynurenic acid inhibits synaptic and acidic amino acid-induced responses in the rat hippocampus and spinal cord. *Brain Res* 273, 170-174.

GAO, J., MAISON, S. F., WU, X., HIROSE, K., JONES, S. M., BAYAZITOV, I., TIAN, Y., MITTLEMAN, G., MATTHEWS, D. B., ZAKHARENKO, S. S., LIBERMAN, M. C. & ZUO, J. (2007). Orphan glutamate receptor delta1 subunit required for high-frequency hearing. *Mol Cell Biol* 27, 4500-4512.

GLIDDON, C. M., SHAO, Z., LEMAISTRE, J. L. & ANDERSON, C. M. (2009). Cellular distribution of the neutral amino acid transporter subtype ASCT2 in mouse brain. *J Neurochem* 108, 372-383.

GONG, X. Q., ZABEK, R. L. & BAI, D. (2007). D-Serine inhibits AMPA receptor-mediated current in rat hippocampal neurons. *Can J Physiol Pharmacol* 85, 546-555.

GRYNKIEWICZ, G., POENIE, M. & TSIEN, R. Y. (1985). A new generation of Ca2+ indicators with greatly improved fluorescence properties. *J Biol Chem* 260, 3440-3450.

GUSTAFSON, E. C., STEVENS, E. R., WOLOSKER, H. & MILLER, R. F. (2007). Endogenous D-serine contributes to NMDA-receptor-mediated light-evoked responses in the vertebrate retina. *J Neurophysiol* 98, 122-130.

HACK, I., FRECH, M., DICK, O., PEICHL, L. & BRANDSTATTER, J. H. (2001). Heterogeneous distribution of AMPA glutamate receptor subunits at the photoreceptor synapses of rodent retina. *Eur J Neurosci* 13, 15-24.

HAMA, Y., KATSUKI, H., TOCHIKAWA, Y., SUMINAKA, C., KUME, T. & AKAIKE, A. (2006). Contribution of endogenous glycine site NMDA agonists to excitotoxic retinal damage in vivo. *Neurosci Res* 56, 279-285.

HANNA, M. C. & CALKINS, D. J. (2007). Expression of genes encoding glutamate receptors and transporters in rod and cone bipolar cells of the primate retina determined by single-cell polymerase chain reaction. *Mol Vis* 13, 2194-2208.

HANSEN, K. B., NAUR, P., KURTKAYA, N. L., KRISTENSEN, A. S., GAJHEDE, M., KASTRUP, J. S. & TRAYNELIS, S. F. (2009). Modulation of the dimer interface at ionotropic glutamate-like receptor delta2 by D-serine and extracellular calcium. *J Neurosci* 29, 907-917.

HARADA, T., HARADA, C., SEKIGUCHI, M. & WADA, K. (1998). Light-induced retinal degeneration suppresses developmental progression of flip-to-flop alternative splicing in GluR1. *J Neurosci* 18, 3336-3343.

HARRIS, E. W., GANONG, A. H. & COTMAN, C. W. (1984). Long-term potentiation in the hippocampus involves activation of N-methyl-D-aspartate receptors. *Brain Res* 323, 132-137.

HARTVEIT, E. (1999). Reciprocal synaptic interactions between rod bipolar cells and amacrine cells in the rat retina. *J Neurophysiol* 81, 2923-2936.

HARTVEIT, E., BRANDSTATTER, J. H., ENZ, R. & WASSLE, H. (1995). Expression of the mRNA of seven metabotropic glutamate receptors (mGluR1 to 7) in the rat retina. An in situ hybridization study on tissue sections and isolated cells. *Eur J Neurosci* 7, 1472-1483.

HARTWICK, A. T., HAMILTON, C. M. & BALDRIDGE, W. H. (2008). Glutamatergic calcium dynamics and deregulation of rat retinal ganglion cells. *J Physiol* 586, 3425-3446.

HARTWICK, A. T., LALONDE, M. R., BARNES, S. & BALDRIDGE, W. H. (2004). Adenosine A1-receptor modulation of glutamate-induced calcium influx in rat retinal ganglion cells. *Invest Ophthalmol Vis Sci* 45, 3740-3748.

HARTWICK, A. T., ZHANG, X., CHAUHAN, B. C. & BALDRIDGE, W. H. (2005). Functional assessment of glutamate clearance mechanisms in a chronic rat glaucoma model using retinal ganglion cell calcium imaging. *J Neurochem* 94, 794-807.

HARVEY, D. M. & CALKINS, D. J. (2002). Localization of kainate receptors to the presynaptic active zone of the rod photoreceptor in primate retina. *Vis Neurosci* 19, 681-692.

HASHIMOTO, A., KANDA, J. & OKA, T. (2000). Effects of N-methyl-D-aspartate, kainate or veratridine on extracellular concentrations of free D-serine and L-glutamate in rat striatum: an in vivo microdialysis study. *Brain Res Bull* 53, 347-351.

HASHIMOTO, A., NISHIKAWA, T., HAYASHI, T., FUJII, N., HARADA, K., OKA, T. & TAKAHASHI, K. (1992). The presence of free D-serine in rat brain. *FEBS Lett* 296, 33-36.

HASHIMOTO, A. & OKA, T. (1997). Free D-aspartate and D-serine in the mammalian brain and periphery. *Prog Neurobiol* 52, 325-353.

HASHIMOTO, A., OKA, T. & NISHIKAWA, T. (1995). Extracellular concentration of endogenous free D-serine in the rat brain as revealed by in vivo microdialysis. *Neuroscience* 66, 635-643.

HAVERKAMP, S. & WASSLE, H. (2004). Characterization of an amacrine cell type of the mammalian retina immunoreactive for vesicular glutamate transporter 3. *J Comp Neurol* 468, 251-263.

HENNEBERGER, C., PAPOUIN, T., OLIET, S. H. & RUSAKOV, D. A. (2010). Long-term potentiation depends on release of D-serine from astrocytes. *Nature* 463, 232-236.

HERMAN, M. A. & JAHR, C. E. (2007). Extracellular glutamate concentration in hippocampal slice. *J Neurosci* 27, 9736-9741.

HESTRIN, S., SAH, P. & NICOLL, R. A. (1990). Mechanisms generating the time course of dual component excitatory synaptic currents recorded in hippocampal slices. *Neuron* 5, 247-253.

HIRANO, T., KASONO, K., ARAKI, K. & MISHINA, M. (1995). Suppression of LTD in cultured Purkinje cells deficient in the glutamate receptor delta 2 subunit. *Neuroreport* 6, 524-526.

HOLLMANN, M. & HEINEMANN, S. (1994). Cloned glutamate receptors. *Annu Rev Neurosci* 17, 31-108.

HONORE, T., DREJER, J., NIELSEN, E. O., WATKINS, J. C., OLVERMAN, H. J. & NIELSEN, M. (1989). Molecular target size analyses of the NMDA-receptor complex in rat cortex. *Eur J Pharmacol* 172, 239-247.

HOSHI, H., LIU, W. L., MASSEY, S. C. & MILLS, S. L. (2009). ON inputs to the OFF layer: bipolar cells that break the stratification rules of the retina. *J Neurosci* 29, 8875-8883.

HUANG, H., LUO, D. G., SHEN, Y., ZHANG, A. J., YANG, R. & YANG, X. L. (2004). AMPA receptor is involved in transmission of cone signal to ON bipolar cells in carp retina. *Brain Res* 1002, 86-93.

HUME, R. I., DINGLEDINE, R. & HEINEMANN, S. F. (1991). Identification of a site in glutamate receptor subunits that controls calcium permeability. *Science* 253, 1028-1031.

IKEDA, K., NAGASAWA, M., MORI, H., ARAKI, K., SAKIMURA, K., WATANABE, M., INOUE, Y. & MISHINA, M. (1992). Cloning and expression of the epsilon 4 subunit of the NMDA receptor channel. *FEBS Lett* 313, 34-38.

IZUMI, Y., CLIFFORD, D. B. & ZORUMSKI, C. F. (1990). Glycine antagonists block the induction of long-term potentiation in CA1 of rat hippocampal slices. *Neurosci Lett* 112, 251-256.

JAKOBS, T. C., BEN, Y. & MASLAND, R. H. (2007). Expression of mRNA for glutamate receptor subunits distinguishes the major classes of retinal neurons, but is less specific for individual cell types. *Mol Vis* 13, 933-948.

JAKOBS, T. C., KOIZUMI, A. & MASLAND, R. H. (2008). The spatial distribution of glutamatergic inputs to dendrites of retinal ganglion cells. *J Comp Neurol* 510, 221-236.

JANE, D. E., LODGE, D. & COLLINGRIDGE, G. L. (2009). Kainate receptors: pharmacology, function and therapeutic potential. *Neuropharmacology* 56, 90-113.

JEON, C. J., STRETTOI, E. & MASLAND, R. H. (1998). The major cell populations of the mouse retina. *J Neurosci* 18, 8936-8946.

JOHNSON, J., SHERRY, D. M., LIU, X., FREMEAU, R. T., JR., SEAL, R. P., EDWARDS, R. H. & COPENHAGEN, D. R. (2004). Vesicular glutamate transporter 3 expression identifies glutamatergic amacrine cells in the rodent retina. *J Comp Neurol* 477, 386-398.

JOHNSON, J. W. & ASCHER, P. (1987). Glycine potentiates the NMDA response in cultured mouse brain neurons. *Nature* 325, 529-531.

JUNJAUD, G., ROUAUD, E., TURPIN, F., MOTHET, J. P. & BILLARD, J. M. (2006). Age-related effects of the neuromodulator D-serine on neurotransmission and synaptic potentiation in the CA1 hippocampal area of the rat. *J Neurochem* 98, 1159-1166.

KALBAUGH, T. L., ZHANG, J. & DIAMOND, J. S. (2009). Coagonist release modulates NMDA receptor subtype contributions at synaptic inputs to retinal ganglion cells. *J Neurosci* 29, 1469-1479.

KAMPHUIS, W., DIJK, F. & O'BRIEN, B. J. (2003a). Gene expression of AMPA-type glutamate receptor subunits in rod-type ON bipolar cells of rat retina. *Eur J Neurosci* 18, 1085-1092.

KAMPHUIS, W., KLOOSTER, J. & DIJK, F. (2003b). Expression of AMPA-type glutamate receptor subunit (GluR2) in ON-bipolar neurons in the rat retina. *J Comp Neurol* 455, 172-186.

KANAI, Y., SMITH, C. P. & HEDIGER, M. A. (1993). A new family of neurotransmitter transporters: the high-affinity glutamate transporters. *Faseb J* 7, 1450-1459.

KAO, J. P., LI, G. & AUSTON, D. A. (2010). Practical aspects of measuring intracellular calcium signals with fluorescent indicators. *Methods Cell Biol* 99, 113-152.

KARRA, D. & DAHM, R. (2010). Transfection techniques for neuronal cells. *J Neurosci* 30, 6171-6177.

KARTVELISHVILY, E., SHLEPER, M., BALAN, L., DUMIN, E. & WOLOSKER, H. (2006). Neuron-derived D-serine release provides a novel means to activate N-methyl-D-aspartate receptors. *J Biol Chem* 281, 14151-14162.

KASHIWABUCHI, N., IKEDA, K., ARAKI, K., HIRANO, T., SHIBUKI, K., TAKAYAMA, C., INOUE, Y., KUTSUWADA, T., YAGI, T., KANG, Y. & *ET AL*. (1995). Impairment of motor coordination, Purkinje cell synapse formation, and cerebellar long-term depression in GluR delta 2 mutant mice. *Cell* 81, 245-252.

KATSUKI, H., NONAKA, M., SHIRAKAWA, H., KUME, T. & AKAIKE, A. (2004). Endogenous D-serine is involved in induction of neuronal death by N-methyl-D-aspartate and simulated ischemia in rat cerebrocortical slices. *J Pharmacol Exp Ther* 311, 836-844.

KATSUKI, H., WATANABE, Y., FUJIMOTO, S., KUME, T. & AKAIKE, A. (2007). Contribution of endogenous glycine and d-serine to excitotoxic and ischemic cell death in rat cerebrocortical slice cultures. *Life Sci* 81, 740-749.

KAWAHARA, Y., ITO, K., SUN, H., KANAZAWA, I. & KWAK, S. (2003). Low editing efficiency of GluR2 mRNA is associated with a low relative abundance of ADAR2 mRNA in white matter of normal human brain. *Eur J Neurosci* 18, 23-33.

KEINANEN, K., WISDEN, W., SOMMER, B., WERNER, P., HERB, A., VERDOORN, T. A., SAKMANN, B. & SEEBURG, P. H. (1990). A family of AMPA-selective glutamate receptors. *Science* 249, 556-560.

KEMP, J. A., FOSTER, A. C., LEESON, P. D., PRIESTLEY, T., TRIDGETT, R., IVERSEN, L. L. & WOODRUFF, G. N. (1988). 7-Chlorokynurenic acid is a selective antagonist at the glycine modulatory site of the N-methyl-D-aspartate receptor complex. *Proc Natl Acad Sci U S A* 85, 6547-6550.

KEMP, J. A. & PRIESTLEY, T. (1991). Effects of (+)-HA-966 and 7-chlorokynurenic acid on the kinetics of N-methyl-D-aspartate receptor agonist responses in rat cultured cortical neurons. *Mol Pharmacol* 39, 666-670.

KESSLER, M., TERRAMANI, T., LYNCH, G. & BAUDRY, M. (1989). A glycine site associated with N-methyl-D-aspartic acid receptors: characterization and identification of a new class of antagonists. *J Neurochem* 52, 1319-1328.

KHORONENKOVA, S. V. & TISHKOV, V. I. (2008). D-amino acid oxidase: physiological role and applications. *Biochemistry (Mosc)* 73, 1511-1518.

KIM, P. M., AIZAWA, H., KIM, P. S., HUANG, A. S., WICKRAMASINGHE, S. R., KASHANI, A. H., BARROW, R. K., HUGANIR, R. L., GHOSH, A. & SNYDER, S. H. (2005). Serine racemase: activation by glutamate neurotransmission via glutamate receptor interacting protein and mediation of neuronal migration. *Proc Natl Acad Sci U S A* 102, 2105-2110.

KLECKNER, N. W. & DINGLEDINE, R. (1988). Requirement for glycine in activation of NMDA-receptors expressed in Xenopus oocytes. *Science* 241, 835-837.

KOHLER, M., BURNASHEV, N., SAKMANN, B. & SEEBURG, P. H. (1993). Determinants of Ca2+ permeability in both TM1 and TM2 of high affinity kainate receptor channels: diversity by RNA editing. *Neuron* 10, 491-500.

KOIKE, C., OBARA, T., URIU, Y., NUMATA, T., SANUKI, R., MIYATA, K., KOYASU, T., UENO, S., FUNABIKI, K., TANI, A., UEDA, H., KONDO, M., MORI, Y., TACHIBANA, M. & FURUKAWA, T. (2010). TRPM1 is a component of the retinal ON bipolar cell transduction channel in the mGluR6 cascade. *Proc Natl Acad Sci U S A* 107, 332-337.

KOLB, H. & FAMIGLIETTI, E. V. (1974). Rod and cone pathways in the inner plexiform layer of cat retina. *Science* 186, 47-49.

KOULEN, P. & BRANDSTATTER, J. H. (2002). Pre- and Postsynaptic Sites of Action of mGluR8a in the mammalian retina. *Invest Ophthalmol Vis Sci* 43, 1933-1940.

KOULEN, P., KUHN, R., WASSLE, H. & BRANDSTATTER, J. H. (1997). Group I metabotropic glutamate receptors mGluR1alpha and mGluR5a: localization in both synaptic layers of the rat retina. *J Neurosci* 17, 2200-2211.

KOULEN, P., KUHN, R., WASSLE, H. & BRANDSTATTER, J. H. (1999). Modulation of the intracellular calcium concentration in photoreceptor terminals by a presynaptic metabotropic glutamate receptor. *Proc Natl Acad Sci U S A* 96, 9909-9914.

KREBS, H. A. (1935). Metabolism of amino-acids: Deamination of amino-acids. *Biochem J* 29, 1620-1644.

KRISTIANSEN, L. V., HUERTA, I., BENEYTO, M. & MEADOR-WOODRUFF, J. H. (2007). NMDA receptors and schizophrenia. *Curr Opin Pharmacol* 7, 48-55.

KRNJEVIC, K. & PHILLIS, J. W. (1963). Iontophoretic studies of neurones in the mammalian cerebral cortex. *J Physiol* 165, 274-304.

KURTH-NELSON, Z. L., MISHRA, A. & NEWMAN, E. A. (2009). Spontaneous glial calcium waves in the retina develop over early adulthood. *J Neurosci* 29, 11339-11346.

KUTSUWADA, T., KASHIWABUCHI, N., MORI, H., SAKIMURA, K., KUSHIYA, E., ARAKI, K., MEGURO, H., MASAKI, H., KUMANISHI, T., ARAKAWA, M. & *ET AL*. (1992). Molecular diversity of the NMDA receptor channel. *Nature* 358, 36-41.

LAMAS, M., LEE-RIVERA, I., RAMIREZ, M. & LOPEZ-COLOME, A. M. (2007). d-Serine regulates CREB phosphorylation induced by NMDA receptor activation in Muller glia from the retina. *Neurosci Lett* 427, 55-60.

LAUBE, B., KURYATOV, A., KUHSE, J. & BETZ, H. (1993). Glycine-glutamate interactions at the NMDA receptor: role of cysteine residues. *FEBS Lett* 335, 331-334.

LEE, S. H., LIU, L., WANG, Y. T. & SHENG, M. (2002). Clathrin adaptor AP2 and NSF interact with overlapping sites of GluR2 and play distinct roles in AMPA receptor trafficking and hippocampal LTD. *Neuron* 36, 661-674.

LEE, S. H., SIMONETTA, A. & SHENG, M. (2004). Subunit rules governing the sorting of internalized AMPA receptors in hippocampal neurons. *Neuron* 43, 221-236.

LEIST, M. & NICOTERA, P. (1998). Apoptosis, excitotoxicity, and neuropathology. *Exp Cell Res* 239, 183-201.

LERMA, J., HERRANZ, A. S., HERRERAS, O., ABRAIRA, V. & MARTIN DEL RIO, R. (1986). In vivo determination of extracellular concentration of amino acids in the rat hippocampus. A method based on brain dialysis and computerized analysis. *Brain Res* 384, 145-155.

LESTER, R. A., TONG, G. & JAHR, C. E. (1993). Interactions between the glycine and glutamate binding sites of the NMDA receptor. *J Neurosci* 13, 1088-1096.

LI, H., GAUGHWIN, P., LI, N. & HE, S. (2004). Localization of dopamine D1-receptor to A-type horizontal cells in the rabbit retina by single cell RT-PCR. *Neurosci Lett* 355, 146-148.

LIU, J., WU, D. C. & WANG, Y. T. (2010). Allosteric potentiation of glycine receptor chloride currents by glutamate. *Nat Neurosci* 13, 1225-1232.

LOMELI, H., SPRENGEL, R., LAURIE, D. J., KOHR, G., HERB, A., SEEBURG, P. H. & WISDEN, W. (1993). The rat delta-1 and delta-2 subunits extend the excitatory amino acid receptor family. *FEBS Lett* 315, 318-322.

LU, W., SHI, Y., JACKSON, A. C., BJORGAN, K., DURING, M. J., SPRENGEL, R., SEEBURG, P. H. & NICOLL, R. A. (2009). Subunit composition of synaptic AMPA receptors revealed by a single-cell genetic approach. *Neuron* 62, 254-268.

LUKASIEWICZ, P. D. & ROEDER, R. C. (1995). Evidence for glycine modulation of excitatory synaptic inputs to retinal ganglion cells. *J Neurosci* 15, 4592-4601.

LUKASIEWICZ, P. D., WILSON, J. A. & LAWRENCE, J. E. (1997). AMPA-preferring receptors mediate excitatory synaptic inputs to retinal ganglion cells. *J Neurophysiol* 77, 57-64.

MARQUARDT, T., ASHERY-PADAN, R., ANDREJEWSKI, N., SCARDIGLI, R., GUILLEMOT, F. & GRUSS, P. (2001). Pax6 is required for the multipotent state of retinal progenitor cells. *Cell* 105, 43-55.

MARTINA, M., KRASTENIAKOV, N. V. & BERGERON, R. (2003). D-Serine differently modulates NMDA receptor function in rat CA1 hippocampal pyramidal cells and interneurons. *J Physiol* 548, 411-423.

MARTINEAU, M., GALLI, T., BAUX, G. & MOTHET, J. P. (2008). Confocal imaging and tracking of the exocytotic routes for D-serine-mediated gliotransmission. *Glia* 56, 1271-1284.

MASLAND, R. H. (2001a). Neuronal diversity in the retina. *Curr Opin Neurobiol* 11, 431-436.

MASLAND, R. H. (2001b). The fundamental plan of the retina. *Nat Neurosci* 4, 877-886.

MATOBA, M., TOMITA, U. & NISHIKAWA, T. (1997). Characterization of 5,7-dichlorokynurenate-insensitive D-[3H]serine binding to synaptosomal fraction isolated from rat brain tissues. *J Neurochem* 69, 399-405.

MATSUDA, K., FLETCHER, M., KAMIYA, Y. & YUZAKI, M. (2003). Specific assembly with the NMDA receptor 3B subunit controls surface expression and calcium permeability of NMDA receptors. *J Neurosci* 23, 10064-10073.

MATSUDA, K., KAMIYA, Y., MATSUDA, S. & YUZAKI, M. (2002). Cloning and characterization of a novel NMDA receptor subunit NR3B: a dominant subunit that reduces calcium permeability. *Brain Res Mol Brain Res* 100, 43-52.

MATSUI, T., SEKIGUCHI, M., HASHIMOTO, A., TOMITA, U., NISHIKAWA, T. & WADA, K. (1995). Functional comparison of D-serine and glycine in rodents: the effect on cloned NMDA receptors and the extracellular concentration. *J Neurochem* 65, 454-458.

MAYAT, E., PETRALIA, R. S., WANG, Y. X. & WENTHOLD, R. J. (1995). Immunoprecipitation, immunoblotting, and immunocytochemistry studies suggest that glutamate receptor delta subunits form novel postsynaptic receptor complexes. *J Neurosci* 15, 2533-2546.

MAYER, M. L. (2005). Glutamate receptor ion channels. *Curr Opin Neurobiol* 15, 282-288.

MAYER, M. L. & VYKLICKY, L., JR. (1989). Concanavalin A selectively reduces desensitization of mammalian neuronal quisqualate receptors. *Proc Natl Acad Sci U S A* 86, 1411-1415.

MAYER, M. L., VYKLICKY, L., JR. & CLEMENTS, J. (1989). Regulation of NMDA receptor desensitization in mouse hippocampal neurons by glycine. *Nature* 338, 425-427.

MCBAIN, C. J. & MAYER, M. L. (1994). N-methyl-D-aspartic acid receptor structure and function. *Physiol Rev* 74, 723-760.

MEGURO, H., MORI, H., ARAKI, K., KUSHIYA, E., KUTSUWADA, T., YAMAZAKI, M., KUMANISHI, T., ARAKAWA, M., SAKIMURA, K. & MISHINA, M. (1992). Functional characterization of a heteromeric NMDA receptor channel expressed from cloned cDNAs. *Nature* 357, 70-74.

MENGER, N., POW, D. V. & WASSLE, H. (1998). Glycinergic amacrine cells of the rat retina. *J Comp Neurol* 401, 34-46.

MENGER, N. & WASSLE, H. (2000). Morphological and physiological properties of the A17 amacrine cell of the rat retina. *Vis Neurosci* 17, 769-780.

MIMURA, Y., MOGI, K., KAWANO, M., FUKUI, Y., TAKEDA, J., NOGAMI, H. & HISANO, S. (2002). Differential expression of two distinct vesicular glutamate transporters in the rat retina. *Neuroreport* 13, 1925-1928.

MIYA, K., INOUE, R., TAKATA, Y., ABE, M., NATSUME, R., SAKIMURA, K., HONGOU, K., MIYAWAKI, T. & MORI, H. (2008). Serine racemase is predominantly localized in neurons in mouse brain. *J Comp Neurol* 510, 641-654.

MONAGHAN, D. T. & COTMAN, C. W. (1985). Distribution of N-methyl-D-aspartate-sensitive L-[3H]glutamate-binding sites in rat brain. *J Neurosci* 5, 2909-2919.

MONYER, H., SPRENGEL, R., SCHOEPFER, R., HERB, A., HIGUCHI, M., LOMELI, H., BURNASHEV, N., SAKMANN, B. & SEEBURG, P. H. (1992). Heteromeric NMDA receptors: molecular and functional distinction of subtypes. *Science* 256, 1217-1221.

MORGANS, C. W., ZHANG, J., JEFFREY, B. G., NELSON, S. M., BURKE, N. S., DUVOISIN, R. M. & BROWN, R. L. (2009). TRPM1 is required for the depolarizing light response in retinal ON-bipolar cells. *Proc Natl Acad Sci U S A* 106, 19174-19178.

MORIKAWA, A., HAMASE, K., INOUE, T., KONNO, R., NIWA, A. & ZAITSU, K. (2001). Determination of free D-aspartic acid, D-serine and D-alanine in the brain of mutant mice lacking D-amino acid oxidase activity. *J Chromatogr B Biomed Sci Appl* 757, 119-125.

MORIYAMA, Y. & YAMAMOTO, A. (2004). Glutamatergic chemical transmission: look! Here, there, and anywhere. *J Biochem* 135, 155-163.

MORIYOSHI, K., MASU, M., ISHII, T., SHIGEMOTO, R., MIZUNO, N. & NAKANISHI, S. (1991). Molecular cloning and characterization of the rat NMDA receptor. *Nature* 354, 31-37.

MOSBACHER, J., SCHOEPFER, R., MONYER, H., BURNASHEV, N., SEEBURG, P. H. & RUPPERSBERG, J. P. (1994). A molecular determinant for submillisecond desensitization in glutamate receptors. *Science* 266, 1059-1062.

MOTHET, J. P., PARENT, A. T., WOLOSKER, H., BRADY, R. O., JR., LINDEN, D. J., FERRIS, C. D., ROGAWSKI, M. A. & SNYDER, S. H. (2000). D-serine is an endogenous ligand for the glycine site of the N-methyl-D-aspartate receptor. *Proc Natl Acad Sci U S A* 97, 4926-4931.

MOTHET, J. P., POLLEGIONI, L., OUANOUNOU, G., MARTINEAU, M., FOSSIER, P. & BAUX, G. (2005). Glutamate receptor activation triggers a calcium-dependent and SNARE protein-dependent release of the gliotransmitter D-serine. *Proc Natl Acad Sci U S A* 102, 5606-5611.

MU, Y., OTSUKA, T., HORTON, A. C., SCOTT, D. B. & EHLERS, M. D. (2003). Activity-dependent mRNA splicing controls ER export and synaptic delivery of NMDA receptors. *Neuron* 40, 581-594.

MUKAI, S., MISHIMA, H. K., SHOGE, K., SHINYA, M., ISHIHARA, K. & SASA, M. (2002). Existence of ionotropic glutamate receptor subtypes in cultured rat retinal ganglion cells obtained by the magnetic cell sorter method and inhibitory effects of 20-hydroxyecdysone, a neurosteroid, on the glutamate response. *Jpn J Pharmacol* 89, 44-52.

MULLE, C., SAILER, A., SWANSON, G. T., BRANA, C., O'GORMAN, S., BETTLER, B. & HEINEMANN, S. F. (2000). Subunit composition of kainate receptors in hippocampal interneurons. *Neuron* 28, 475-484.

MUSTAFA, A. K., KIM, P. M. & SNYDER, S. H. (2004). D-Serine as a putative glial neurotransmitter. *Neuron Glia Biol* 1, 275-281.

NAKANISHI, N., AXEL, R. & SHNEIDER, N. A. (1992). Alternative splicing generates functionally distinct N-methyl-D-aspartate receptors. *Proc Natl Acad Sci U S A* 89, 8552-8556.

NAKANISHI, S., NAKAJIMA, Y., MASU, M., UEDA, Y., NAKAHARA, K., WATANABE, D., YAMAGUCHI, S., KAWABATA, S. & OKADA, M. (1998). Glutamate receptors: brain function and signal transduction. *Brain Res Brain Res Rev* 26, 230-235.

NAMEKATA, K., OKUMURA, A., HARADA, C., NAKAMURA, K., YOSHIDA, H. & HARADA, T. (2006). Effect of photoreceptor degeneration on RNA splicing and expression of AMPA receptors. *Mol Vis* 12, 1586-1593.

NAUR, P., HANSEN, K. B., KRISTENSEN, A. S., DRAVID, S. M., PICKERING, D. S., OLSEN, L., VESTERGAARD, B., EGEBJERG, J., GAJHEDE, M., TRAYNELIS, S. F. & KASTRUP, J. S. (2007). Ionotropic glutamate-like receptor delta2 binds D-serine and glycine. *Proc Natl Acad Sci U S A* 104, 14116-14121.

NEVIAN, T. & HELMCHEN, F. (2007). Calcium indicator loading of neurons using single-cell electroporation. *Pflugers Arch* 454, 675-688.

NEWMAN, E. A. (2005). Calcium increases in retinal glial cells evoked by light-induced neuronal activity. *J Neurosci* 25, 5502-5510.

NILSSON, A., DUAN, J., MO-BOQUIST, L. L., BENEDIKZ, E. & SUNDSTROM, E. (2007). Characterisation of the human NMDA receptor subunit NR3A glycine binding site. *Neuropharmacology* 52, 1151-1159.

NISWENDER, C. M. & CONN, P. J. (2010). Metabotropic glutamate receptors: physiology, pharmacology, and disease. *Annu Rev Pharmacol Toxicol* 50, 295-322.

NONG, Y., HUANG, Y. Q., JU, W., KALIA, L. V., AHMADIAN, G., WANG, Y. T. & SALTER, M. W. (2003). Glycine binding primes NMDA receptor internalization. *Nature* 422, 302-307.

NOWAK, L., BREGESTOVSKI, P., ASCHER, P., HERBET, A. & PROCHIANTZ, A. (1984). Magnesium gates glutamate-activated channels in mouse central neurones. *Nature* 307, 462-465.

NYITRAI, G., KEKESI, K. A. & JUHASZ, G. (2006). Extracellular level of GABA and Glu: in vivo microdialysis-HPLC measurements. *Curr Top Med Chem* 6, 935-940.

O'BRIEN, K. B. & BOWSER, M. T. (2006). Measuring D-serine efflux from mouse cortical brain slices using online microdialysis-capillary electrophoresis. *Electrophoresis* 27, 1949-1956.

O'BRIEN, K. B., MILLER, R. F. & BOWSER, M. T. (2005). D-Serine uptake by isolated retinas is consistent with ASCT-mediated transport. *Neurosci Lett* 385, 58-63.

OKUBO, Y. & IINO, M. (2010). Visualization of glutamate as a volume transmitter. *J Physiol*, doi: 10.1113/jphysiol.2010.199539.

OLIVER, M. W., SHACKLOCK, J. A., KESSLER, M., LYNCH, G. & BAIMBRIDGE, K. G. (1990). The glycine site modulates NMDA-mediated changes of intracellular free calcium in cultures of hippocampal neurons. *Neurosci Lett* 114, 197-202.

PALMER, C. L., COTTON, L. & HENLEY, J. M. (2005). The molecular pharmacology and cell biology of alpha-amino-3-hydroxy-5-methyl-4-isoxazolepropionic acid receptors. *Pharmacol Rev* 57, 253-277.

PANATIER, A., THEODOSIS, D. T., MOTHET, J. P., TOUQUET, B., POLLEGIONI, L., POULAIN, D. A. & OLIET, S. H. (2006). Glia-derived D-serine controls NMDA receptor activity and synaptic memory. *Cell* 125, 775-784.

PATERNAIN, A. V., COHEN, A., STERN-BACH, Y. & LERMA, J. (2003). A role for extracellular Na+ in the channel gating of native and recombinant kainate receptors. *J Neurosci* 23, 8641-8648.

PEI, W., HUANG, Z. & NIU, L. (2007). GluR3 flip and flop: differences in channel opening kinetics. *Biochemistry* 46, 2027-2036.

PEI, W., HUANG, Z., WANG, C., HAN, Y., PARK, J. S. & NIU, L. (2009). Flip and flop: a molecular determinant for AMPA receptor channel opening. *Biochemistry* 48, 3767-3777.

PENG, Y. W., BLACKSTONE, C. D., HUGANIR, R. L. & YAU, K. W. (1995). Distribution of glutamate receptor subtypes in the vertebrate retina. *Neuroscience* 66, 483-497.

PEREZ DE SEVILLA MULLER, L., SHELLEY, J. & WEILER, R. (2007). Displaced amacrine cells of the mouse retina. *J Comp Neurol* 505, 177-189.

PERKEL, D. J., HESTRIN, S., SAH, P. & NICOLL, R. A. (1990). Excitatory synaptic currents in Purkinje cells. *Proc Biol Sci* 241, 116-121.

PERRY, V. H. & WALKER, M. (1980). Amacrine cells, displaced amacrine cells and interplexiform cells in the retina of the rat. *Proc R Soc Lond B Biol Sci* 208, 415-431.

PINA-CRESPO, J. C., TALANTOVA, M., MICU, I., STATES, B., CHEN, H. S., TU, S., NAKANISHI, N., TONG, G., ZHANG, D., HEINEMANN, S. F., ZAMPONI, G. W., STYS, P. K. & LIPTON, S. A. (2010). Excitatory glycine responses of CNS myelin mediated by NR1/NR3 "NMDA" receptor subunits. *J Neurosci* 30, 11501-11505.

PINHEIRO, P. & MULLE, C. (2006). Kainate receptors. *Cell Tissue Res* 326, 457-482.

PLESTED, A. J. & MAYER, M. L. (2007). Structure and mechanism of kainate receptor modulation by anions. *Neuron* 53, 829-841.

PLESTED, A. J., VIJAYAN, R., BIGGIN, P. C. & MAYER, M. L. (2008). Molecular basis of kainate receptor modulation by sodium. *Neuron* 58, 720-735.

PRIESTLEY, T., LAUGHTON, P., MYERS, J., LE BOURDELLES, B., KERBY, J. & WHITING, P. J. (1995). Pharmacological properties of recombinant human N-methyl-D-aspartate receptors comprising NR1a/NR2A and NR1a/NR2B subunit assemblies expressed in permanently transfected mouse fibroblast cells. *Mol Pharmacol* 48, 841-848.

PRILLOFF, S., NOBLEJAS, M. I., CHEDHOMME, V. & SABEL, B. A. (2007). Two faces of calcium activation after optic nerve trauma: life or death of retinal ganglion cells in vivo depends on calcium dynamics. *Eur J Neurosci* 25, 3339-3346.

PURO, D. G., YUAN, J. P. & SUCHER, N. J. (1996). Activation of NMDA receptor-channels in human retinal Muller glial cells inhibits inward-rectifying potassium currents. *Vis Neurosci* 13, 319-326.

RABE, C. S. & TABAKOFF, B. (1990). Glycine site-directed agonists reverse the actions of ethanol at the N-methyl-D-aspartate receptor. *Mol Pharmacol* 38, 753-757.

RAFIKI, A., BERNARD, A., MEDINA, I., GOZLAN, H. & KHRESTCHATISKY, M. (2000). Characterization in cultured cerebellar granule cells and in the developing rat brain of mRNA variants for the NMDA receptor 2C subunit. *J Neurochem* 74, 1798-1808.

RAUEN, T., TAYLOR, W. R., KUHLBRODT, K. & WIESSNER, M. (1998). High-affinity glutamate transporters in the rat retina: a major role of the glial glutamate transporter GLAST-1 in transmitter clearance. *Cell Tissue Res* 291, 19-31.

REED, B. T., SULLIVAN, S. J., TSAI, G., COYLE, J. T., ESGUERRA, M. & MILLER, R. F. (2009). The glycine transporter GlyT1 controls N-methyl-D-aspartic acid receptor coagonist occupancy in the mouse retina. *Eur J Neurosci* 30, 2308-2317.

RIBEIRO, C. S., REIS, M., PANIZZUTTI, R., DE MIRANDA, J. & WOLOSKER, H. (2002). Glial transport of the neuromodulator D-serine. *Brain Res* 929, 202-209.

RILLICH, K., GENTSCH, J., REICHENBACH, A., BRINGMANN, A. & WEICK, M. (2009). Light stimulation evokes two different calcium responses in Muller glial cells of the guinea pig retina. *Eur J Neurosci* 29, 1165-1176.

RODRIGUEZ-MORENO, A. & SIHRA, T. S. (2007). Metabotropic actions of kainate receptors in the CNS. *J Neurochem* 103, 2121-2135.

ROSENBERG, D., KARTVELISHVILY, E., SHLEPER, M., KLINKER, C. M., BOWSER, M. T. & WOLOSKER, H. (2010). Neuronal release of D-serine: a physiological pathway controlling extracellular D-serine concentration. *Faseb J* 24, 2951-2961.

ROWAN, M. J., RIPPS, H. & SHEN, W. (2010). Fast glutamate uptake via EAAT2 shapes the cone-mediated light offset response in bipolar cells. *J Physiol* 588, 3943-3956.

RUTTER, A. R., FRADLEY, R. L., GARRETT, E. M., CHAPMAN, K. L., LAWRENCE, J. M., ROSAHL, T. W. & PATEL, S. (2007). Evidence from gene knockout studies implicates Asc-1 as the primary transporter mediating d-serine reuptake in the mouse CNS. *Eur J Neurosci* 25, 1757-1766.

SALT, T. E. (1989). Modulation of NMDA receptor-mediated responses by glycine and D-serine in the rat thalamus in vivo. *Brain Res* 481, 403-406.

SANES, J. R. & ZIPURSKY, S. L. (2010). Design principles of insect and vertebrate visual systems. *Neuron* 66, 15-36.

SASAKI, T. & KANEKO, A. (2007). Elevation of intracellular ca(2+) concentration induced by hypoxia in retinal ganglion cells. *Jpn J Ophthalmol* 51, 175-180.

SCHELL, M. J., BRADY, R. O., JR., MOLLIVER, M. E. & SNYDER, S. H. (1997). D-serine as a neuromodulator: regional and developmental localizations in rat brain glia resemble NMDA receptors. *J Neurosci* 17, 1604-1615.

SCHELL, M. J., MOLLIVER, M. E. & SNYDER, S. H. (1995). D-serine, an endogenous synaptic modulator: localization to astrocytes and glutamate-stimulated release. *Proc Natl Acad Sci U S A* 92, 3948-3952.

SCHIFFER, H. H., SWANSON, G. T. & HEINEMANN, S. F. (1997). Rat GluR7 and a carboxy-terminal splice variant, GluR7b, are functional kainate receptor subunits with a low sensitivity to glutamate. *Neuron* 19, 1141-1146.

SEKARAN, S., FOSTER, R. G., LUCAS, R. J. & HANKINS, M. W. (2003). Calcium imaging reveals a network of intrinsically light-sensitive inner-retinal neurons. *Curr Biol* 13, 1290-1298.

SHEN, W. & JIANG, Z. (2007). Characterization of glycinergic synapses in vertebrate retinas. *J Biomed Sci* 14, 5-13.

SHEN, W. & SLAUGHTER, M. M. (2002). A non-excitatory paradigm of glutamate toxicity. *J Neurophysiol* 87, 1629-1634.

SHEN, Y., HEIMEL, J. A., KAMERMANS, M., PEACHEY, N. S., GREGG, R. G. & NAWY, S. (2009). A transient receptor potential-like channel mediates synaptic transmission in rod bipolar cells. *J Neurosci* 29, 6088-6093.

SHLEPER, M., KARTVELISHVILY, E. & WOLOSKER, H. (2005). D-serine is the dominant endogenous coagonist for NMDA receptor neurotoxicity in organotypic hippocampal slices. *J Neurosci* 25, 9413-9417.

SIKKA, P., WALKER, R., COCKAYNE, R., WOOD, M. J., HARRISON, P. J. & BURNET, P. W. (2010). D-Serine metabolism in C6 glioma cells: Involvement of alanine-serine-cysteine transporter (ASCT2) and serine racemase (SRR) but not D-amino acid oxidase (DAO). *J Neurosci Res* 88, 1829-1840.

SILVER, R. A., TRAYNELIS, S. F. & CULL-CANDY, S. G. (1992). Rapid-time-course miniature and evoked excitatory currents at cerebellar synapses in situ. *Nature* 355, 163-166.

SLAUGHTER, M. M. & MILLER, R. F. (1981). 2-amino-4-phosphonobutyric acid: a new pharmacological tool for retina research. *Science* 211, 182-185.

SOMMER, B., KOHLER, M., SPRENGEL, R. & SEEBURG, P. H. (1991). RNA editing in brain controls a determinant of ion flow in glutamate-gated channels. *Cell* 67, 11-19.

ST JULES, R., KENNARD, J., SETLIK, W. & HOLTZMAN, E. (1992). Frog cones as well as Muller cells have peroxisomes. *Exp Eye Res* 54, 1-8.

STANDLEY, S., TOCCO, G., TOURIGNY, M. F., MASSICOTTE, G., THOMPSON, R. F. & BAUDRY, M. (1995). Developmental changes in alpha-amino-3-hydroxy-5-methyl-4-isoxazole propionate receptor properties and expression in the rat hippocampal formation. *Neuroscience* 67, 881-892.

STEPHENSON, F. A., COUSINS, S. L. & KENNY, A. V. (2008). Assembly and forward trafficking of NMDA receptors (Review). *Mol Membr Biol* 25, 311-320.

STEVENS, E. R., ESGUERRA, M., KIM, P. M., NEWMAN, E. A., SNYDER, S. H., ZAHS, K. R. & MILLER, R. F. (2003). D-serine and serine racemase are present in the vertebrate retina and contribute to the physiological activation of NMDA receptors. *Proc Natl Acad Sci U S A* 100, 6789-6794.

STEVENS, E. R., GUSTAFSON, E. C., SULLIVAN, S. J., ESGUERRA, M. & MILLER, R. F. (2010). Light-evoked NMDA receptor-mediated currents are reduced by blocking D-serine synthesis in the salamander retina. *Neuroreport* 21, 239-244.

STOSIEK, C., GARASCHUK, O., HOLTHOFF, K. & KONNERTH, A. (2003). In vivo two-photon calcium imaging of neuronal networks. *Proc Natl Acad Sci U S A* 100, 7319-7324.

STRETTOI, E. & MASLAND, R. H. (1996). The number of unidentified amacrine cells in the mammalian retina. *Proc Natl Acad Sci U S A* 93, 14906-14911.

SUCHER, N. J., KOHLER, K., TENNETI, L., WONG, H. K., GRUNDER, T., FAUSER, S., WHEELER-SCHILLING, T., NAKANISHI, N., LIPTON, S. A. & GUENTHER, E. (2003). N-methyl-D-aspartate receptor subunit NR3A in the retina: developmental expression, cellular localization, and functional aspects. *Invest Ophthalmol Vis Sci* 44, 4451-4456.

SUCHER, N. J., LIPTON, S. A. & DREYER, E. B. (1997). Molecular basis of glutamate toxicity in retinal ganglion cells. *Vision Res* 37, 3483-3493.

SULLIVAN, S. J. & MILLER, R. F. (2010). AMPA receptor mediated D-serine release from retinal glial cells. *J Neurochem* 115, 1681-1689.

SUN, W., LI, N. & HE, S. (2002a). Large-scale morophological survey of rat retinal ganglion cells. *Vis Neurosci* 19, 483-493.

SUN, W., LI, N. & HE, S. (2002b). Large-scale morphological survey of mouse retinal ganglion cells. *J Comp Neurol* 451, 115-126.

SUN, Y., JIANG, X. D., LIU, X., GONG, H. Q. & LIANG, P. J. (2010). Synaptic contribution of Ca2+-permeable and Ca2+-impermeable AMPA receptors on isolated carp retinal horizontal cells and their modulation by Zn2+. *Brain Res* 1317, 60-68.

TAKAYASU, N., YOSHIKAWA, M., WATANABE, M., TSUKAMOTO, H., SUZUKI, T., KOBAYASHI, H. & NODA, S. (2008). The serine racemase mRNA is expressed in both neurons and glial cells of the rat retina. *Arch Histol Cytol* 71, 123-129.

TASCHENBERGER, H., ENGERT, F. & GRANTYN, R. (1995). Synaptic current kinetics in a solely AMPA-receptor-operated glutamatergic synapse formed by rat retinal ganglion neurons. *J Neurophysiol* 74, 1123-1136.

TAYLOR, W. R., CHEN, E. & COPENHAGEN, D. R. (1995). Characterization of spontaneous excitatory synaptic currents in salamander retinal ganglion cells. *J Physiol* 486 (Pt 1), 207-221.

TEHRANI, A., WHEELER-SCHILLING, T. H. & GUENTHER, E. (2000). Coexpression patterns of mGLuR mRNAs in rat retinal ganglion cells: a single-cell RT-PCR study. *Invest Ophthalmol Vis Sci* 41, 314-319.

THONGKHAO-ON, K., KOTTEGODA, S., PULIDO, J. S. & SHIPPY, S. A. (2004). Determination of amino acids in rat vitreous perfusates by capillary electrophoresis. *Electrophoresis* 25, 2978-2984.

THORESON, W. B. & WITKOVSKY, P. (1999). Glutamate receptors and circuits in the vertebrate retina. *Prog Retin Eye Res* 18, 765-810.

TSIEN, R. Y. (1980). New calcium indicators and buffers with high selectivity against magnesium and protons: design, synthesis, and properties of prototype structures. *Biochemistry* 19, 2396-2404.

UNSOELD, T., STRADOMSKA, A. M., WANG, R., RATHJEN, F. G. & JUTTNER, R. (2008). Early maturation of GABAergic synapses in mouse retinal ganglion cells. *Int J Dev Neurosci* 26, 233-238.

VANDENBRANDEN, C. A., KAMPHUIS, W., NUNES CARDOZO, B. & KAMERMANS, M. (2000). Expression and localization of ionotropic glutamate receptor subunits in the goldfish retina--an in situ hybridization and immunocytochemical study. *J Neurocytol* 29, 729-742.

VANEY, D. (1990). The mosaic of amacrine cells in the mammalian retina. *Prog Ret Res* 9, 49-100.

VANEY, D. I., GYNTHER, I. C. & YOUNG, H. M. (1991). Rod-signal interneurons in the rabbit retina: 2. AII amacrine cells. *J Comp Neurol* 310, 154-169.

VESSEY, J. P., STRATIS, A. K., DANIELS, B. A., DA SILVA, N., JONZ, M. G., LALONDE, M. R., BALDRIDGE, W. H. & BARNES, S. (2005). Proton-mediated feedback inhibition of presynaptic calcium channels at the cone photoreceptor synapse. *J Neurosci* 25, 4108-4117.

VICINI, S., WANG, J. F., LI, J. H., ZHU, W. J., WANG, Y. H., LUO, J. H., WOLFE, B. B. & GRAYSON, D. R. (1998). Functional and pharmacological differences between recombinant N-methyl-D-aspartate receptors. *J Neurophysiol* 79, 555-566.

VIGNES, M., BLEAKMAN, D., LODGE, D. & COLLINGRIDGE, G. L. (1997). The synaptic activation of the GluR5 subtype of kainate receptor in area CA3 of the rat hippocampus. *Neuropharmacology* 36, 1477-1481.

VIGNES, M. & COLLINGRIDGE, G. L. (1997). The synaptic activation of kainate receptors. *Nature* 388, 179-182.

VITANOVA, L. (2007a). AMPA and kainate receptors in turtle retina: an immunocytochemical study. *Cell Mol Neurobiol* 27, 407-421.

VITANOVA, L. (2007b). Non-NMDA receptors in frog retina: an immunocytochemical study. *Acta Histochem* 109, 154-163.

VOLGYI, B., CHHEDA, S. & BLOOMFIELD, S. A. (2009). Tracer coupling patterns of the ganglion cell subtypes in the mouse retina. *J Comp Neurol* 512, 664-687.

VYKLICKY, L., JR., BENVENISTE, M. & MAYER, M. L. (1990). Modulation of N-methyl-D-aspartic acid receptor desensitization by glycine in mouse cultured hippocampal neurones. *J Physiol* 428, 313-331.

WADICHE, J. I. & JAHR, C. E. (2001). Multivesicular release at climbing fiber-Purkinje cell synapses. *Neuron* 32, 301-313.

WASHBOURNE, P. & MCALLISTER, A. K. (2002). Techniques for gene transfer into neurons. *Curr Opin Neurobiol* 12, 566-573.

WASSLE, H. (2004). Parallel processing in the mammalian retina. *Nat Rev Neurosci* 5, 747-757.

WASSLE, H., CHUN, M. H. & MULLER, F. (1987). Amacrine cells in the ganglion cell layer of the cat retina. *J Comp Neurol* 265, 391-408.

WASSLE, H., GRUNERT, U., COOK, N. J. & MOLDAY, R. S. (1992). The cGMP-gated channel of rod outer segments is not localized in bipolar cells of the mammalian retina. *Neurosci Lett* 134, 199-202.

WASSLE, H., HEINZE, L., IVANOVA, E., MAJUMDAR, S., WEISS, J., HARVEY, R. J. & HAVERKAMP, S. (2009). Glycinergic transmission in the Mammalian retina. *Front Mol Neurosci* 2, 6.

WASSLE, H., REGUS-LEIDIG, H. & HAVERKAMP, S. (2006). Expression of the vesicular glutamate transporter vGluT2 in a subset of cones of the mouse retina. *J Comp Neurol* 496, 544-555.

WATANABE, Y., HIMI, T., SAITO, H. & ABE, K. (1992). Involvement of glycine site associated with the NMDA receptor in hippocampal long-term potentiation and acquisition of spatial memory in rats. *Brain Res* 582, 58-64.

WEAVER, J. C. (1995). Electroporation theory. Concepts and mechanisms. *Methods Mol Biol* 55, 3-28.

WEE, K. S., ZHANG, Y., KHANNA, S. & LOW, C. M. (2008). Immunolocalization of NMDA receptor subunit NR3B in selected structures in the rat forebrain, cerebellum, and lumbar spinal cord. *J Comp Neurol* 509, 118-135.

WENTHOLD, R. J., PETRALIA, R. S., BLAHOS, J., II & NIEDZIELSKI, A. S. (1996). Evidence for multiple AMPA receptor complexes in hippocampal CA1/CA2 neurons. *J Neurosci* 16, 1982-1989.

WIESSNER, M., FLETCHER, E. L., FISCHER, F. & RAUEN, T. (2002). Localization and possible function of the glutamate transporter, EAAC1, in the rat retina. *Cell Tissue Res* 310, 31-40.

WILLIAMS, S. M., DIAZ, C. M., MACNAB, L. T., SULLIVAN, R. K. & POW, D. V. (2006). Immunocytochemical analysis of D-serine distribution in the mammalian brain reveals novel anatomical compartmentalizations in glia and neurons. *Glia* 53, 401-411.

WOLLMUTH, L. P., KUNER, T. & SAKMANN, B. (1998). Adjacent asparagines in the NR2-subunit of the NMDA receptor channel control the voltage-dependent block by extracellular Mg2+. *J Physiol* 506 (Pt 1), 13-32.

WOLOSKER, H., BLACKSHAW, S. & SNYDER, S. H. (1999a). Serine racemase: a glial enzyme synthesizing D-serine to regulate glutamate-N-methyl-D-aspartate neurotransmission. *Proc Natl Acad Sci U S A* 96, 13409-13414.

WOLOSKER, H., SHETH, K. N., TAKAHASHI, M., MOTHET, J. P., BRADY, R. O., JR., FERRIS, C. D. & SNYDER, S. H. (1999b). Purification of serine racemase: biosynthesis of the neuromodulator D-serine. *Proc Natl Acad Sci U S A* 96, 721-725.

WONG, A. Y., FAY, A. M. & BOWIE, D. (2006). External ions are coactivators of kainate receptors. *J Neurosci* 26, 5750-5755.

WONG, A. Y., MACLEAN, D. M. & BOWIE, D. (2007). Na+/Cl- dipole couples agonist binding to kainate receptor activation. *J Neurosci* 27, 6800-6809.

WONG, H. K., LIU, X. B., MATOS, M. F., CHAN, S. F., PEREZ-OTANO, I., BOYSEN, M., CUI, J., NAKANISHI, N., TRIMMER, J. S., JONES, E. G., LIPTON, S. A. & SUCHER, N. J. (2002). Temporal and regional expression of NMDA receptor subunit NR3A in the mammalian brain. *J Comp Neurol* 450, 303-317.

WROBLEWSKI, J. T., FADDA, E., MAZZETTA, J., LAZAREWICZ, J. W. & COSTA, E. (1989). Glycine and D-serine act as positive modulators of signal transduction at N-methyl-D-aspartate sensitive glutamate receptors in cultured cerebellar granule cells. *Neuropharmacology* 28, 447-452.

WU, S. Z., BODLES, A. M., PORTER, M. M., GRIFFIN, W. S., BASILE, A. S. & BARGER, S. W. (2004). Induction of serine racemase expression and D-serine release from microglia by amyloid beta-peptide. *J Neuroinflammation* 1, 2.

WURM, A., ERDMANN, I., BRINGMANN, A., REICHENBACH, A. & PANNICKE, T. (2009). Expression and function of P2Y receptors on Muller cells of the postnatal rat retina. *Glia* 57, 1680-1690.

YAMAZAKI, M., ARAKI, K., SHIBATA, A. & MISHINA, M. (1992a). Molecular cloning of a cDNA encoding a novel member of the mouse glutamate receptor channel family. *Biochem Biophys Res Commun* 183, 886-892.

YAMAZAKI, M., MORI, H., ARAKI, K., MORI, K. J. & MISHINA, M. (1992b). Cloning, expression and modulation of a mouse NMDA receptor subunit. *FEBS Lett* 300, 39-45.

YANG, J. H., MAPLE, B., GAO, F., MAGUIRE, G. & WU, S. M. (1998). Postsynaptic responses of horizontal cells in the tiger salamander retina are mediated by AMPA-preferring receptors. *Brain Res* 797, 125-134.

YANG, Y., GE, W., CHEN, Y., ZHANG, Z., SHEN, W., WU, C., POO, M. & DUAN, S. (2003). Contribution of astrocytes to hippocampal long-term potentiation through release of D-serine. *Proc Natl Acad Sci U S A* 100, 15194-15199.

YANG, Z. J., APPLEBY, V. J., COYLE, B., CHAN, W. I., TAHMASEB, M., WIGMORE, P. M. & SCOTTING, P. J. (2004). Novel strategy to study gene expression and function in developing cerebellar granule cells. *J Neurosci Methods* 132, 149-160.

YAO, Y. & MAYER, M. L. (2006). Characterization of a soluble ligand binding domain of the NMDA receptor regulatory subunit NR3A. *J Neurosci* 26, 4559-4566.

YOSHIKAWA, M., OKA, T., KAWAGUCHI, M. & HASHIMOTO, A. (2004). MK-801 upregulates the expression of d-amino acid oxidase mRNA in rat brain. *Brain Res Mol Brain Res* 131, 141-144.

YOUNG, H. M. & VANEY, D. I. (1990). The retinae of Prototherian mammals possess neuronal types that are characteristic of non-mammalian retinae. *Vis Neurosci* 5, 61-66.

YU, J., DANIELS, B. A. & BALDRIDGE, W. H. (2009). Slow excitation of cultured rat retinal ganglion cells by activating group I metabotropic glutamate receptors. *J Neurophysiol* 102, 3728-3739.

ZERANGUE, N. & KAVANAUGH, M. P. (1996). ASCT-1 is a neutral amino acid exchanger with chloride channel activity. *J Biol Chem* 271, 27991-27994.

ZHANG, J. & DIAMOND, J. S. (2006). Distinct perisynaptic and synaptic localization of NMDA and AMPA receptors on ganglion cells in rat retina. *J Comp Neurol* 498, 810-820.

ZHANG, J. & DIAMOND, J. S. (2009). Subunit- and pathway-specific localization of NMDA receptors and scaffolding proteins at ganglion cell synapses in rat retina. *J Neurosci* 29, 4274-4286.

ZHUANG, Z., YANG, B., THEUS, M. H., SICK, J. T., BETHEA, J. R., SICK, T. J. & LIEBL, D. J. (2010). EphrinBs regulate D-serine synthesis and release in astrocytes. *J Neurosci* 30, 16015-16024.